(NASA-CR-142878) PLANETARY QUARANTINE: SUPPORTING RESEARCH AND TECHNOLOGY Semiannual Review, 1 Jul. - 31 Dec. 1974 (Jet Propulsion Lab.) 119 p HC $5.25 CSCL 22B G3/54

N75-24362

Unclas 22220

JET PROPULSION LABORATORY
CALIFORNIA INSTITUTE OF TECHNOLOGY
PASADENA, CALIFORNIA

900-701

PLANETARY QUARANTINE

Semi-Annual Review
Supporting Research and Technology

1 July - 31 December 1974

April 18, 1975

APPROVED, Sections
I, II, III, and IV

D. M. Taylor, Supervisor
Life Sciences Research

A. R. Hoffman, Supervisor
Planetary Quarantine Analysis

D. S. Hess, Manager
Environmental Requirements
Section

APPROVED, Sections
V and VI

D. Alcorn for
J. R. Puleo, Supervisor
Planetary Quarantine Laboratory

D. Alcorn, Manager
Systems Test and Launch
Operations Section

JET PROPULSION LABORATORY
CALIFORNIA INSTITUTE OF TECHNOLOGY
PASADENA, CALIFORNIA

PREFACE

This document contains a report on Research and Advanced Development at the Jet Propulsion Laboratory during the period 1 July 1974 to 31 Dec 1974, sponsored by the Planetary Quarantine branch of the NASA Office of Space Science and Applications.

CONTENTS

I. PLANETARY QUARANTINE STRATEGIES FOR ADVANCED MISSIONS (NASA No. 193-58-61-01)

1.1 STRATEGIES FOR SATELLITE ENCOUNTER 1-1

1.1.1 Subtask A Introduction 1-1

1.1.2 Significant Accomplishments 1-1

1.1.3 Future Activities 1-2

1.1.4 Presentations 1-3

1.2 OUTER PLANET ENTRY ANALYSIS 1-4

1.2.1 Subtask B Introduction 1-4

1.2.2 Significant Accomplishments 1-4

1.2.3 Future Activities 1-9

1.2.4 Presentations 1-9

II. NATURAL SPACE ENVIRONMENT STUDIES (NASA No. 193-58-61-02)

2.1 EFFECT OF PLANETARY TRAPPED RADIATION BELT ON MICROORGANISMS 2-1

2.1.1 Subtask A Introduction 2-1

2.1.2 Significant Accomplishments 2-1

2.1.3 Future Activities 2-1

2.1.4 Presentations 2-2

2.2 EFFECT OF SOLAR WIND RADIATION ON MICROORGANISMS 2-3

2.2.1 Subtask B Introduction 2-3

2.2.2 Approach 2-3

2.2.3 Significant Accomplishments 2-4

2.2.4 Future Activities 2-12

2.2.5 Presentations 2-12

2.2.6 References 2-13

2.3 EFFECT OF SPACE VACUUM ON MICROORGANISMS 2-14

2.3.1 Subtask C Introduction 2-14

2.3.2 Significant Accomplishments 2-14

2.3.3 Future Activities 2-14

2.3.4 Presentations 2-14

PRECEDING PAGE BLANK NOT FILMED

CONTENTS (contd)

2.4 PROBABILITY OF GROWTH IN PLANETARY ATMOSPHERES AND SATELLITES 2-15

2.4.1 Subtask D Introduction 2-15

2.4.2 Significant Accomplishments 2-15

2.4.3 Future Activities 2-16

2.4.4 Presentations 2-16

2.5 EFFECT OF SOLAR ELECTROMAGNETIC RADIATION ON MICROORGANISMS 2-17

2.5.1 Subtask E Introduction 2-17

2.5.2 Approach 2-17

2.5.3 Significant Accomplishments 2-18

2.5.4 Future Actitivies 2-24

2.5.5 Presentations 2-24

2.5.6 References 2-24

III. POST LAUNCH RECONTAMINATION STUDIES (NASA No. 193-58-62-03)

3.1 POST LAUNCH RECONTAMINATION STUDIES 3-1

3.1.1 Introduction 3-1

3.1.2 Significant Accomplishments 3-1

3.1.3 Future Activities 3-10

3.1.4 Presentations 3-10

3.1.5 References 3-10

IV. SPACECRAFT CLEANING AND DECONTAMINATION TECHNIQUES (NASA No. 193-58-63-02)

4.1 PHYSICAL REMOVAL OF SPACECRAFT MICROBIAL BURDEN 4-1

4.1.1 Subtask A Introduction 4-1

4.1.2 Approach 4-2

4.1.3 Significant Accomplishments 4-8

4.1.4 Summary 4-20

4.1.5 Conclusions. 4-21

4.1.6 Future Activities 4-22

4.1.7 Presentations 4-22

CONTENTS (contd)

4.2 EVALUATION OF PLASMA CLEANING AND DECONTAMINATION TECHNIQUES 4-24

4.2.1 Subtask B Introduction 4-24

4.2.2 Approach 4-24

4.2.3 Significant Accomplishments 4-27

4.2.4 Summary and Conclusion 4-29

4.2.5 Future Activities 4-30

4.2.6 Presentation 4-30

4.3 PLANETARY QUARANTINE CONSIDERATION FOR SHUTTLE LAUNCHED SPACECRAFT 4-31

4.3.1 Subtask C Introduction 4-31

4.3.2 Significant Accomplishments 4-31

4.3.3 Future Activities 4-33

4.3.4 Presentation 4-33

V. PLANETARY QUARANTINE LABORATORY ASSAY ACTIVITIES (AFETR) (NASA No. 193-58-63-05)

5.1 PLANETARY QUARANTINE LABORATORY ASSAY ACTIVITIES (AFETR) 5-1

5.1.1 Subtask A Introduction 5-1

5.1.2 Significant Accomplishments 5-1

5.1.3 Future Activities 5-2

5.1.4 Presentations 5-2

VI. PLANETARY QUARANTINE LABORATORY - RESEARCH ACTIVITIES (NASA No. 193-58-63-06)

6.1 TEFLON RIBBON EXPERIMENTS 6-1

6.1.1 Subtask A Introduction 6-1

6.1.2 Significant Accomplishments 6-1

6.1.3 Future Activities 6-12

6.1.4 Presentations 6-12

6.1.5 References 6-12

CONTENTS (contd)

6.2 PYROLYSIS GAS - LIQUID CHROMATOGRAPHY STUDY 6-13

6.2.1 Subtask B Introduction 6-13

6.2.2 Approach 6-13

6.2.3 Experimental Conditions 6-14

6.2.4 Future Activities 6-19

6.2.5 Presentation 6-19

6.2.6 References 6-19

CONTENTS (contd)

FIGURES

2-B. 1	Solar wind electron source, overview of system	2-5
2-B. 2	Solar wind electron source instrumentation	2-6
2-B. 3	Solar wind electron source, interior view showing dosimetry fixture and electron gun	2-7
2-B. 4	View of dosimetry test fixture through vacuum window with the source in operation	2-9
2-B. 5	Cultured organism test fixture	2-11
2-E. 1	Solar cell fixture for naturally occurring population collection	2-20
2-E. 2	Naturally occurring population fixture mounted in vacuum chamber	2-21
2-E. 3	Effect of SER at 0. 1 Sun, -125°C	2-23
2-E. 4	Effect of SER at 0. 5 Sun, -15°C	2-23
2-E. 5	Effect of SER at 1. 0 Sun, +70°C	2-25
2-E. 6	Effect of SER on naturally occurring microorganisms	2-25
3-A. 1	Grain charging in shade	3-3
3-A. 2	Electric field	3-3
3-A. 3	Recontamination simulation of LRC run 6	3-4
3-A. 4	Release velocity distribution	3-4
3-A. 5	Angular distribution escaped grain direction	3-7
3-A. 6	Mission micrometeoroid fluence distribution over mass and velocity groups	3-8
3-A. 7	Mission grain recontamination distribution over meteoroid mass and velocity groups	3-8
3-A. 8	Mission safe-hit distribution over meteoroid mass and velocity groups	3-9

CONTENTS (contd)

FIGURES (contd)

3-A. 9	Mission grain escape distribution over meteoroid mass and velocity groups	3-9
4-A. 1	Diagram of brush evaluation test set up	4-3
4-A. 2	Linear brush test apparatus working position	4-5
4-A. 3	Linear brush test apparatus view at test brush and accessories	4-6
4-A. 4	Apparatus accessories; top - plutonium ship and vacuum grids; bottom - test brushes	4-7
4-A. 5	Arrangement of samples and counting areas	4-9
4-A. 6	Brush adjustment	4-9
4-A. 7	Effect of tip shape and static charge on particle adherence to	4-11
4-A. 8	Single fiber shedding test; T - trimmed fibers; F - flagged fibers	4-12
4-A. 9	Typical efficiency distribution across test sample with uncharged fiber	4-14
4-A. 10	Restoration of fiber - cleanliness of striker bar in vacuum flow	4-14
4-A. 11	Typical particle distribution over length of shedding sample	4-15
4-A. 12	Typical lateral particle distribution on a shedding slide	4-15
4-A. 13	Effect of moisture and number of sweeps on removal efficiency	4-16
4-A. 14	Effect of moisture and number of sweeps on edge-shedding	4-16
4-A. 15	Effect of static charge on step-efficiency	4-18
4-A. 16	Effect of static charge on accumulative removal efficiency	4-18

CONTENTS (contd)

FIGURES (contd)

4-A. 17	Effect of static charge on edge shedding	4-18
4-A. 18	Effect of static charge on particle adherence to brush	4-18
4-A. 19	Experimental rotary brush 25.4 (1 inch) sweep width	4-23
4-B. 1	Schematic of test sample orientation	4-26
4-B. 2	Schematic of mated surface test stack	4-26
6-A. 1	Expected effects of thermal processes on naturally occurring spores	6-11
6-B. 1	Chromatographic Equipment	6-15
6-B. 2	Assay Techniques	6-17
6-B. 3	Chromatogram of B. circulans	6-18
6-B. 4	Chromatogram of B. firmus	6-18
6-B. 5	Chromatogram of B. subtilis	6-20
6-B. 6	Chromatogram of B. subtilis (90% spores)	6-21
6-B. 7	Chromatogram of heat survivor Bacillus V-52-26	6-21

TABLES

2-B. 1	Preliminary data for BSN	2-13
3-A. 1	Summary of results of recontamination analysis for Viking-type spacecraft	3-6
4-A. 1	Effect of static charge on edge shedding and adherence to fiber	4-19
4-B. 1	Test matrix to determine the effectiveness of helium plasma in penetrating and sterilizing various sample configurations	4-25
4-B. 2	Mean percent survival of Bacillus subtilus var. niger spores in glass tubing after exposure to helium plasma	4-27

CONTENTS (contd)

TABLES (contd)

4-B.3 Mean percent survival of Bacillus subtilus var. niger spores in stainless steel tubing after exposure to helium plasma 4-28

4-B.4 Mean percent survial of Bacillus subtilus var. niger spores in stainless steel tubing after exposure to helium plasma[a] 4-30

4-B.5 Bacillus subtilus var. niger spores recovered from mated metal surfaces exposed to helium plasma for sixty minutes[a] 4-31

6-A.1 Thermal resistance of bacterial spores collected on teflon ribbons - VAB - KSC (1.2mg/L water) 6-3

6-A.2 Thermal resistance of bacterial spores collected on teflon ribbons - JPL/Pasadena (1.2 mg/L water). 6-4

6-A.3 Thermal resistance of bacterial spores collected on teflon ribbons - Martin-Marietta/Denver (1.2mg/L water). 6-5

6-A.4 Positive cultures detected at various incubation periods 6-7

6-A.5 Biochemical test reactions of heat-stressed environmental isolates (Martin Marietta Aerospace). . . . 6-8

6-A.6 Biochemical test reactions of heat-stressed environmental isolates (JPL/Pasadena) 6-9

6-A.7 Biochemical test reactions of heat-stressed environmental isolates (VAB - KSC) . . . . . .

6-B.1 Pyrolysis conditions 6-16

6-B.2 Chromatography conditions 6-16

SECTION I

PLANETARY QUARANTINE STRATEGIES FOR ADVANCED MISSIONS (NASA NO. 193-58-61-01)

Contents	Title and Related Personnel
Subtask A para. 1.1	STRATEGIES FOR SATELLITE ENCOUNTER Cognizance: C. Gonzalez Associate Personnel: W. Brady
Subtask B para. 1.2	OUTER PLANET ENTRY ANALYSIS Cognizance: C. Gonzalez Associate Personnel: W. Jaworski, A. McRonald

1.1 STRATEGIES FOR SATELLITE ENCOUNTER

1.1.1 Subtask A Introduction

The objectives of this task are to determine the impact of satisfying satellite quarantine on current outer planet mission and spacecraft designs; and to develop tools required to perform trajectory and navigation analyses for determining satellite impact probabilities.

1.1.2 Significant Accomplishments

1.1.2.1 Jupiter Orbiter Mission. The progress so far has been to develop a general framework for evaluating potential strategies used to develop and check out the necessary software for the analysis. This is being done in order to determine the impact of the quarantine constraints on the maneuver requirements and determine what maneuver-strategies are preferable in terms of reducing the impact of quarantine constraints on the mission.

It is important to minimize propellant consumption while satisfying all the mission constraints. The constraints are of three types. The flyby conditions must be kept within allowable bounds to achieve the proper orbital change. They must also satisfy the conditions imposed by the science objectives of the mission. Finally, and of most concern here, is the planetary and satellite quarantine constraint.

One sample orbit from a typical orbiter mission has been considered. This is a 33.4 day Callisto to Callisto transfer orbit. It is called a crank orbit because it involves a swingby above the planet to provide an orbit plane change and no period change. The orbit has a period twice that of Callisto. This sample was chosen for study because results were available for comparison. Prior studies (preproject non-PQ related) indicate that the orbital trim maneuvers should be performed shortly after the Callisto encounter at the beginning of the transfer (encounter 1), at apoapse, and shortly before the Callisto encounter at the end of the transfer (encounter 2). The delivery errors at encounter 1 are removed by the first two maneuvers and the third maneuver removes the errors resulting from the first two.

The close swingbys require precise delivery accuracy. The dispersions must be small enough to provide an appropriately small probability of impact at the immediate encounter. Also, the dispersions are magnified by the swingby and could cause large dispersions at the next encounter. Therefore, there must be constraints which keep the dispersions at the next encounter within bounds. One parameter of interest is the period of the next orbit. Other orbital parameters might also be considered. For the orbital transfers being considered, it is efficient to try to target the first maneuver to a specific aim point. The three maneuvers should be considered together and the total velocity gain should be minimized subject to the desired set of constraints. Constraints can be added to limit the first two maneuvers to aim points outside a contour to satisfy PQ.

A computer program was tried out on the sample Callisto to Callisto transfer and it was found that the constraints used did not provide enough control over the dispersions on the post flyby orbit. The semi-major axis was controlled well enough, but the lateral components of velocity apparently propagated very large dispersions in the orbital plane equivalent to an apsidal rotation. The post flyby orbit must be controlled to maintain reasonable errors for successive orbits.

1.1.3 Future Activities

Once an acceptable set of constraints has been found, the influence of quarantine constraints on the maneuver ΔV requirements will be studied. The limit on probability of impact, spacecraft reliability and orbit determination accuracy will be varied. It is expected that the ΔV requirements will increase with reductions in the allowable probability of impact or in the spacecraft reliability and decrease with improved orbit determination accuracy. The probability of impact (P_I) is being used to account for variations in both the estimate of the probability of contamination given impact ($P_{C/I}$) and the limit on probability of contamination (P_C) since $P_I = P_C/P_{C/I}$. In this case the P_C is the probability of contamination allocated to this flyby of this satellite.

Another sample transfer orbit will also be studied. The trajectory data are currently being generated for an Io to Io pump orbit. The period of the orbit is reduced from 32 to 21 days by flying by Io at a 1020 km altitude. The effect on satellite quarantine of coming within this distance of Io will be investigated in the next reporting period.

1.1.4 Presentations

None

1.2 OUTER PLANET ENTRY ANALYSIS

1.2.1 Subtask B Introduction

The objectives of the outer planet atmospheric entry analysis subtask is to develop and use the tools to determine the thermal response characteristics of a typical spacecraft and related debris upon entry into the atmospheres of Jupiter, Saturn, Uranus or Titan.

1.2.2 Significant Accomplishments

The entry heating analyses for Jupiter have been completed. The work during the past six months included tests performed at the Martin Marietta, Denver Plasma arc test facility. These tests were performed on samples of components and materials similar to those which will be flown on outer planet missions.

The analyses performed previously for the SR&T outer planet atmospheric entry heating task indicated that a typical outer planet spacecraft would break up upon entering the Jovian atmosphere due to the entry heating and dynamic pressure. Upon break up various components and materials, such as cabling, which would be contaminated with microorganisms, would be exposed to the atmosphere. These analyses also led to the conclusion that under certain conditions some detached components, such as cabling would not be heated enough to cause significant microbial burden reduction. In performing the analyses, advantage was taken of simplifications which were not conservative. The purpose for the tests described here was to obtain some experimental indication of the correctness of these assumptions.

Facilities do not exist to test large samples or to test samples in conditions simulating Jovian entry. These tests were not a simulation* of Jovian entry but were used to provide guidelines for interpreting the analytical work. Samples of components and materials, similar to those which analyses indicated could contain survivors, were prepared and used in the test. These

*Among other things, the test facility used was not equipped to simulate radiative heating.

samples were size limited because of the test facilities. Therefore, in general, compared to an actual Jovian entry: the test conditions provided lower heat levels; the effects proceeded more slowly; single components were isolated from their surroundings; and radiative heating was not available.

The following were the test objectives:

1) To test the effects of side heating on a component. The analyses performed prior to the test consider only the stagnation heat flux at the front end of the component. Side heating was assumed to be negligible.

2) To compare the thermal response of cabling attached to structural members or a subchassis with cabling which is unattached. The analyses were performed for a piece of unattached cabling. However, although some detached cabling would be present in entry, the thermal response of attached cabling also needed to be considered.

3) To determine the thermal response of actual combinations of materials such as those in cabling, i. e., copper wire and teflon insulation. The previous analyses were simplified; for example, teflon insulated copper cabling was simulated by a teflon rod. The tests afforded an opportunity to see the combined thermal response of the actual materials in a cable.

4) To observe the combined effects of heat and pressure on cabling, i. e., the response of a cable spreading apart to the thermal environment.

5) To observe any anomalies not accounted for in the previous analyses.

Seven samples were tested. These included four cable samples instrumented with thermocouples. A precurser sample was tested, and as it was rotated into the plasma stream by the holder, the constraining ties quickly disintegrated and the cable wires spread apart. The cable wires were quickly consumed by the plasma and only small pieces were left at the bottom of the

chamber. In order to prevent quick disintegration of the next samples they were secured by beryllium wires. This had the additional advantage of simulating either short spaced cable clamping or additional external encasement. In addition, one cable sample consisted of a nominal cable attached to an aluminum angle to which a thin fiberglass plate was bonded; the entire sample was wrapped in a thin teflon tape. Two fiberglass boards were tested: one consisted of a sandwich of fiberglass boards, with printed circuit type components attached over an aluminum honeycomb structure; the other consisted only of one fiberglass board with nothing attached. Both samples were instrumented with thermocouples. The last sample was a piece of the carbon epoxy strut.

Test results were obtained through visual inspection of the samples, before, during, and after the tests and inspection of black and white, and color photographs, and color movies taken during the test. The color movies were taken at high frame (i. e., slow motion) speeds in order to allow one to observe the tests slowly enough to understand what occurred. The results, and conclusions derived therefrom, and discussed here are based mainly on visual observation of the movies and of the samples. The test results are in agreement with the simplifying assumptions made in the previous analyses. Therefore, the conservatism used in those analyses appears to be justified, bearing in mind that the tests were performed with small samples in a much milder environment. In other words, since the tests were not a scaled down version of an actual entry simulation any conclusions based on the tests must take this into account. The test objectives were met.

The results of the tests conducted on the simple and isolated samples showed negligible side heating. Insignificant side heating also was concluded from the tests on the fiberglass board and subchassis sample.

The tests showed that the susceptibility of a cable to disintegration increases if it is not bound securely and spreads apart. Previous analyses showed that a cable (intact and not spreading) which has separated from a spacecraft, and coming in lengthwise without tumbling is resistant to heating at the back end. However, this situation represents an extreme case.

It must be borne in mind that because of juxtapositioning and in situ positioning of components in a chassis or subchassis, the actual situation in that case might differ from that implied from the tests described here. In the tests, which simply used a juxtapositioning of a cable with an aluminum angle and a piece of fiberglass, the aluminum and glass melt to provide a heat sink and blockage which slowed down the disintegration. The gases resulting from the ablation also provided heat blockage. Previous analyses performed on circuit boards which were stacked together indicated survival of micro-organisms on the boards toward the back of the stacks. The single sample circuit board tested here (fiberglass board on the aluminum honeycomb structure) was placed edge-on. The test indicated that no significant side heating occurred. However, if a number of boards which were stacked entered edge-on, one would expect heating of the sides of the interior boards. It is more difficult, at this point, to conclude positively from the test on one circuit board that a stack of boards (either edge-on or face on) would not experience any side heating. However, in an entry situation, breakup of a stack of circuit boards could occur leading to clusters of a single or a few circuit boards. In this case the tests results indicate that side heating would be negligible.

The results of total Jupiter study (past several years) have demonstrated a rather small but finite probability or survival of the congested plastic chunks and debris resulting from the initial spacecraft breakup due primarily to heating. The study has also revealed that small particles released, prior to spacecraft entry into the atmosphere, will survive within predetermined entry corridors, and their survivability depends on the entry angle into the atmosphere. Particles released after entry of the spacecraft into the atmosphere and breakup will not survive. For the three atmospheres studied (cool, normal and warm) a steep entry into the cool atmosphere indicated a higher probability of survival of large chunks; mainly due to shorter duration of the heat pulse. Very shallow entries into the warm atmosphere, however, offer a higher degree of survivability for very small debris and particles because the analysis has shown that their entry corridor is wider than in the case of the cool atmosphere.

The word survivability, as used here, means that local temperatures within the material may not reach a high enough level to ensure a desirable microbial kill.

Work was also performed in connection with Titan and Uranus. With regard to Titan, thermochemistry and radiative flux computations were completed for three model atmospheres (the Titan light model atmosphere will not radiate), and the computer coding was completed for the heavy model. This will allow the computation of convective and radiative entry heating and trajectories for entry of a spacecraft and its major fragments into the various model atmospheres of Titan. Values of heating per unit mass were determined for the Titan heavy atmosphere and an entry speed of 16 km/sec. In general, time-integrated heating in Titan entry will generally be less (up to a factor of three) than for the corresponding case of Saturn or Uranus entry.

With regard to Uranus and based on preliminary considerations the following conclusions are appropriate: (1) steep entry of a spacecraft into Uranus will give much less time-integrated heating (probably by a factor of from 3 to 10) than for the corresponding entry into Saturn; (2) entry at $\theta_e = 15°$ or less into Uranus will give integrated heating that is comparable (up to a factor of two less) to a Saturn entry, for the nominal atmosphere, and up to a factor of three greater for the cool atmosphere; (3) entry heating analysis should concern itself, in general, with objects for which the product (nose radius × mass/unit area in the flight direction) is large; for Uranus this statement is precise for the nominal atmosphere, in view of the dominance of convective heating over radiative (and similarly for the Titan medium and light atmospheres); (4) small particle pre-peak and post-peak corridors will fall between those for Saturn and Titan.

Accidental entry of a spacecraft from circular orbit was considered in a preliminary way leading to the following conclusions: (1) for the Jupiter case, one can say that decay from a posigrade equatorial circular orbit, or atmospheric penetration while in an imperfect circular orbit, is very closely similar to shallow entry into Saturn while on a flyby mission (aerodynamic entry speed is 30 km/sec for Jupiter circular decay, vis-a-vis 28 km/sec for

shallow Saturn flyby). Thus, no special treatment for Jupiter circular orbit decay appears to be warranted; (2) for Saturn the inertial circular speed is 25.1 km/sec, and thus the aerodynamic entry speed for posigrade equatorial entry is 14.9 km/sec; for small particles the corridors will be similar to those for Titan (similar entry speed) but with no hyperbolic skip-out boundaries, and possible skip-up boundaries at smaller angles than the previous Saturn boundaries; (3) circular orbits at large angles to the equator are unlikely for the first orbiters of Jupiter and Saturn, from fuel load considerations. The aerodynamic entry speeds in decay from polar orbits for Jupiter and Saturn would be 44.3 and 27.1 km/sec, respectively, and the heating could again be estimated from existing shallow entry results for Jupiter and Saturn.

1.2.3 Future Activities

The parts of the spacecraft whose non-survivability, when entering the Jupiter atmosphere, have been demonstrated in this study will be reanalyzed for Saturn and Titan. The objective of these analyses will be to show the relative degree of spacecraft parts survival to aid in the assessment of the microbic burden reduction problem involved when entering the atmospheres of these bodies.

1.2.4 Presentations

None

SECTION II

NATURAL SPACE ENVIRONMENT STUDIES
(NASA NO. 193-58-61-02)

Contents	Title and Related Personnel
Subtask A para. 2.1	EFFECT OF PLANETARY TRAPPED RADIATION BELT ON MICROORGANISMS Cognizance: D. Taylor Associate Personnel: C. Hagen (Bionetics) J. Barengoltz Y. Yelinek (Bionetics)
Subtask B para. 2.2	EFFECT OF SOLAR WIND ON MICROORGANISMS Cognizance: J. Barengoltz Associate Personnel: T. Laue (Bionetics) J. Farber (Bionetics) S. Donovan (Bionetics)
Subtask C para. 2.3	EFFECT OF SPACE VACUUM ON MICROORGANISMS Cognizance: C. Hagen (Bionetics) D. Taylor Associate Personnel: G. Simko (Bionetics) C. Smith (Bionetics) J. Yelinek (Bionetics) A. Ferreira (Bionetics)
Subtask D para. 2.4	PROBABILITY OF GROWTH IN PLANETARY ATMOSPHERE AND SATELLITES Cognizance: D. Taylor Associate Personnel: C. Myers N. Divine

PRECEDING PAGE BLANK NOT FILMED

Subtask E
para. 2.5

EFFECT OF SOLAR ELECTROMAGNETIC RADIATION ON MICROORGANISMS

Cognizance: M. Wardle

Associate Personnel:
D. Taylor
C. Hagen (Bionetics)
D. Ross
A. Ferreira (Bionetics)

2.1 EFFECT OF PLANETARY TRAPPED RADIATION BELT ON MICROORGANISMS

2.1.1 Subtask A Introduction

The objective of this subtask is to determine the effect of planetary trapped radiation belts on the survival of microorganisms associated with an unsterile spacecraft.

With flyby missions now planned for Jupiter and Saturn and possible Jupiter orbiters and probes, the trapped radiation belts may represent an environment lethal to microorganisms and thereby reduce the requirements for decontamination of spacecraft before launch.

The major components of planetary trapped radiation belts are electrons and protons. The approach of the present task is to evaluate possible biological effects of these belts by subjecting spacecraft microbial isolates to different energies, exposures, and dose rates of those particles.

2.1.2 Significant Accomplishments

During this period the Jupiter trapped radiation belt models were updated utilizing the Pioneer 10 radiation environment measurements. These models were used to compute specific radiation environments for Jupiter orbiters. Values of peak flux, peak dose rate, fluence and dose were computed as functions of energy for several trajectories including both equatorial and inclined orbits (the values for inclined orbits because of the absence of high latitude measurements in the Pioneer 10 data are highly uncertain). These values can be used to estimated bioburden reduction due to the radiation environment.

2.1.3 Future Activities

The radiation environment for Jupiter orbiters is provisional and will be recomputed as additional Pioneer 11 radiation measurements are incorporated into the radiation belt models. Additional activities will be to formulate statements of work to evaluate the effect of radiation on the survival of

encapsulated microorganisms and for the procurement of a high energy proton facility for the purpose of investigating the effects of high energy protons similar to those present in planetary trapped radiation belts. Finally, the evaluation of external radiation environments in terms of electron test data and the evaluation of the effect of secondary radiation will be conducted with the use of the updated Jupiter electron radiation belt models.

2.1.4. Presentations

None

2.2 EFFECT OF SOLAR WIND RADIATION ON MICROORGANISMS

2.2.1 Subtask B Introduction

The objective of this subtask is to determine the effect of solar wind radiation on microorganisms associated with nonsterile spacecraft.

This study is directed towards determining the reduction in spacecraft-associated microbial burden attributable to solar wind radiation. The data obtained will be utilized to update probability constants in the assessment of mission planetary quarantine constraints.

2.2.2 Approach

In order to fulfill the objectives of this task, an initial test program to investigate the effect of solar wind electrons on test microorganisms held in a vacuum has been established. A literature survey indicates biological effectiveness for electrons with energy in excess of 1 keV. Measurements and models of the solar wind electron spectrum imply an upper limit to the energy range of interest at about 5 keV. Parametric tests in this energy range, 1-5 keV, will be conducted at accelerated dose rates to permit typical mission doses (fluences) in acceptable test durations. Although other radiation effects data indicate significant dose rate effects are unlikely, this factor will be investigated for this environment. At each energy and dose rate (flux), tests with varying doses will be performed to obtain survival curves.

The first formal experimental phase will consist of tests with MM'71 isolates (sporeformers and non-sporeformers) and Staphylococcus epidermidis and spores of Bacillus subtilis var. niger as comparative organisms. A second phase will be an analogous program with naturally occurring microbial populations as samples.

In long range planning with the electron source, close-to-real time exposures and sequential exposures with varying energy to simulate the spectrum are being considered.

2.2.3 Significant Accomplishments

During this reporting period, the solar wind electron source (SWES) has been installed and tested, and preliminary experiments to establish the dose range versus energy of interest have been conducted.

2.2 3.1 The Solar Wind Electron Source. The SWES system consists of three subsystems: an electron gun subsystem, a dosimetry subsystem, and a vacuum subsystem (Fig. 2-B.1, 2, and 3).

The electron gun and its power supply and instrumentation package comprise the electron gun subsystem*. The electron gun, visible in the upper right hand corner of Fig. 2-B.3, may be mounted on the vacuum chamber centerline (as shown) or at one of four off-axis positions. The two-axis gimbal mount permits the beam to be centered in either case. This capability will allow combined environment experiments to be conducted in the future.

The electrons are initially emitted at thermal energies by the "uni-potential high temperature" cathode held at a large negative potential (the accelerating voltage or energy) with respect to the chamber ground. The cathode emission level is adjustable to change the dose rate. The spatial profile of the beam (divergence) is varied by a solid angle electrode. A pre-acceleration element accelerates the electrons to an intermediate energy before they gain the desired total energy in falling to the test fixture (ground). The power supply and instrumentation package (Fig. 2-B.2) allows adjustment and monitoring of all of the previous parameters, as well as a beam current monitor.

The electron gun subsystem can produce electrons in the energy range of 1 to 5 keV (± 5%) at current densities variable from 0.1 nanoamp/cm^2 to 5 μamp/cm^2. This current density range is equivalent to a flux (dose rate) range of 6×10^8 to 3×10^{13} e/cm^{2}sec. With the present configuration, the subsystem can cover a circular area of 25 cm with a 20% overall radial uniformity and a local uniformity (azimuthal) of 10%. A straightforward modification of the electron gun by the addition of a pre-acceleration grid and a

*Custom designed and manufactured by Dr. C. Crawford of Kimball Physics, Inc., Wilton, New Hampshire.

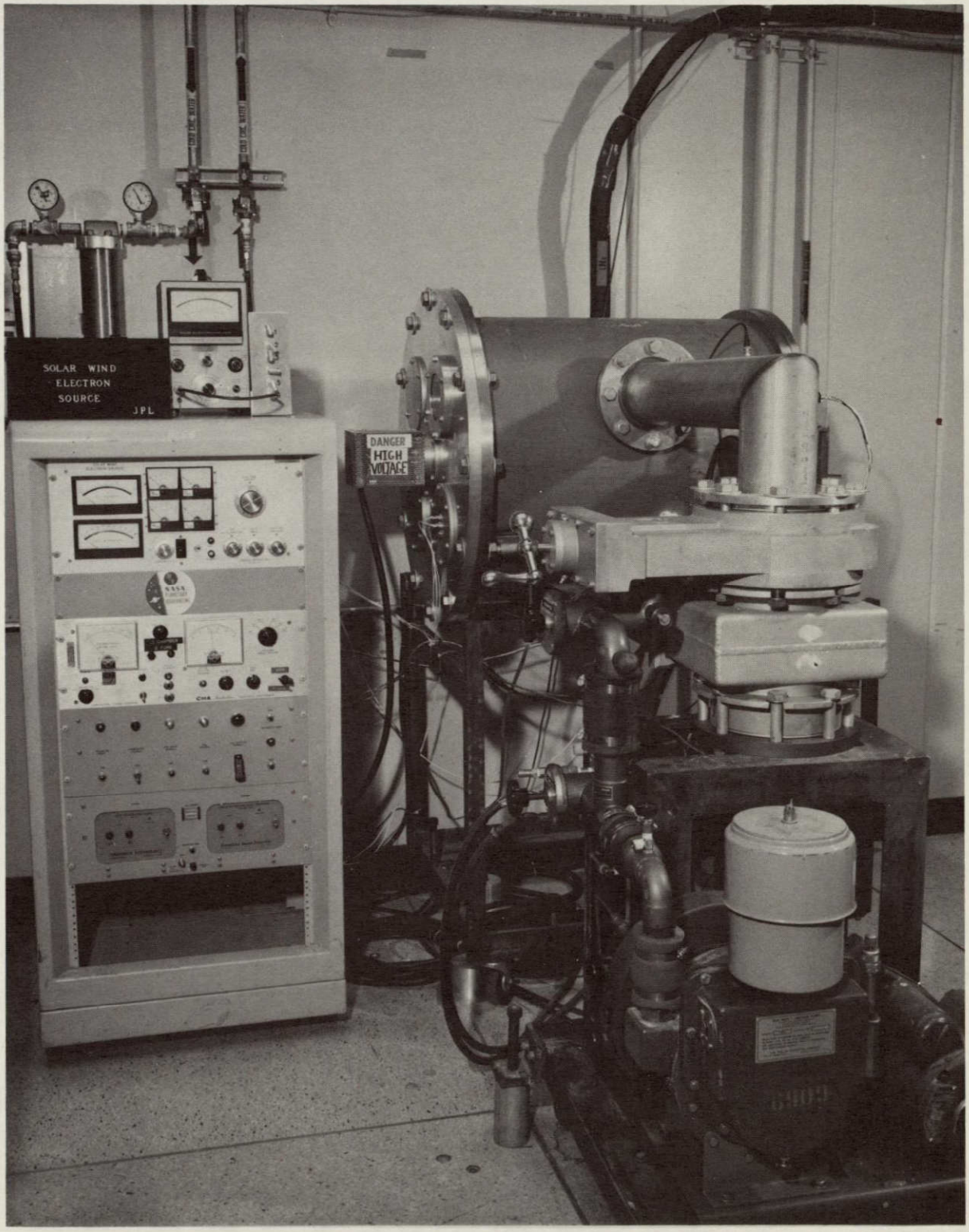

Fig. 2-B. 1. Solar wind electron source, overview of system

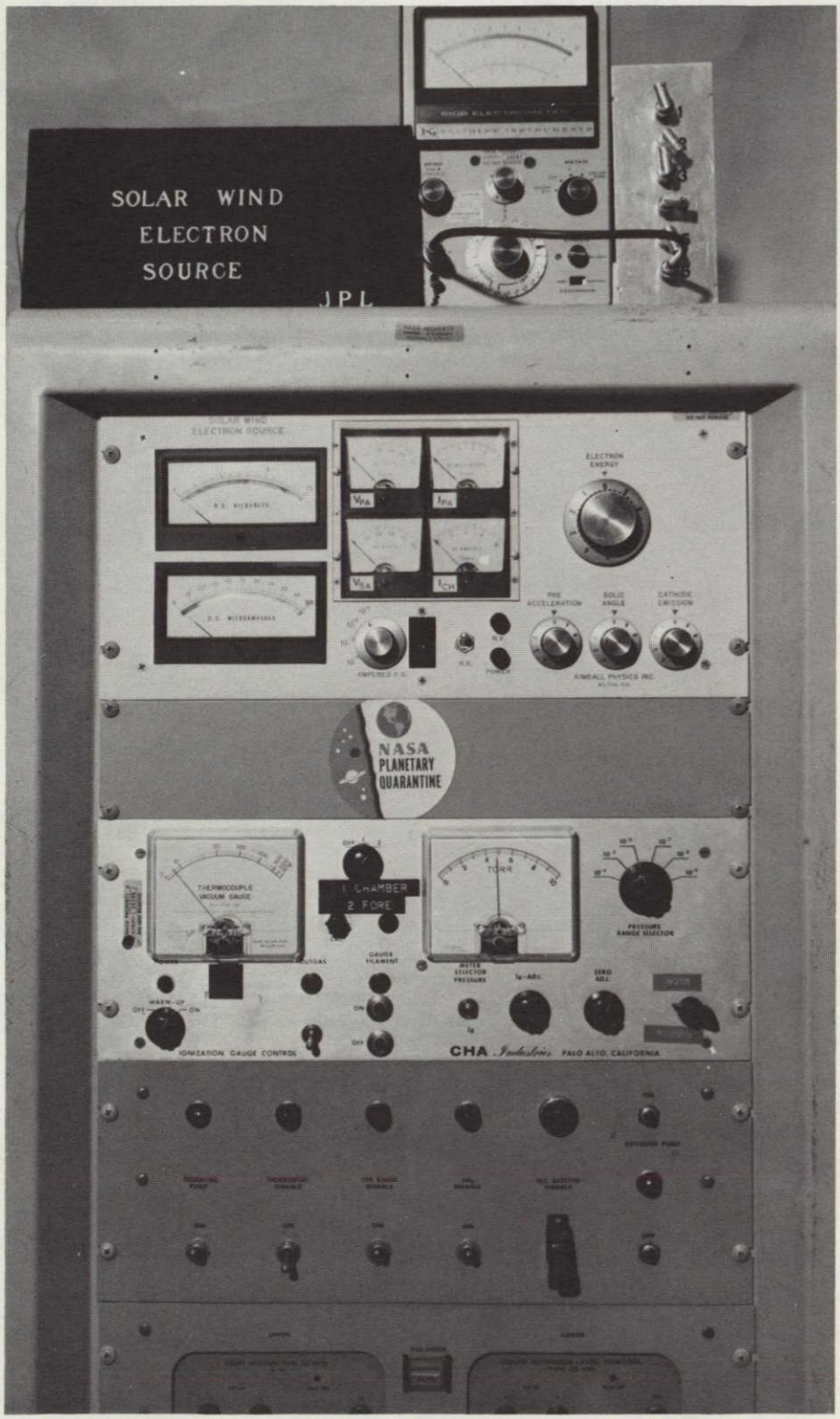

Fig. 2-B. 2. Solar wind electron source instrumentation

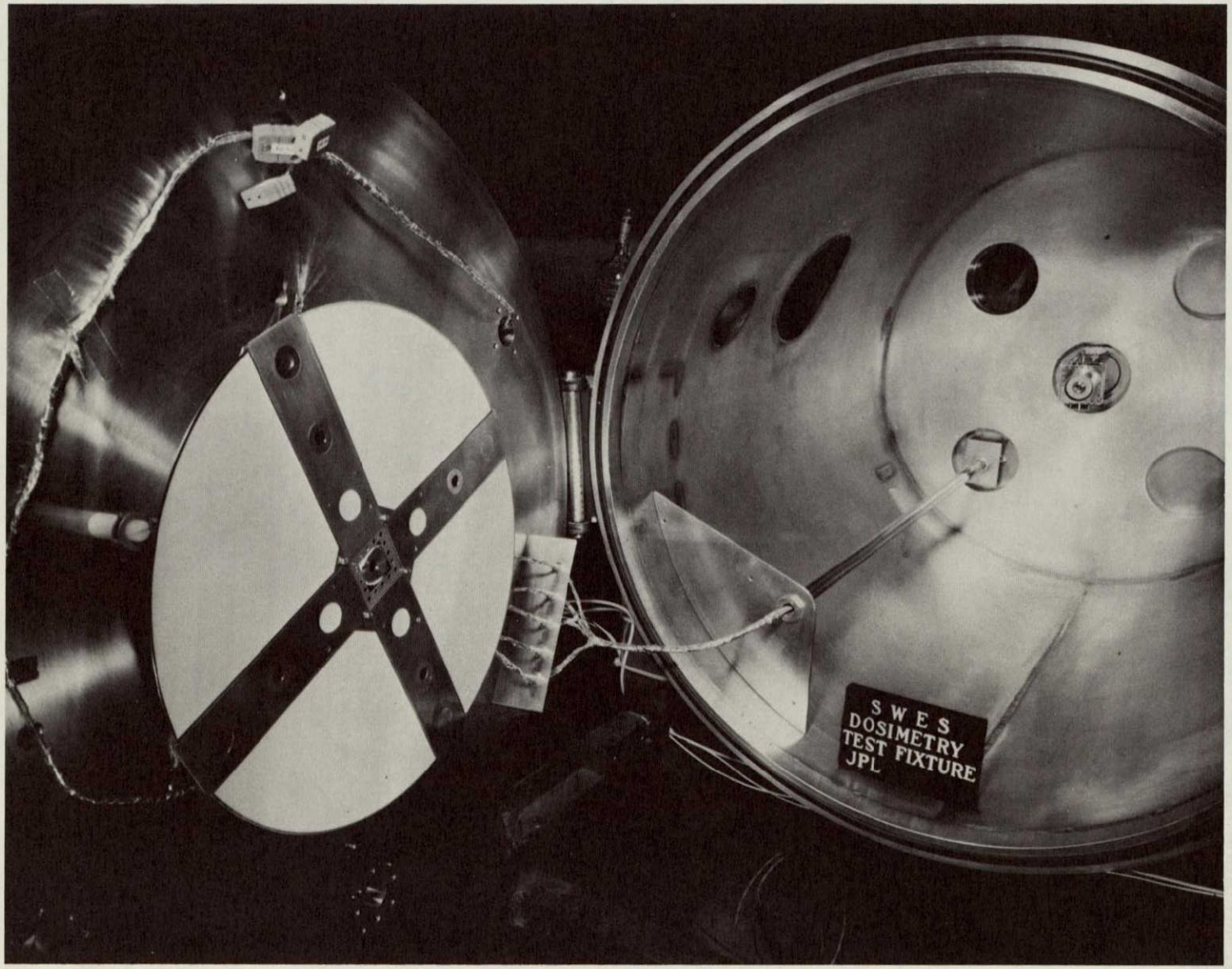

Fig. 2-B. 3. Solar wind electron source, interior view showing dosimetry fixture and electron gun

ground grid provides a much larger radially uniform coverage at the cost of larger inhomogenieties.

The dosimetry subsystem consists of a dosimetry test fixture, a monitor Faraday cup, a Keithley Model 610B electrometer, and the necessary cabling, vacuum feedthroughs, and connectors. The dosimetry test fixture* is comprised of an array of four Faraday cups mountable on 10, 20, or 30 cm diameter circles on a phosphor screen plate. These Faraday cups, together with the monitor Faraday cup on the beam axis, provide a direct reading of the incident current density (proportional to flux) at discrete locations. The cup currents are monitored by the electrometer. The phosphor screen glows under electron bombardment to provide a check of local uniformity and overall profile of the beam. It may be inspected through a vacuum window at the gun end of the chamber (Figs. 2-B. 3 and 2-B. 4). The use of the dosimetry subsystem is described in para. 2. 2. 3. 2.

The vacuum subsystem is a 61 cm i. d. × 70 cm long cylindrical vacuum chamber pumped by a LN2 trapped 6 in. diffusion pump stand (Fig. 2-B. 1).

The subsystem is capable of obtaining a vacuum of 1×10^{-3} nt/m^2 (8×10^{-6} torr) from ambient pressure (dry nitrogen) in 1 hour or less. The oil backstreaming, of particular importance to cathode life and beam uniformity, was measured by quartz crystal microbalance techniques over 63 hours of segmented vacuum operation with approximately two hours of gun operation. The deposition rate either exposed to the beam or near the pump inlet was less than 5×10^{-11} g/cm^2 sec.

2 2. 3. 2 Experimental Activities.

1. Beam Profile and Dosimetry Measurements. The measurements of the beam profile and other dosimetry matters were accomplished with the use of the dosimetry subsystem described in para. 2. 2. 3. 1. The dosimetry test fixture was mounted inside the vacuum chamber access door and the cup

*Custom designed and manufactured by Dr. Crawford of Kimball Physics, Inc., Wilton, New Hampshire.

Fig. 2-B.4. View of dosimetry test fixture through vacuum window with the source in operation

cables connected (see Fig. 2-B. 3). A complete profile, as in the case of the SWES acceptance tests, at a particular energy and flux was obtained by consecutive runs with the movable Faraday cups placed on the 10, 20, and 30 cm diameter circles. These runs were normalized for comparative purposes by resetting all controls by the meters and then adjusting the cathode emission precisely with the monitor (center-fixed) Faraday cup.

For the preliminary biological tests and the formal pure culture tests, only a single beam mapping run with the movable cups on the 10 cm diameter circle was required. This dosimetry run, which was performed before each experimental run, allowed an optimization of azimuthal symmetry on the circle corresponding to the cultured organism test fixture annulus. When the proper control settings had been noted, the monitor Faraday cup reading to produce the desired flux at the sample annulus was also recorded. During an experimental run, with the dosimetry test fixture replaced by the cultured organism test fixture (Fig. 2-B. 5), the flux was monitored by the monitor Faraday cup. Note that the test fixture has a hole on the beam axis to allow the cup to see the beam. The required fluence was then obtained by timing the duration of the exposure.

2. Preparation and Assay of Test Samples. For the preliminary experiments, pure cultures of *Bacillus subtilis* var. *niger* (BSN) were prepared. The organisms were sporulated in the liquid synthetic medium of Lazzarini and Santangelo (J. Bacteriol. 94: 125-130, 1967) modified by the addition of 25 mg of both L-methionine and L-tryptophan to one liter of medium. Mature spores were harvested and washed (7 times with sterile distilled water) by centrifugation (10 min at 9750 relative centrifugal force) with final suspension in distilled water.

An appropriate dilution of the final suspension was used to innoculate the test stages with approximately 10^4 spores. The stages were then placed on the cultured organism test fixture (Fig. 2-B. 5). Ten stages were placed on each side of the fixture, ten exposed and ten controls, and in addition three controls were mounted.

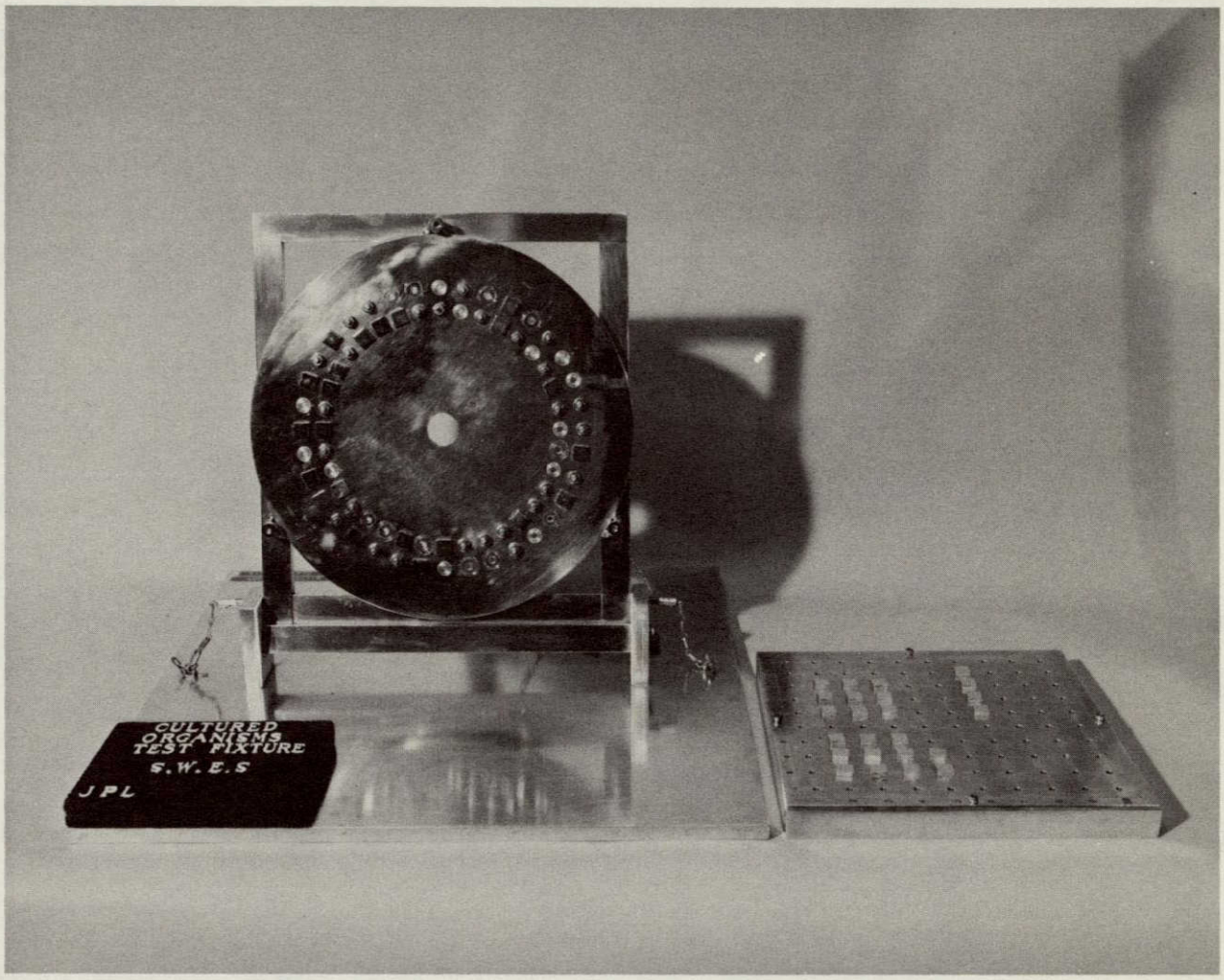

Fig. 2-B.5. Cultured organism test fixture

After the test exposure, the fixture was assayed in a rapid, consistent manner. Stages were removed from the fixture, placed individually into tubes containing 10 ml of 0. 1% sterile peptone water, and exposed to ultrasonic treatment (25 kHz for 12 min) in an ultrasonic bath. Upon removal from the bath the tube contents were thoroughly mixed prior to 10-fold serial 1. 0 ml dilutions and triplicate 1. 0 ml platings of designated dilutions with TSA. The organisms were incubated at 37° C for 48 hours under dark conditions.

3. Microbiological Data. Dilution plates with 30 to 300 colony forming units (CFU) were enumerated for survivors after the incubation period. Survival fractions were computed by ratioing the bacterial population recovered from the exposed stages to that from the "dark" side stages (controls). These populations were expressed as geometric means.

The resultant survival fractions for the eight preliminary runs with BSN are given in Table 2-B. 1, as well as a predictive model based on Ref. 1 and previously presented at the San Francisco 1974 Seminar (Ref. 2). The data exhibited here are consistently more sensitive (lower survival fractions) than the predictions. Perhaps the BSN are more sensitive than the Bacillus subtilis (Marburg strain) of Reference 1.

2. 2. 4 Future Activities

In the immediate future, the formal test program for cultured organisms will be conducted.

A plan is currently in the formative stage for a naturally occurring population study. A test fixture such as employed in the Solar Electromagnetic Radiation subtask (Ref. 3) may be used.

2. 2. 5 Presentations

Barengoltz, J., "Effect of Solar Wind Radiation on Microorganisms", presented at NASA Spacecraft Technology Seminar, San Francisco, Calif. February, 1974.

Table 2-B. 1. Preliminary Data For BSN

Run No.	Energy (keV)	Fluence (e/cm^2)	Survival Fraction (2σ Range†)	Prediction
1	1.5	10^{14}	0.041 (0.014-0.12)	0.16
5	1.5	10^{14}	0.037 (0.015-0.092)	0.16
2	1.5	5×10^{14}	0.0049 (0.0025-0.0097)	0.065
6	1.5	5×10^{14}	0.0058 (0.0029-0.012)	0.065
3	4.5	5×10^{11}	0.020 (0.011-0.035)	0.19
7	4.5	5×10^{11}	0.026 (0.012-0.059)	0.19
4	4.5	2×10^{12}	0.0025 (0.0011-0.0059)	0.0013
8	4.5	2×10^{12}	0.0020 (0.0012-0.0034)	0.0013

†Variation within an experimental run due to beam inhomogeneity, sample clumping, and sample innoculation.

2.2.6 References

1. Davis, M., Arch. Biochem. and Biophys. 48, pp. 469-481 (1954).
2. Barengoltz, J., "Effect of Solar Wind Radiation on Microorganisms," presented at NASA Spacecraft Technology Seminar, San Francisco, California, February, 1974 (unpublished).
3. Planetary Quarantine Semi-Annual Review, Space Research and Technology, 1 January - 30 June 1974, JPL Doc. 900-675, pp. 2-13 and 14 (1974).

2.3 EFFECT OF SPACE VACUUM ON MICROORGANISMS

2.3.1 Subtask C Introduction

This study was designed to examine the combined effects of space vacuum and spacecraft temperatures on the survival of microorganisms. The scope of study has changed slightly to incorporate higher temperatures that may be experienced by the Viking solar panels into the test matrix.

2.3.2 Significant Accomplishments

Extensive refurbishment of existing vacuum temperature equipment was completed. The refurbished equipment will be used in subsequent vacuum temperature tests involving naturally occurring (uncultured) microbial populations. Heater elements were incorporated into the fallout strips that will be used to collect naturally occurring microbial propulations from spacecraft assembly areas. A test fixture was designed and fabricated to hold the fallout strips. Additional effort was involved with thermocouple and heater rewiring of the equipment.

2.3.3 Future Activities

Future activities of the vacuum temperature task will be to conduct equipment check test runs. Upon successful completion of the engineering tests, the thermal vacuum resistance of naturally occurring microbial population present in spacecraft assembly areas will be investigated.

2.3.4 Presentations

None

2.4 PROBABILITY OF GROWTH IN PLANETARY ATMOSPHERES AND SATELLITES

2.4.1 Subtask D Introduction

The objectives of this subtask are to relate environmental parameters affecting microbial growth to conditions present in the atmospheres of Jupiter and Saturn, and to identify and study satellites of Jupiter and Saturn having possible biological interest.

2.4.2 Significant Accomplishments

2.4.2.1 Jupiter Atmosphere Study. During this period a contract was established to conduct a study of the structure and dynamics of the Jovian atmosphere. The principal investigator is Dr. Andrew P. Ingersoll of the California Institute of Technology. The objective of this task is to provide a quantitative, state-of-the-art model of Jupiter's atmosphere considering recent observations, particularly those of Pioneers-10 and -11. The study will include the application of the model to the determination of aerosol mixing and transport properties within and between different regions of the atmosphere over a range of particle characteristics for the purpose of evaluating survival and growth probabilities for anaerobic organisms. The numerical results will include temperature, pressure, density, chemical composition, scale heights, horizontal and vertical wind speeds, turbulence and convection cell sizes, circulation times, and transport proprieties as functions of altitude and latitude. Estimates of possible ranges of values for these quantities will be provided and all values will be consistent with observations.

This numerical model will be the first application of the Pioneer data to a comprehensive analysis of the Jovian atmosphere and should lead to a reduction of the uncertainties in Pg estimates for Jupiter.

The principal results will be available as follows:

1) 30 June 1975, Status Report.

2) 30 August, 1975, Outline of Major Results.

3) 31 October 1975, Preliminary draft of final report.

4) 31 December 1975, Final Report.

2.4.3 Future Activities

As the results of the Jovian Atmosphere study become available, the first-order effort will be to apply the results to the problem of assessing growth probabilities for Jupiter. Also, as the study progresses, most of the results will be in a publishable form and will appear in appropriate Journals.

Another promising area for future activity involves an evaluation of the Pioneer 10 and 11 radio-occultation observations. These observations which have, for other planetary missions, yielded highly significant atmospheric temperature and pressure measurements, produced results which, when applied to the structure of Jupiter's atmosphere, give values which conflict with those from infrared and microwave observations. Consideration should be given to establishing a contract which would evaluate the relationship of the radio-occultation measurements to the small scale turbulent structure of Jupiter's atmosphere.

2.4.4 Presentations

None

2.5 EFFECT OF SOLAR ELECTROMAGNETIC RADIATION ON MICROORGANISMS

2.5.1 Subtask E Introduction

The objective of this task is to estimate the effect of solar electromagnetic radiation (SER) on the survival of microbial populations in a space environment. Efforts will be addressed to the investigation of the photobiological effect of SER in a fashion that permits direct transference of the results to considerations of planetary quarantine. Such information will enable the updating of probability constants in the assessment of applicable planetary quarantine constraints for a mission.

2.5.2 Approach

In line with the objective of this task, the initial approach will involve the subjection of test species to SER in a manner that will yield interpretive data on the response of spacecraft biocontaminants to the SER of space. Primarily, this will entail the high vacuum irradiation of microorganisms with broad spectrum SER (far ultraviolet to infrared).

The first stage of experimentation has involved the testing of pure cultured species to study the effect of SER under different dose, dose rate and temperature conditions. Seven isolates (5 sporeformers and 2 nonsporeformers) from Mariner Mars 1971, Staphylococcus epidermidis and spores of Bacillus subtilis var. niger were tested as pure cultures. Irradiation was conducted at solar constants* (dose rates) of 0.1, 0.5 and 1.0 sun with temperatures at irradiation of -125, -15 and +70°C, respectively. These conditions respectively correspond to representative near Jupiter, Mars and Earth environments. In order to obtain survivor curves, organisms were exposed to varying doses for each temperature-dose rate condition.

*For this task, 1.0 solar constant is defined as a beam intensity, at the plane of irradiance, of 0.54 $mWcm^{-2}$ in the wavelength interval from 200 to 270 nanometers.

The second stage of experimentation has been directed towards the testing of naturally occurring microbial populations. The populations are collected on Viking-type solar cell fixtures (Fig. 2-E.1) and exposed to SER in a natural state; i.e., no laboratory treatment of the organisms is instituted prior to their testing. As with the axenic cultures, dose, dose rate and temperature are imposed as experimental variables. The temperatures to be studied (-15° C and +65° C) are those expected to nominally occur on the sun side of the Viking solar panels (see JPL-PQ Semi Annual, Sept. 30, 1974, p. 2-15).

Work to date comprises pure culture tests at 0.1, 0.5 and 1.0 sun and naturally occurring population tests at 0.5 sun, +65°C.

2.5.3 Significant Accomplishments

2.5.3.1 Solar Electromagnetic Radiation Test System. A complete account of the solar electromagnetic test system is given in the JPL-PQ Semi Annual, Sept. 30, 1974.

2.5.3.2 Naturally Occurring Population Test Fixture. The solar cell fixture for naturally occurring population collection is shown in Fig. 2-E.1. The fixture was composed of a 6061 aluminum base plate, 35.56 cm square and 0.635 cm thick, to which solar cells were attached. Kapton film heaters, 34.29 cm square, were bonded to the backside (nonirradiated side) of the plate and painted black. To the front of the base plate were attached 9, 10.16 cm square, 0.318 cm thick, 6061 aluminum pieces to which were bonded Viking-type solar cells. The configuration of the solar cells, as bonded to the squares, was identical to that of their functional mode; i.e., electrical connection, spacing and topography were duplicated.

Five thermocouples were attached to the backside of the plate to monitor and profile temperature. Temperature control was ±2° C.

2.5.3.3 Experimental Activities.

1. Pure cultured organisms. A complete account of the preparation, irradiation and assay of pure cultured organisms is given in the JPL-PQ Semi Annual, Sept. 30, 1974.

2. Collection of Naturally Occurring Microorganisms. Eighteen, 10.16 cm square, sterile, solar cell fixtures were placed onto a 35.56 × 71.12 cm aluminum tray positioned 1 m above the floor. The placement of the fixtures on the tray was per a random scheme.

After 5 to 7 days of exposure the fixtures were picked up with sterile forceps and loaded onto two aluminum base plates (nine per plate). Twelve stainless steel screws, each torqued to 15 in-lbs, held each fixture to the base plate. Upon completion of base plate loading, one plate was removed to the SER test facility and one (control), to the microbiology laboratory.

3. Irradiation of Naturally Occurring Microorganisms. Upon arrival at the SER facility, the base plate (with solar cells attached) was mounted on a support frame within the vacuum chamber (Fig. 2-E.2). The frame was situated on a track that enabled placement of the test fixture exactly 1.37 m from the point of entry of the light beam into the vacuum chamber.

The five thermocouple leads (from the backside (darkside) of the plate) were then connected to a recorder that provided continous readout of the fixture temperature throughout the test. (Engineering tests were run to map the temperature profile of the frontside (sunside) of the fixture as a function of backside readouts.)

Once the fixture had equilibrated to the required temperature under a vacuum of approximately 2×10^{-6} torr, the samples were irradiated. (The vacuum cycle and SER protocol were as previously described for pure cultured organism tests.) Following irradiation, the test fixture was removed to the microbiology laboratory for assay.

4. Assay of Naturally Occurring Microorganisms. Solar cell fixtures were unscrewed from the base plate and placed (solar cell surface facing downward) into crystalline beakers (one per beaker) containing 100 ml of 0.1% peptone water and exposed to ultrasonic bath treatment (25 KHz for 2 min). Upon removal from the bath, the beaker contents were thoroughly mixed prior to plating of aliquots with TSA. A fraction of the immersion fluid was heat shocked by placing an aliquot into a test tube and exposing the tube to 80°C for 18 minutes in a water bath, followed by cooling in an ice water

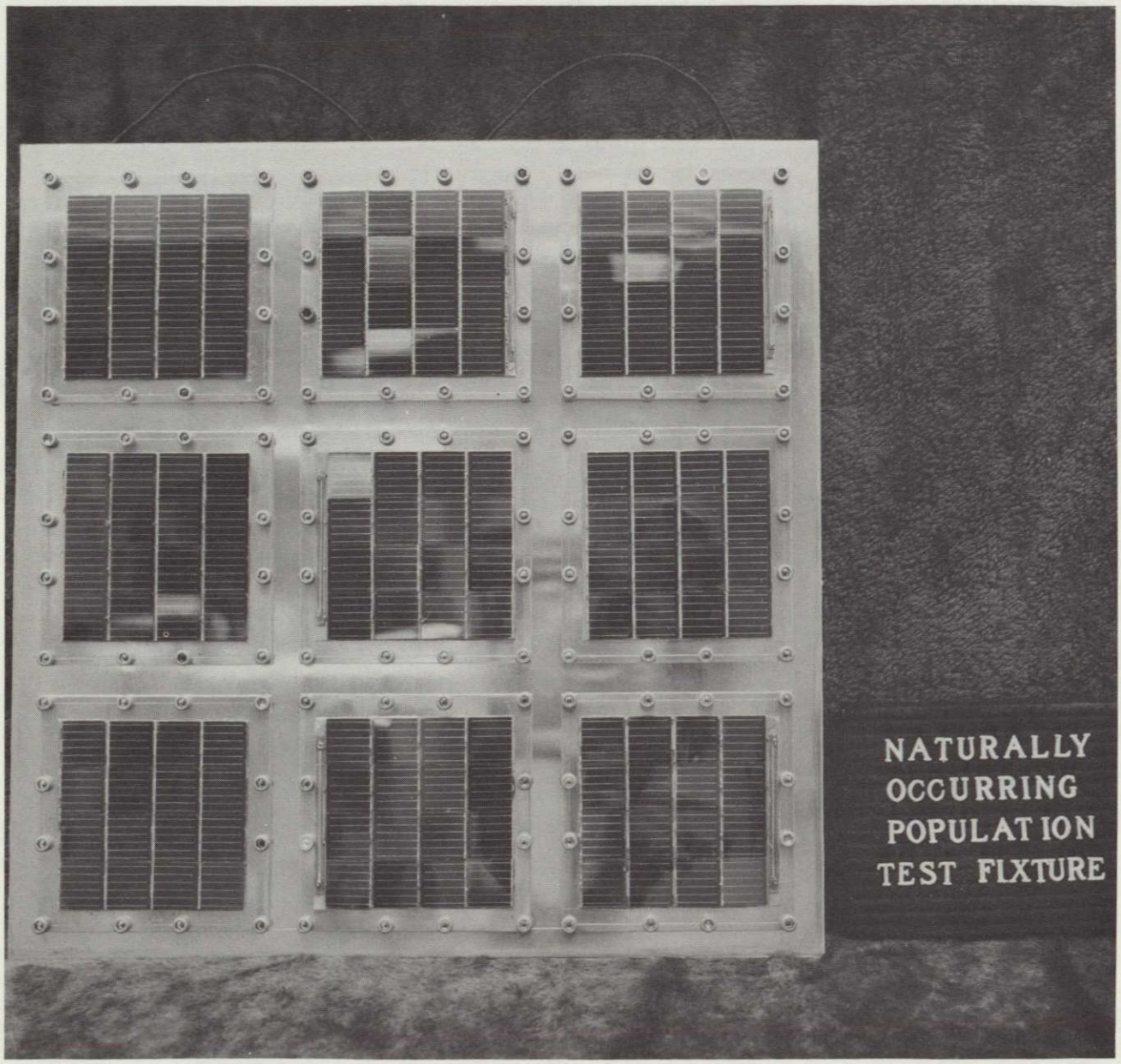

Fig. 2-E.1. Solar cell fixture for naturally occurring population collection

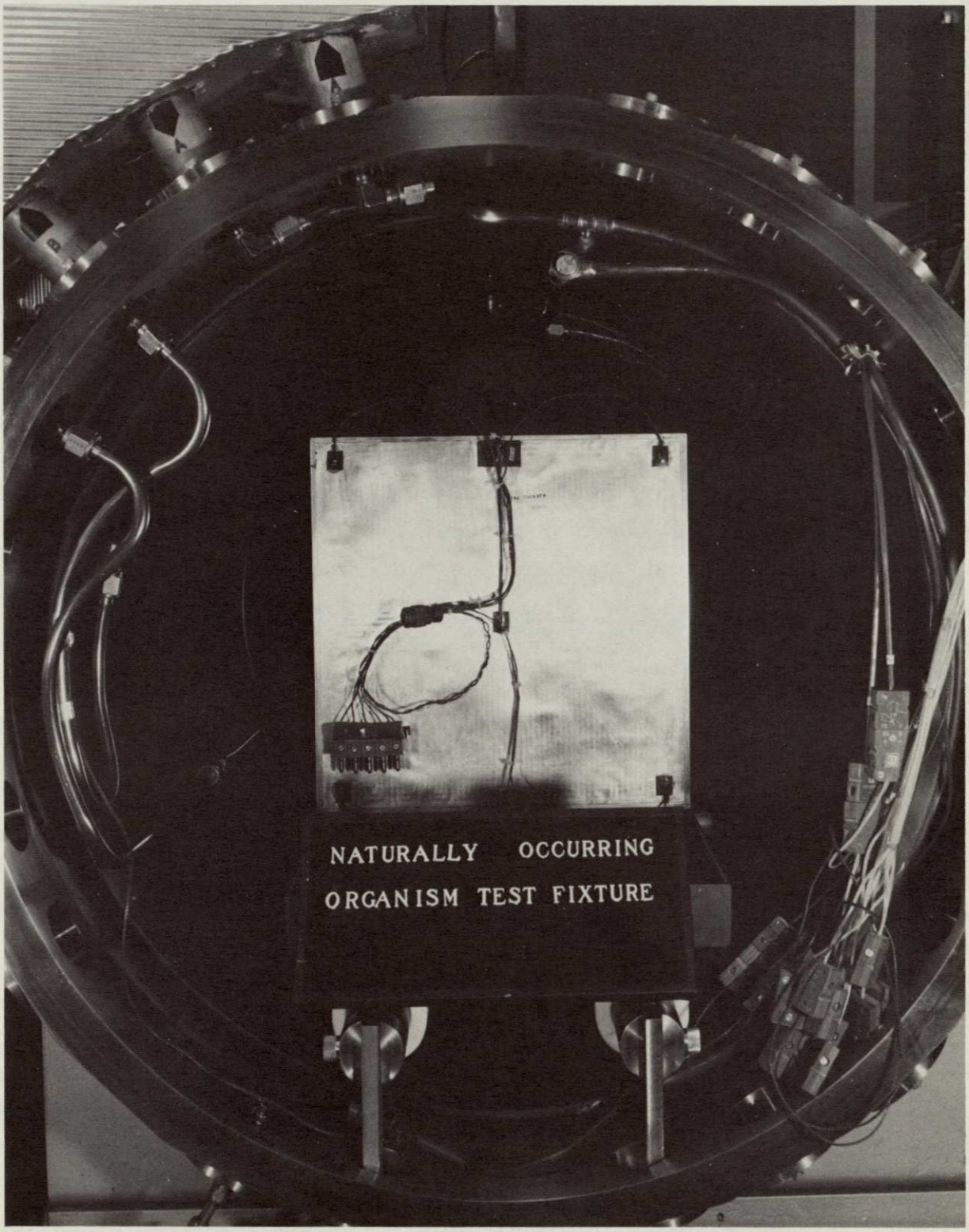

Fig. 2-E.2. Naturally occurring population fixture mounted in vacuum chamber (nonirradiated side showing with unpainted film heaters)

bath prior to TSA pour plate formation. After plates were formed they were overlayed with agar to help control spreaders. Plates were dark incubated at 32° C for 72 hours.

5. Microbiological Data. Studies of the effect of SER on pure cultured microorganisms were conducted by irradiating populations at dose rates of 0.1, 0.5 and 1.0 sun under temperature conditions of -125, -15 and +70° C, respectively. The results of these studies are shown in Figures 2-E.3, 2-E.4, and 2-E.5.

In the majority of cases, spore populations exhibited a greater resistance to the SER conditions imposed than did nonsporeformers. However, for both population types the major inactivation effect was seen within the first 2,000 ergs mm^{-2} of irradiation. Thereafter, a much more gradual slope was generally observed in the survivor curves. Two of the nonsporeformers, Micrococcus (Type II) and S. epidermidis, were inactivated at very low doses and these data are not shown. Micrococcus (Type VI) exhibited a percent survival on the order of 10^{-3} at 8,000 ergs mm^{-2}, 0.1 sun; and at 6 and 8,000 ergs mm^{-2}, 1.0 sun. (10^{-3} percent survival was considered the "zero" point on the survivor curves based on an inoculum level of approximately 10^6 colony forming units per stage.) Micrococcus (Type VI) evidenced a 10^{-2} percent survival at the highest 0.5 sun dose: 4,000 ergs mm^{-2}. Spore populations survived at the 8 and 4 x 10^{-2} levels respectively for the highest 0.1 and 0.5 sun doses (8 and 4,000 ergs mm^{-2} respectively), and at the 5 x 10^{-3} level for 1.0 sun (8,000 ergs mm^{-2}).

As pointed out in the last semi-annual report, the seeming inability to significantly reduce some of the test populations beyond a certain level, irrespective of dose, points to the possibility that a fraction of the population surviving irradiation was in fact shielded from the lethal spectra by organisms, and/or, nonviable impurities on the inoculated stages. Scanning electron micrographs seemed to support this hypothesis. This factor quite possibly added to the degree of dispersion exhibited by the data. On occasion, replicate tests for certain organisms showed significantly different percents survival which were most likely explainable as a function of random clumping-shielding events leading to the protection of significant fractions of the population from the SER.

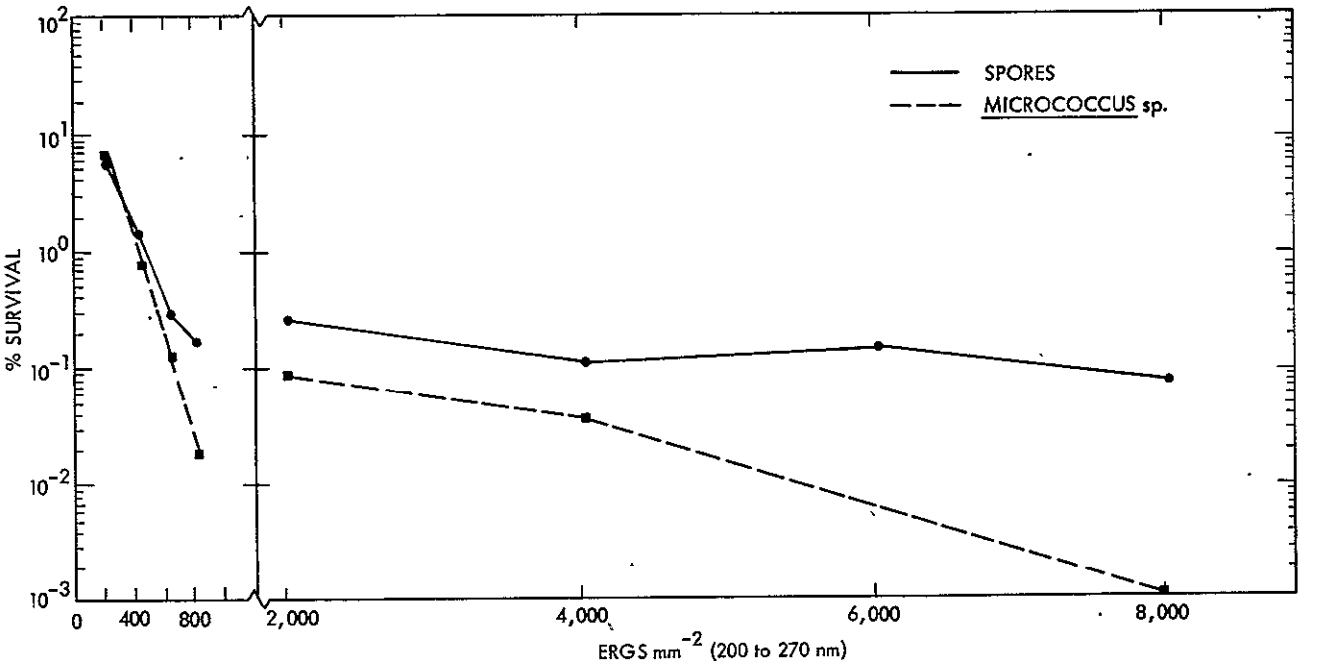

Fig. 2-E. 3. Effect of SER at 0.1 Sun, -125° C

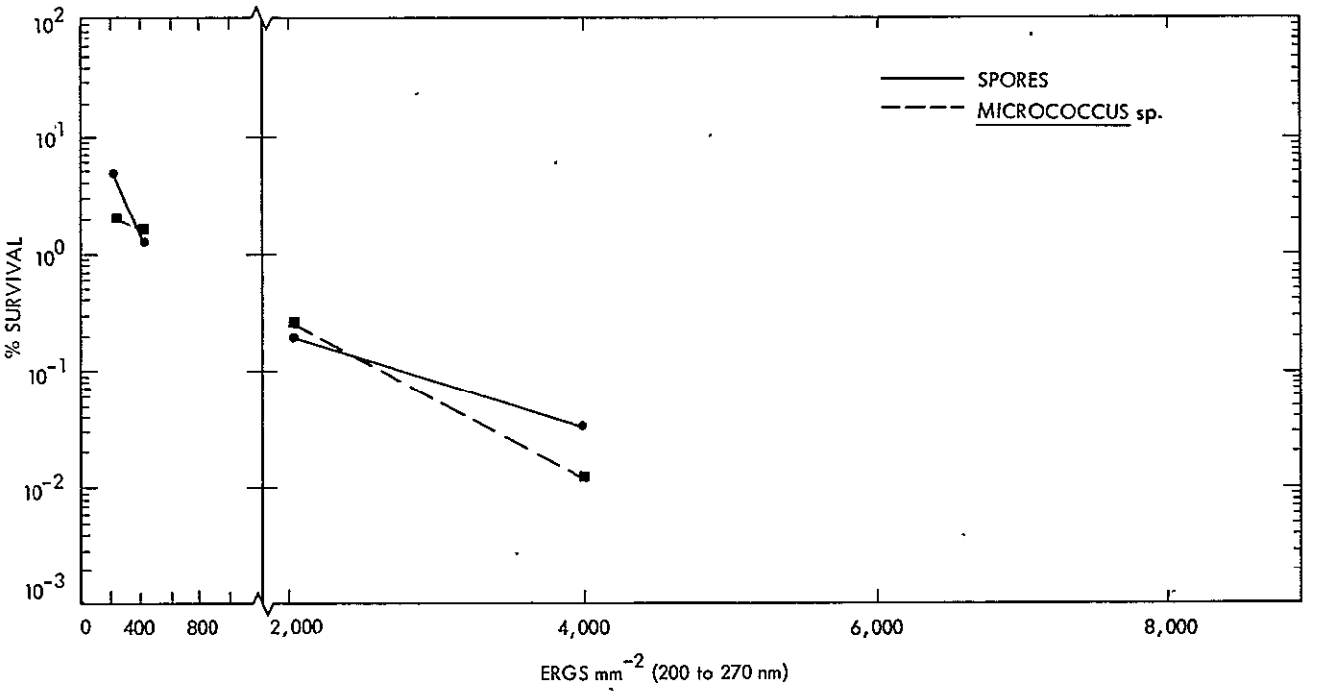

Fig. 2-E. 4. Effect of SER at 0.5 Sun, -15° C

Figure 2-E.6 shows the results of initial testing of the resistance of naturally occurring microorganisms to SER at 0.5 sun, +65° C conditions. The comparison of these data to those obtained from pure cultured organisms is quite interesting. As with the pure cultured tests, the major drop in the number of survivors occurred within the first 2000 ergs mm^{-2} of exposure. Most interesting was the fact that an increase in the dosage from 8,000 up to 80,000 ergs mm^{-2} produced no significant reduction in the percent survival. A number of the pure cultured studies indicated the possibility of a comparable situation, but were not carried beyond 8,000 ergs mm^{-2}.

The magnitude of the surviving fraction of naturally occurring microorganisms at high doses was much greater than could be demonstrated for pure cultures. The data indicate an average percent survival of 7 for naturally occurring organisms exposed to SER doses of 8,000 to 80,000 as compared to 8×10^{-2} to 5×10^{-3} for pure cultured spore populations exposed to 8,000 ergs mm^{-2}.

2.5.4 Future Activities

Additional work will be conducted to further define and statistically evaluate the resistance of pure cultured and naturally occurring microorganisms to SER as a function of dose, dose rate and temperature. Collateral experimentation will be initiated to define the effect of viable and nonviable particulate shielding on survival. In addition, studies will be conducted on the photoreactivability of naturally occurring microbial populations.

2.5.5 References

None

2.5.6 Presentations and Publications

Wardle, M. D., "Effect of Solar Electromagnetic Radiation on Microorganisms," presented at the NASA Spacecraft Sterilization Technology Seminar, Cocoa Beach, Florida, December, 1974.

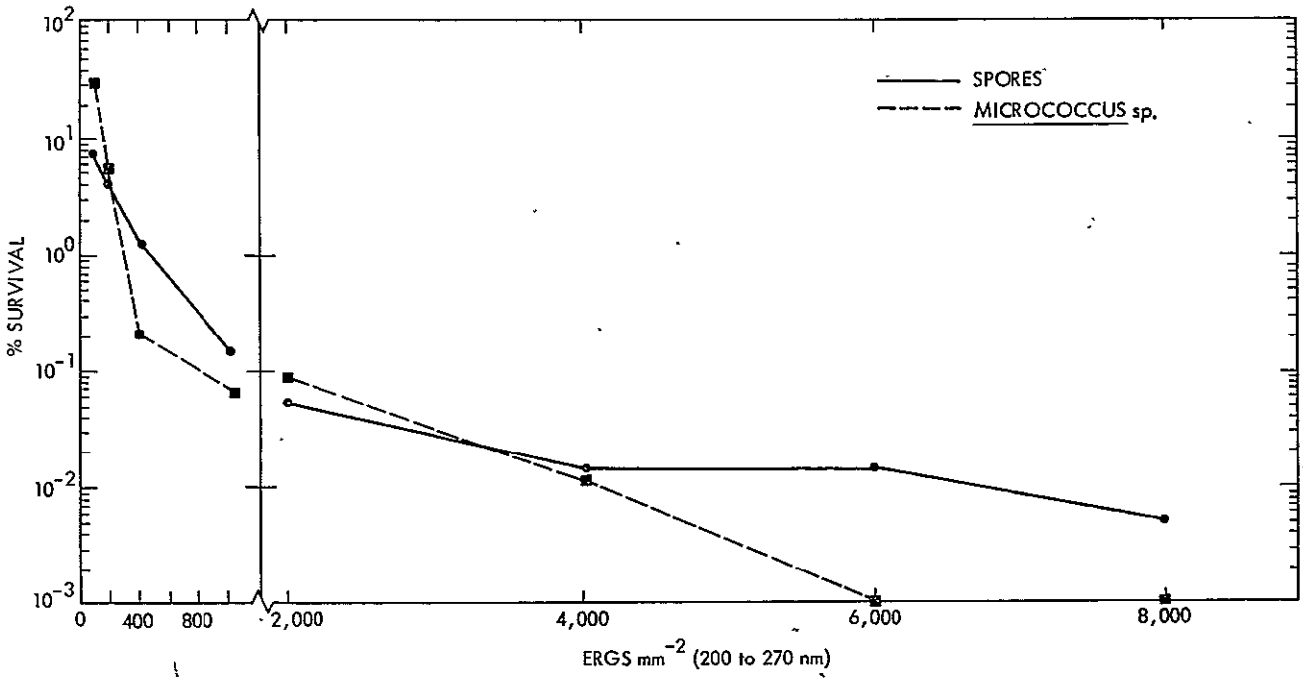

Fig. 2-E. 5. Effect of SER at 1.0 Sun, +70°C

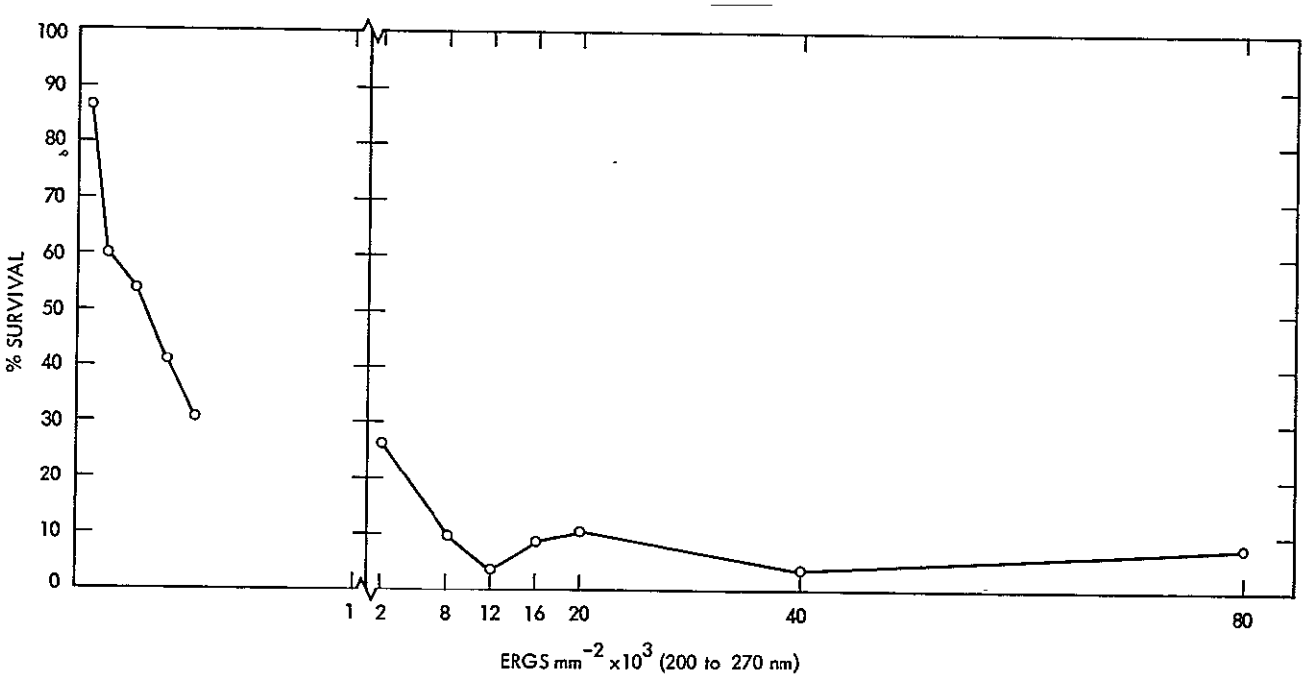

Fig. 2-E. 6. Effect of SER at 0.5 Sun, +65°C on naturally occurring microorganisms (not heat shocked)

SECTION III

POST LAUNCH RECONTAMINATION STUDIES
(NASA No. 193-58-62-03)

Contents	Title and Related Personnel
Subtask A para. 3.1	POST LAUNCH RECONTAMINATION STUDIES
	Cognizance: J. Barengoltz
	Associate Personnel: D. Edgars (Bionetics)

PRECEDING PAGE BLANK NOT FILMED

3.1 POST LAUNCH RECONTAMINATION STUDIES

3.1.1 Subtask A Introduction

The objective of the task is the development of an analytical technique for the evaluation of the probability of the relocation of particles from nonsterile to sterile areas on a spacecraft. The recontamination process is important for all multiple missions with separate microbiological burden allocations for various major spacecraft systems, and critical for life detection experiments that risk contamination from nonsterile components.

The approach has been to study the effects of typical mission environments on the redistribution of particles on spacecraft surfaces both analytically and experimentally. This study consists of three logical components, which have been reflected in the effort: (1) particle adhesion, (2) dynamic release mechanisms, and (3) particle transport. The effort in particle adhesion has been principally a particle release experiment, together with analytical work and attempts to correlate other data found in the literature and elsewhere. Under dynamic release mechanisms, meteoroid impact and pyro firing have been modeled. The particle transport activity is an analytical effort which includes the development of codes for spacecraft geometry and orientation, forces acting on released particles, and trajectory.

Finally all of these components were to be assembled into an operational, integrated computer code. For a demonstration calculation with this computer code, a geometrical model based on a Viking-type spacecraft and the spaceflight phase between Earth orbit and Mars encounter were chosen.

3.1.2 Significant Accomplishments

During this report period a final form of the electrostatic force was developed, comparative calculations of the meteoroid impact/particle release code were performed, and the final demonstration calculation for the spaceflight phase of a Viking-type orbiter/lander spacecraft was completed.

A summary discussion of the meteoroid impact model and the particle adhesion model may be found in Ref. 1.

3.1.2.1 Electrostatic Force: The electrostatic force acting on a particle is equal to its electrical charge times the electric field acting on it. The charge is due to the effect of charged particle impingement and sunlight; the field (of the spacecraft) arises in an analogous manner.

The description of the charge state of an illuminated particle has been completed and reported previously (Ref. 1). Since then the case of a shaded particle, also discussed in Ref. 1, has been calculated and is shown in Fig. 3-A.1.

A one-dimensional electric field has been developed and reported previously (Ref. 2). During this report period a computer code was written which approximates the real electric field by the one-dimensional solution for the near case (within an effective Debye length). In the far-field case, the electric field due to an equivalent sphere of an area-averaged surface charge and an area-averaged effective Debye length is employed. A wake region in the anti-sun direction is also modeled (Ref. 1). A spacecraft outline with the conventional sense of the electric field, as well as the far-field analytical form, is shown in Fig. 3-A-2.

3.1.2.2 Calculations with Meteoroid Impact/Particle Release Code. Comparisons of calculations of particle release due to meteoroid impact by the YANG1/RELEAS code with the results of experimental simulations have been performed previously in terms of removal fractions (Ref. 1). Recently a report on removal velocities has been published (Ref. 3). A comparison of the YANG1/RELEAS code with the results of this independent experimental study is favorable (Figs. 3-A.3 and 4). The apparent disagreement in Fig. 3-A.4 of the velocity distributions is due to an unfair comparison. The experimental results are for a very restricted seeded area at a fixed distance from the impact locus and show a sharp distribution. The analytical results of the model show the broad distribution resulting from the integration of particles released at all ranges, including very low velocity events at large ranges. A more detailed comparison indicates reasonable agreement for the restricted range case. The recontamination study requires, in fact, the velocity distribution of all particles of a given size dislodged anywhere by a meteoroid impact.

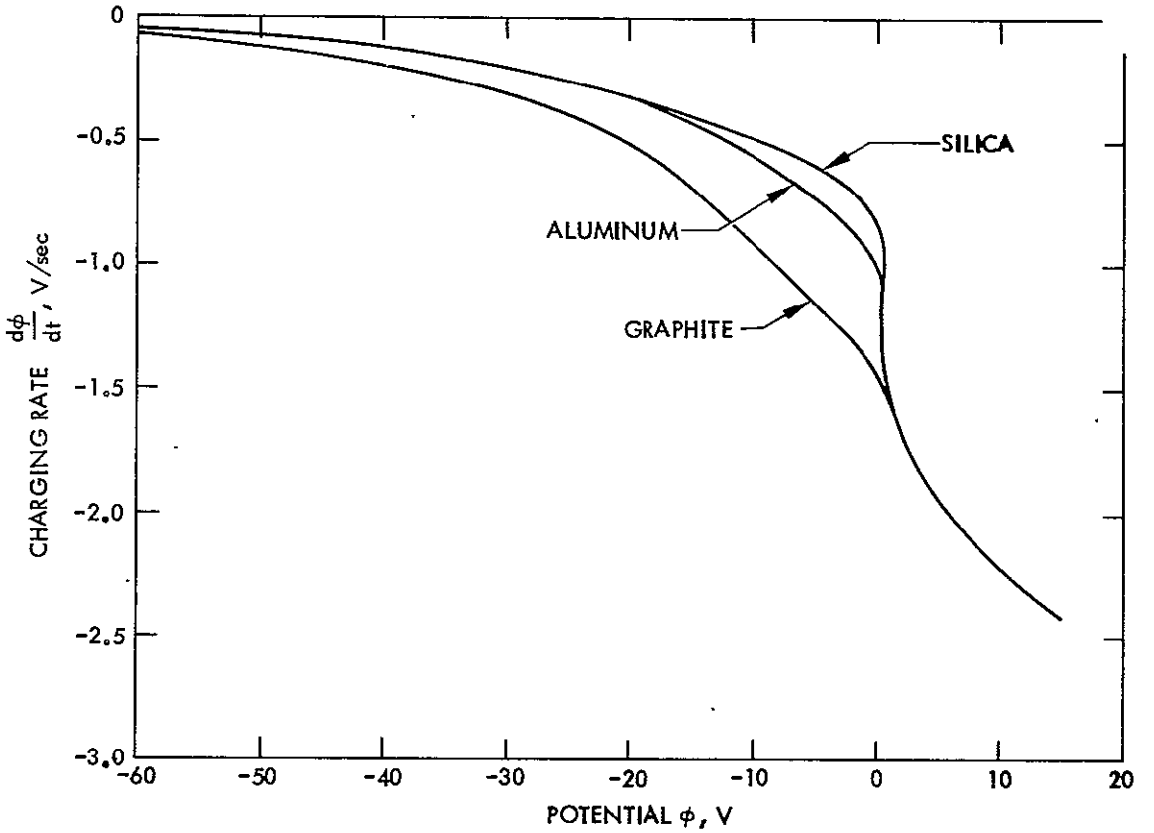

Fig. 3-A. 1. Grain charging in shade

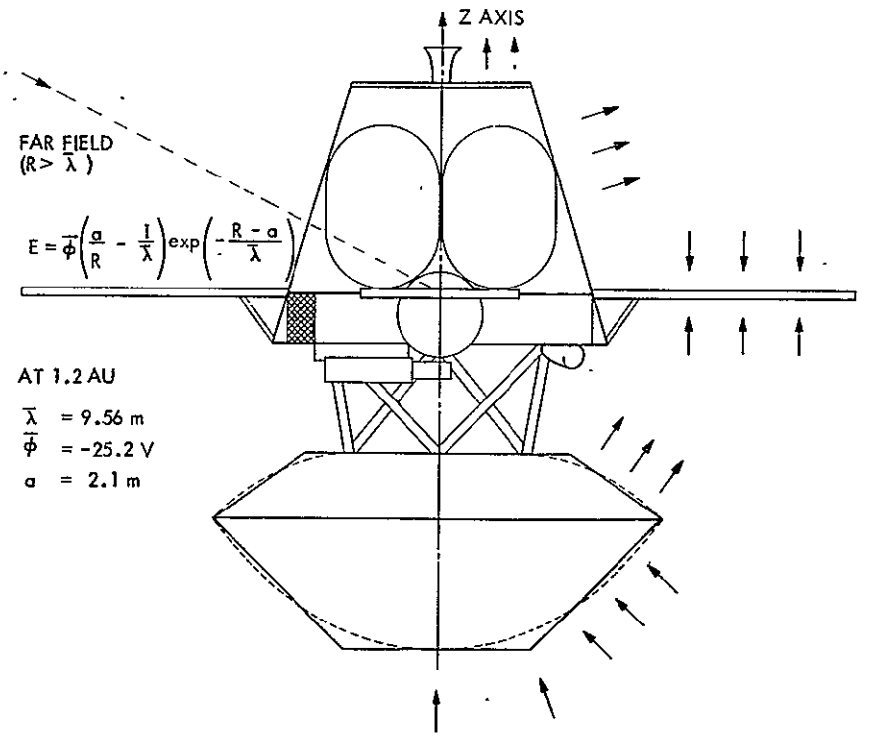

Fig. 3-A. 2. Electric field

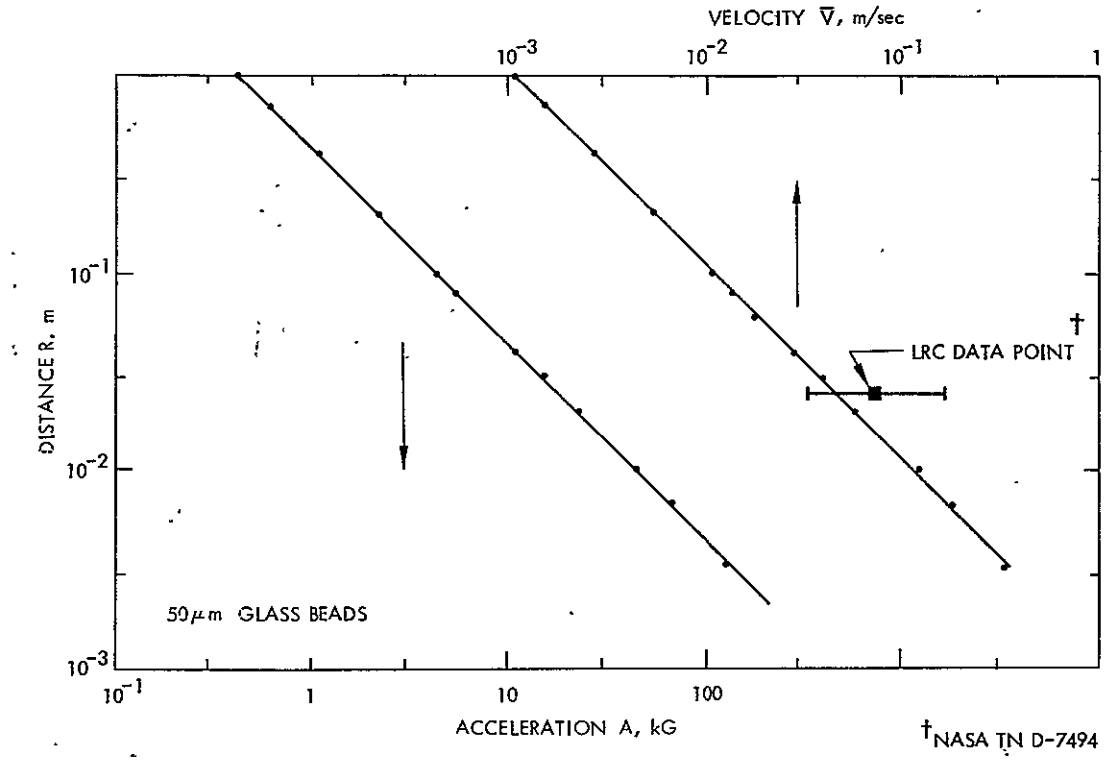

Fig. 3-A.3. Recontamination simulation of LRC run 6

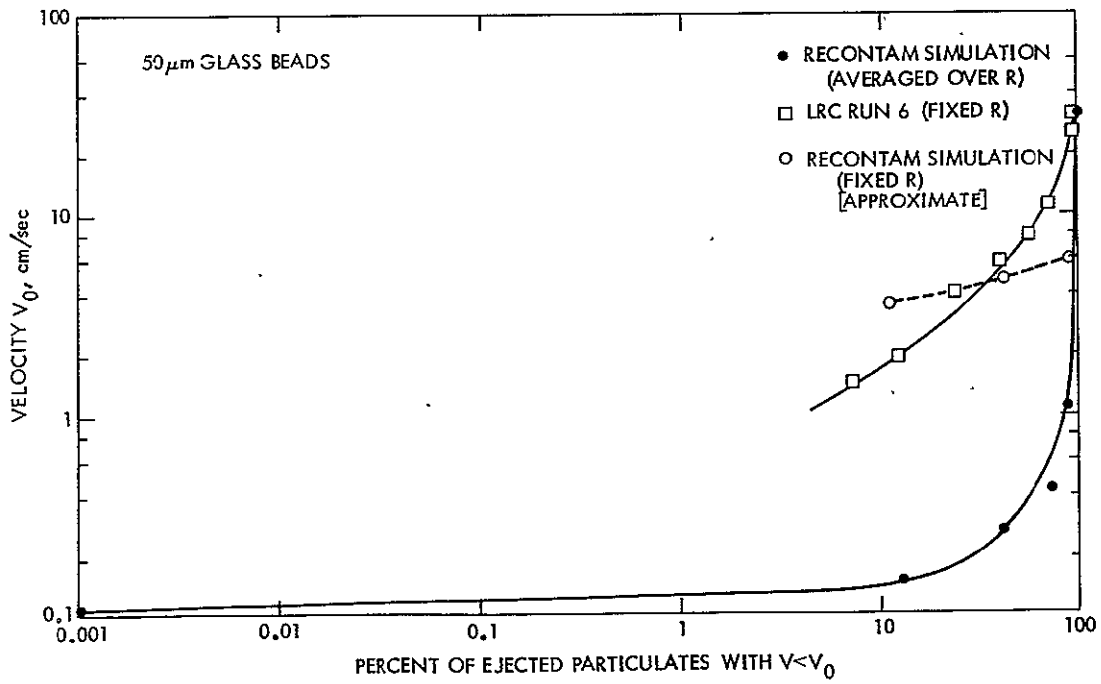

Fig. 3-A.4. Release velocity distribution

3.1.2.3 Spaceflight Recontamination Code. The logic and flowchart of the integrated computer code has been reported (Ref. 4). Several changes have been made since that report in order to produce a code which could be run in a reasonable duration on the computer. Instead of an inner Monte Carlo loop on impact location, released grain size and released grain velocity, only the impact location is randomly selected. The grain size and velocity are considered deterministically by a 10 × 10 group calculation (5 μm to 105 μm in 10 μm steps and an adaptive velocity grouping based on the calculated velocity distribution for the meteoroid impact under consideration). Similarly the outer Monte Carlo loop on meteoroid mass and velocity has been replaced by a 10 mass group × 3 velocity group calculation. In addition to a large computer time saving, this modification permitted a segmented approach to the total calculation. The first stage of the calculation consisted of executing the complete meteoroid-induced surface effects array and producing surface response data on computer cards. Then the balance of the computer calculation could be performed for several meteoroid groups at a time (or just one if desired). Finally the results for each meteoroid group appropriately weighted were summed to provide the total simulation of the entire meteoroid environment.

This approach also permits an easy identification of the important meteoroid events and estimations of the effect of modifying the meteoroid environment model.

3.1.2.4 Results of Calculation. The following quantities have been estimated by by a simulation of a 300 day spaceflight from Earth to Mars for a Viking-type spacecraft:

1) expected number of recontamination hits - particulates released from the orbiter and upper surfaces of the lander which strike the lower surfaces of the lander.

2) expected number of safe hits - particulates released from the orbiter and upper surfaces of the lander which strike other locations than the lower surfaces of the lander.

3) expected number of escapes - also in the form of a polar distribution of direction (orbiter-lander axis referenced)

4) average velocity of escapes.

The results for these quantities are summarized in Table 3-A. 1 for two meteoroid models and a pyro event simulation. The conservative model includes some high velocity impacts (groups 2 and 3) that would result from some choices of spacecraft trajectory. The other model represents a nominal trajectory selection by only low velocity impacts (group 1) in the range 1.2 to 2.0 $\times 10^4$ m/s (group velocity 1.6 $\times 10^4$ m/s). The directional distribution of the escapes is shown in Fig. 3-A. 5. Finally the meteoroid group model and the first three quantities listed above, as a function of meteoroid group, are displayed graphically in Figs. 3-A.6, 7, 8 and 9.

Table 3-A. 1. Summary of Results of Recontamination Analysis for Viking-type Spaceflight

	Conservative Meteoroid Velocity	Nominal Meteoroid Velocity	Pyro
Recontamination Hits	33	10	1
Safehits	21,215	7281	849
Escapes	126,778	34,349	35,000
Average Escape Velocity	1.15 m/s	0.69 m/s	1.94 m/s
Meteoroid Impacts	28,279	18,842	4
Pyro Events			

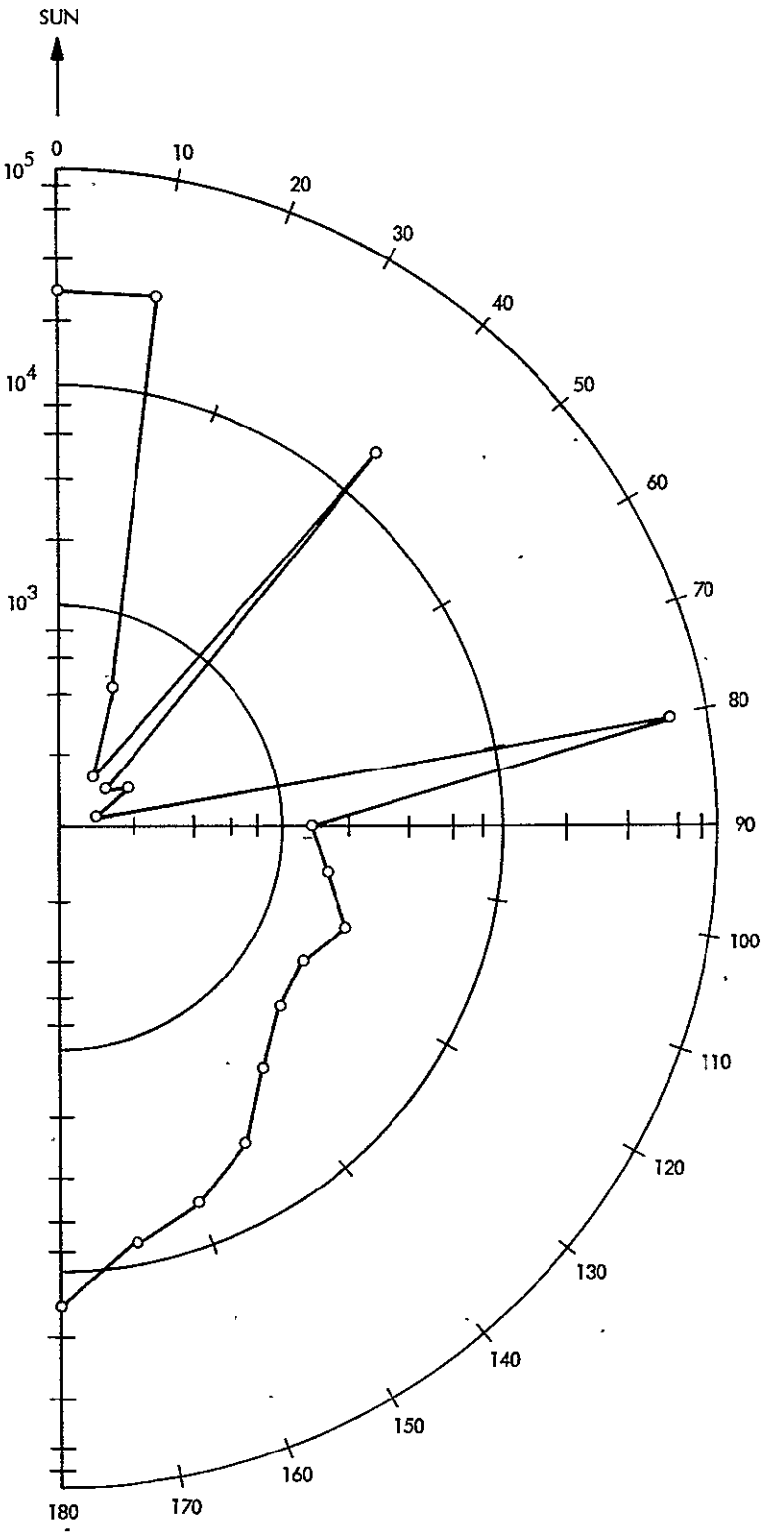

Fig. 3-A. 5. Angular distribution escaped grain direction

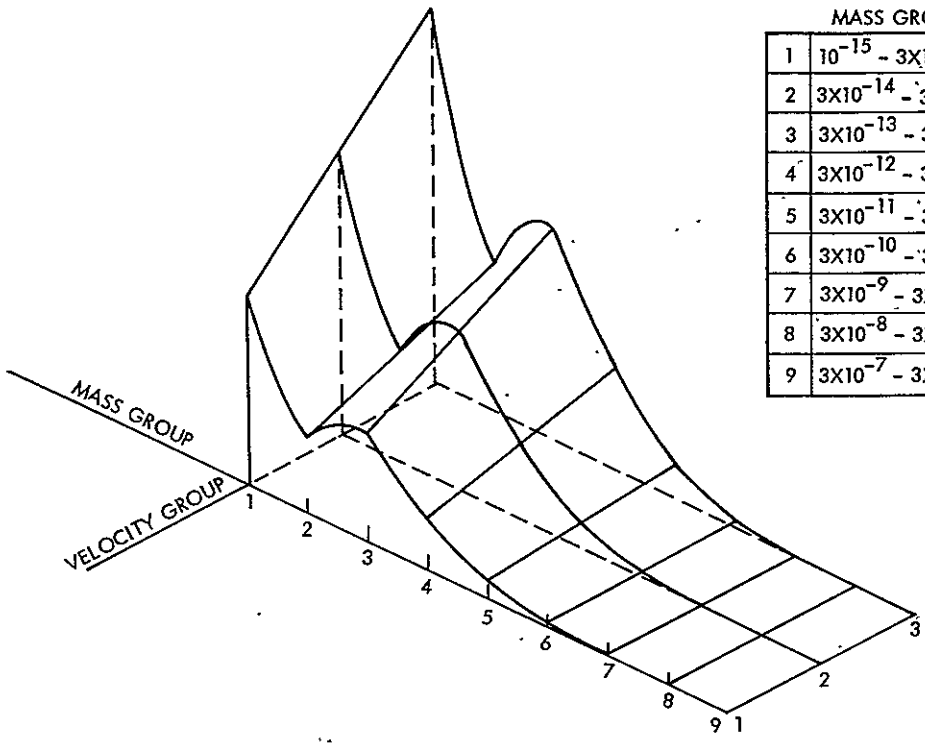

	MASS GROUPS		VELOCITY GROUPS
1	10^{-15} - $3X10^{-14}$ kg	1	1.2 - 2.0X10^4 m/s
2	$3X10^{-14}$ - $3X10^{-13}$ kg	2	2.0 - 2.8X10^4 m/s
3	$3X10^{-13}$ - $3X10^{-12}$ kg	3	2.8 - 3.6X10^4 m/s
4	$3X10^{-12}$ - $3X10^{-11}$ kg		
5	$3X10^{-11}$ - $3X10^{-10}$ kg		
6	$3X10^{-10}$ - $3X10^{-9}$ kg		
7	$3X10^{-9}$ - $3X10^{-8}$ kg		
8	$3X10^{-8}$ - $3X10^{-7}$ kg		
9	$3X10^{-7}$ - $3X10^{-6}$ kg		

Fig. 3-A.6. Mission micrometeoroid fluence distribution over mass and velocity groups

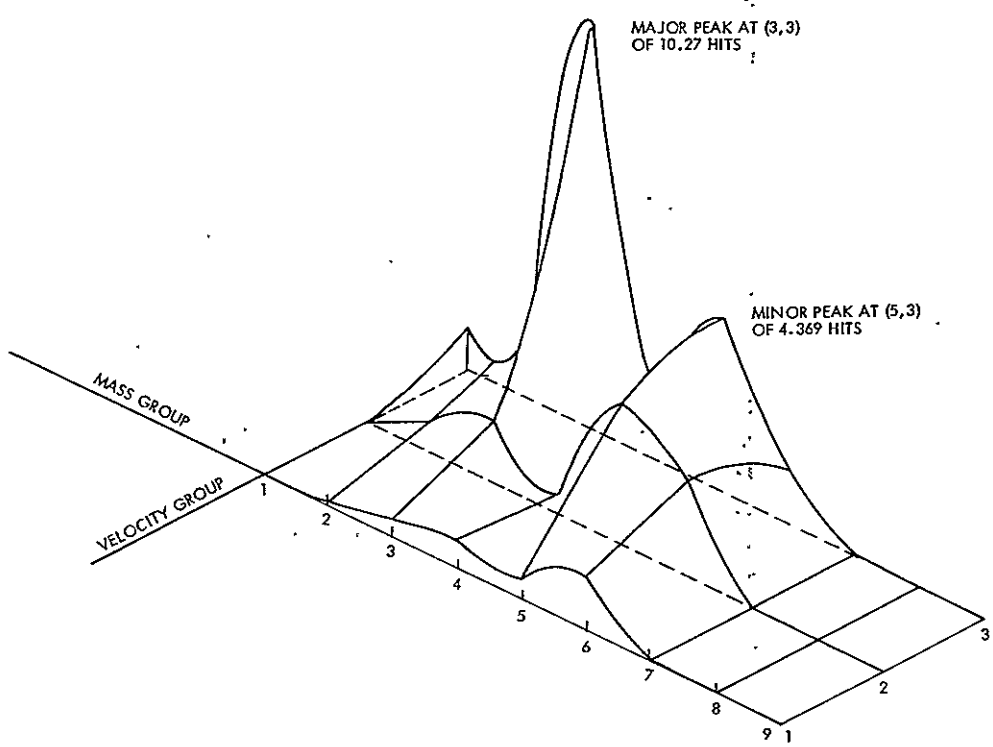

Fig. 3-A.7. Mission grain recontamination distribution over meteoroid mass and velocity groups

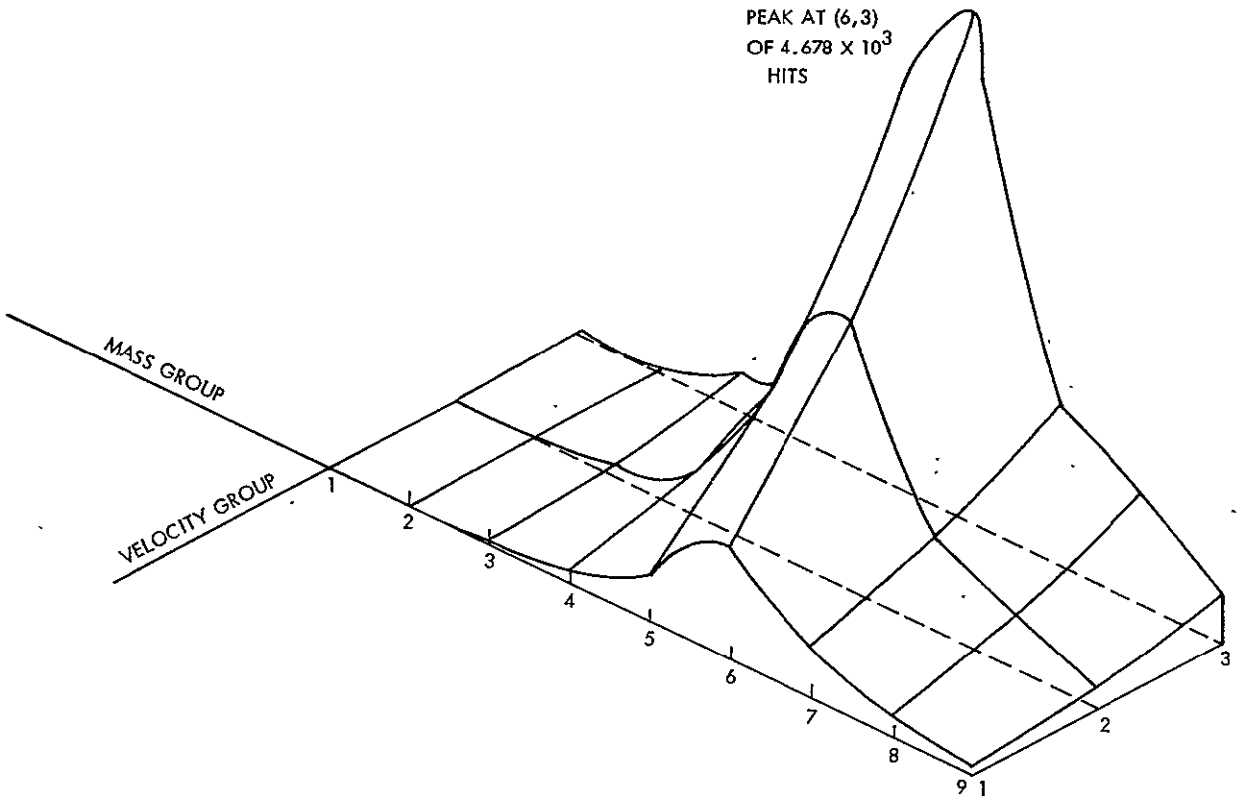

Fig. 3-A. 8. Mission safe-hit distribution over meteoroid mass and velocity groups

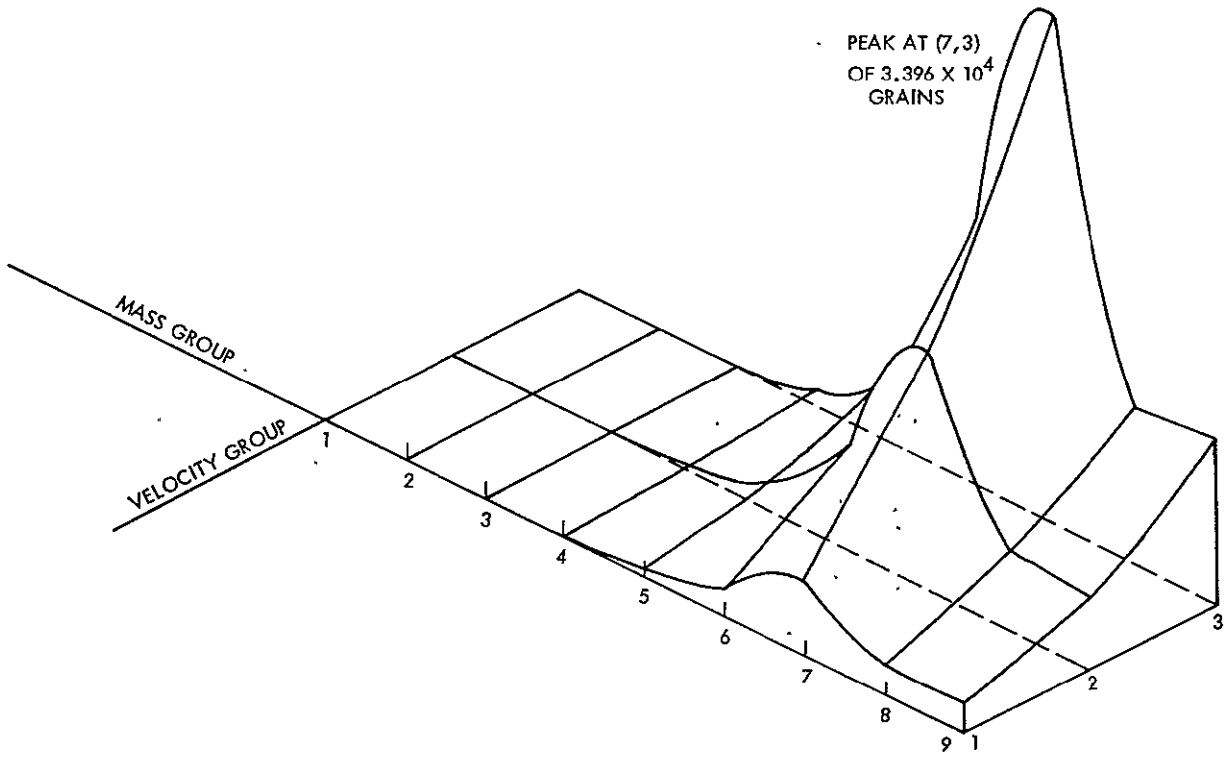

Fig. 3-A. 9. Mission grain escape distribution over meteoroid mass and velocity groups

3.1.3 Future Activities

A comprehensive final report on the spaceflight phase recontamination computer program and calculations is currently being prepared and will be available by June, 1975.

Two additional areas of concern will be investigated, particle adhesion as a function of ambient pressure in the range from 1 atmosphere to hard vacuum and the creation and release of particulates by abrasive mechanisms.

These technical areas reflect some of the needs for the new direction of the study, the STS shuttle-launched spacecraft recontamination study.

3.1.4 Presentations

Barentoltz, J., "Post Launch Recontamination Studies," presented at NASA Spacecraft Sterilization Technology Seminar, Cocoa Beach, Florida, December, 1974.

3.1.5 References

1. Planetary Quarantine Semi-Annual Review, Space Research and Technology, 1 July - 31 December 1973, JPL Doc. 900-655, p. 3-1 (1974).

2. Planetary Quarantine Semi-Annual Review, Space Research and Technology, 1 January - 30 June 1973, JPL Doc. 900-636, pp. 3-8 and 9 (1973).

3. Goad, J. H., Jr., DiBattista, J. D., Robinson, D. M., and Chu, W. P., "Removal of Spacecraft-Surface Particulate Contaminants by Simulated Micrometeoroid Impacts," NASA TN D-7494 (1974).

4. Planetary Quarantine Semi-Annual Review, Space Research and Technology, 1 January - 30 June 1974, JPL Doc. 900-675, p. 3-1 (1974).

SECTION IV

SPACECRAFT CLEANING AND DECONTAMINATION TECHNIQUES (NASA No. 193-58-63-02)

Contents	Title and Related Personnel	
Subtask A para. 4.1	PHYSICAL REMOVAL OF SPACECRAFT MICROBIAL BURDEN	
	Cognizance:	H. Schneider
	Associate Personnel:	W. Neiderheiser (Bionetics)
Subtask B para. 4.2	EVALUATION OF PLASMA CLEANING AND DECONTAMINATION TECHNIQUES	
	Cognizance:	S. Fraser (Boeing) D. Taylor
	Associate Personnel:	R. Olson (Boeing) W. Leavens (Boeing)
Subtask C para. 4.3	PQ CONSIDERATION FOR SHUTTLE LAUNCHED SPACECRAFT	
	Cognizance:	M. Christensen
	Associate Personnel:	R. Wingfield (Bionetics)

PRECEDING PAGE BLANK NOT FILMED

4.1 PHYSICAL REMOVAL OF SPACECRAFT MICROBIAL BURDEN

4.1.1 Subtask A Introduction

Present planetary quarantine constraints for flyby and orbiter vehicles require maintaining the microbial burden on the spacecraft below a certain critical level. State-of-the-art clean room facilities and contamination control techniques do not assure that this critical level can be maintained throughout necessary assembly and test operations.

Previous activities under this task concentrated on the study of vacuum techniques with and without the use of a brush, and on steady state as well as pulse blow cleaning techniques using extra dry, high-purity nitrogen. A test device was developed that would allow for the simulation and evaluation of these techniques under controllable conditions with an observation of the behavior of the test particulates under a 100X microscope. Studies to establish the mechanical properties of candidate brush-materials were conducted in the JPL materials test laboratory. As described in detail in JPL documents 900-597, 900-636, and 900-675, the following findings were made so far:

1) Brushes efficiently detach particles of the smallest discernible sizes (2-3 μm) but the flow resistance across the bristles is very high, the flow velocities near the surface are too low to accomplish entrainment and to transport detached particles into the vacuum system. Consequently, the brushes quickly become saturated with particles, and become a shedding source rather than a cleaning tool.

2) Vacuum flow alone efficiently detaches and removes particles larger than 10 μm if, a) the surface is dry, b) flow velocities are near critical (chocked flow) and, c) the nozzle stand-off distance from the surface is not larger than 150-200 μm. The removal efficiency drops off sharply at larger stand-off distances.

3) Blow cleaning efficiently removes particles greater than 5 μm from normally dry (i.e., 50% RH) surfaces at pressures of 30 psig across the blow nozzle. Pressures on the order of 50 to 80 psig are necessary to efficiently remove particulate matter smaller than 50 μm from oily (fingerprinted) surfaces.

4) A periodic blocking of the jet noticeably enhances removal efficiency (20-30%) where otherwise relatively low removal efficiencies (<50%) are achieved. Best results are obtained at blow pressures between 10 and 15 psig (just critical expansion), and at pulse frequencies below 50 Hz.

5) Jet deflection induced by blowing over wedges and oscillating rods did not improve detachment. Efficient (nearly 100%) removal of particulates of all sizes, however, could be produced by feeding liquid (isopropyl alcohol) through a hollow rod blown across its open end at pressures between 1 and 3 psig.

6) The application of ultrasonic techniques (Hartmann generator) in a synergistic mode with flow cleaning was negative, possibly because of insufficient power output of the existing apparatus (140 db max).

7) The cleaning of moist surfaces was very inefficient under all of the conditions tested.

8) Natural sable hair (presently in use for spacecraft cleaning) has a very low fatigue resistance and tends to break up during use. Dupont Felor fiber was found to have the most acceptable properties as a substitute material for cleaning brushes, particularly in regard to an application on motorized (rotary or oscillating) brushes.

4.1.2 Approach

The primary objective during this reporting period was to establish the basic cleaning properties of Felor fiber which, as reported earlier, has been chosen as a substitute material for natural Sable hair. A special apparatus was designed that would allow to accomplish this in a controllable and repeatable manner.

The schematic of the device is shown in Fig. 4-A.1. It consists mainly of a flat stationary base (1) and a sliding rectangular vacuum chamber (2), the test brush (3), which consists of five 0.1 inch diameter 0.65 in. long

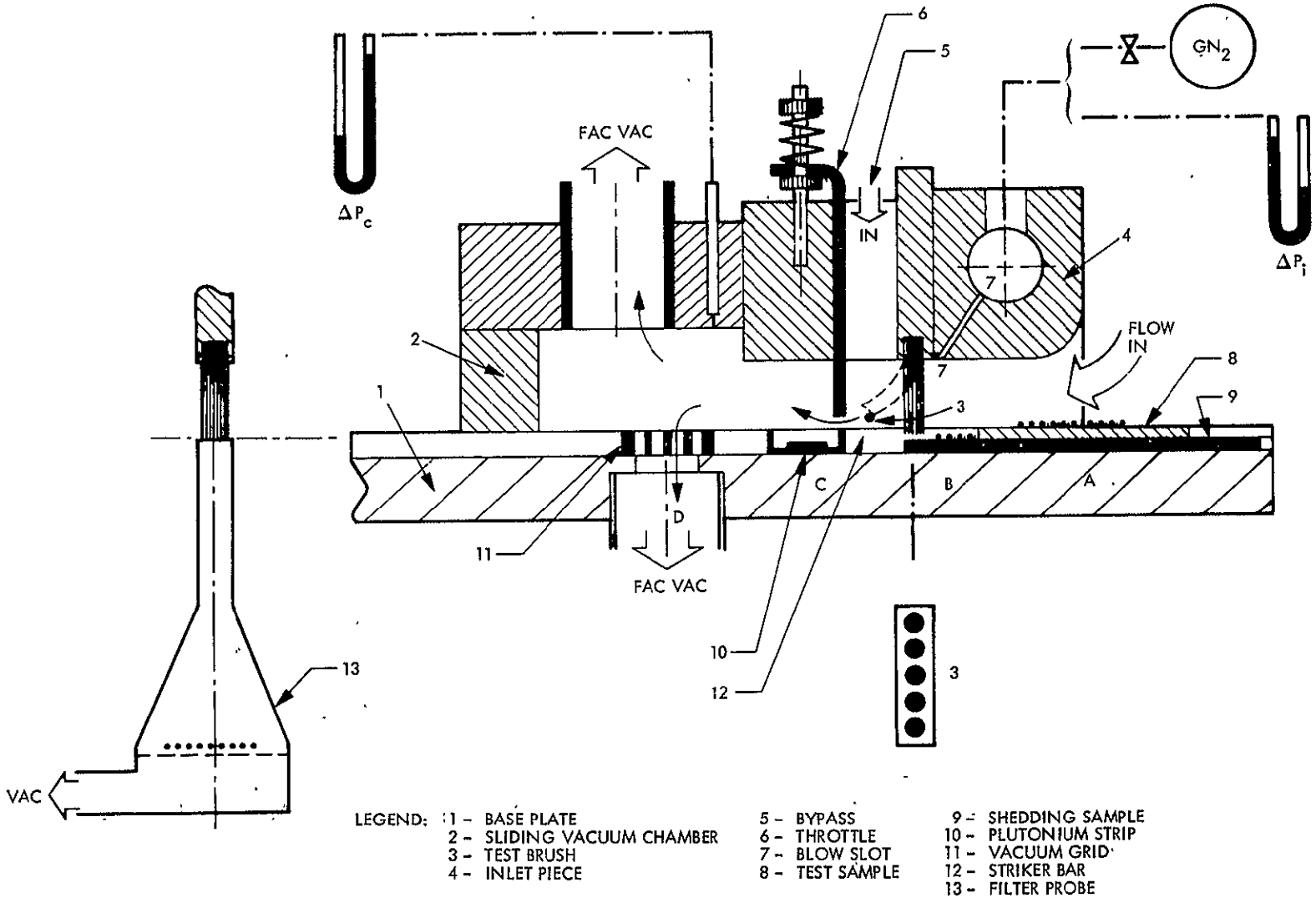

Fig. 4-A. 1. Diagram of brush evaluation test setup

tufts of Felor hair, spaced 0.2 inches apart from each other. The inlet piece (4) and the test brush (3) can be adjusted in height relative to the base (1). The flow across the test brush (3) can be controlled by means of the bypass (5) and the throttle (6). Clean air or GN_2 can be blown against the test brush (3) through a slot (7) incorporated into the inlet piece (4). The base plate (1) is grooved to receive and to position the samples (8, 9), a neutralizing device (10), (platonium strip), and a vacuum grid (11). A striker bar (12) can be installed behind the test brush (3).

Two samples are used for test. A 2 × 2 in. optical slide (8), to establish removal capability, and a standard bio-slide (9), to establish the amounts of particles swept over the edge of sample (8), or shed from the brush. The amounts of particles adhering to the brush are established by vacuuming the brush by means of a filter probe (13) after the test. Photos Fig. 4-A.2, 4-A.3, and 4-A.4 show the described devices and its accessories.

Tests are accomplished by sweeping the test brush (3), together with the entire upper plenum (2) over the stations (A), (B), (C) and (D) in a prescribed sequence. In contrast to the apparatus used in earlier tests with flow, the samples have to be removed from the device for counting under a 100X microscope. The discussed tests were conducted as indicated, with GM 1543637 standard dust or with 5-10 μm size glass beads seeded to an approximate density of 800-1000 particles per mm^2 on sample (8). The samples were cleaned with freon TF and with isopropyl alcohol prior to each test, and were fogged (where indicated) by chilling after they were seeded, to simulate accidental moisture condensation. The fibers were charged (where indicated) by rubbing a plastic stick until it would pick up paper chips from a 1 cm distance, followed by a sweep with the stick over the test brush. The room environment varied between 25-28°C and 50-60% RH. All tests were conducted on a laminer flow bench.

Counts prior to and after tests were taken over a 1/4 mm^2 area each from the locations indicated in Fig. 4-A.5. Except where indicated otherwise, all data presented are averages across the indicated reference lines from two identical determinations each. The term "relative line count," where indicated, designates line count averages related to the original line count average of the test sample, Station A.

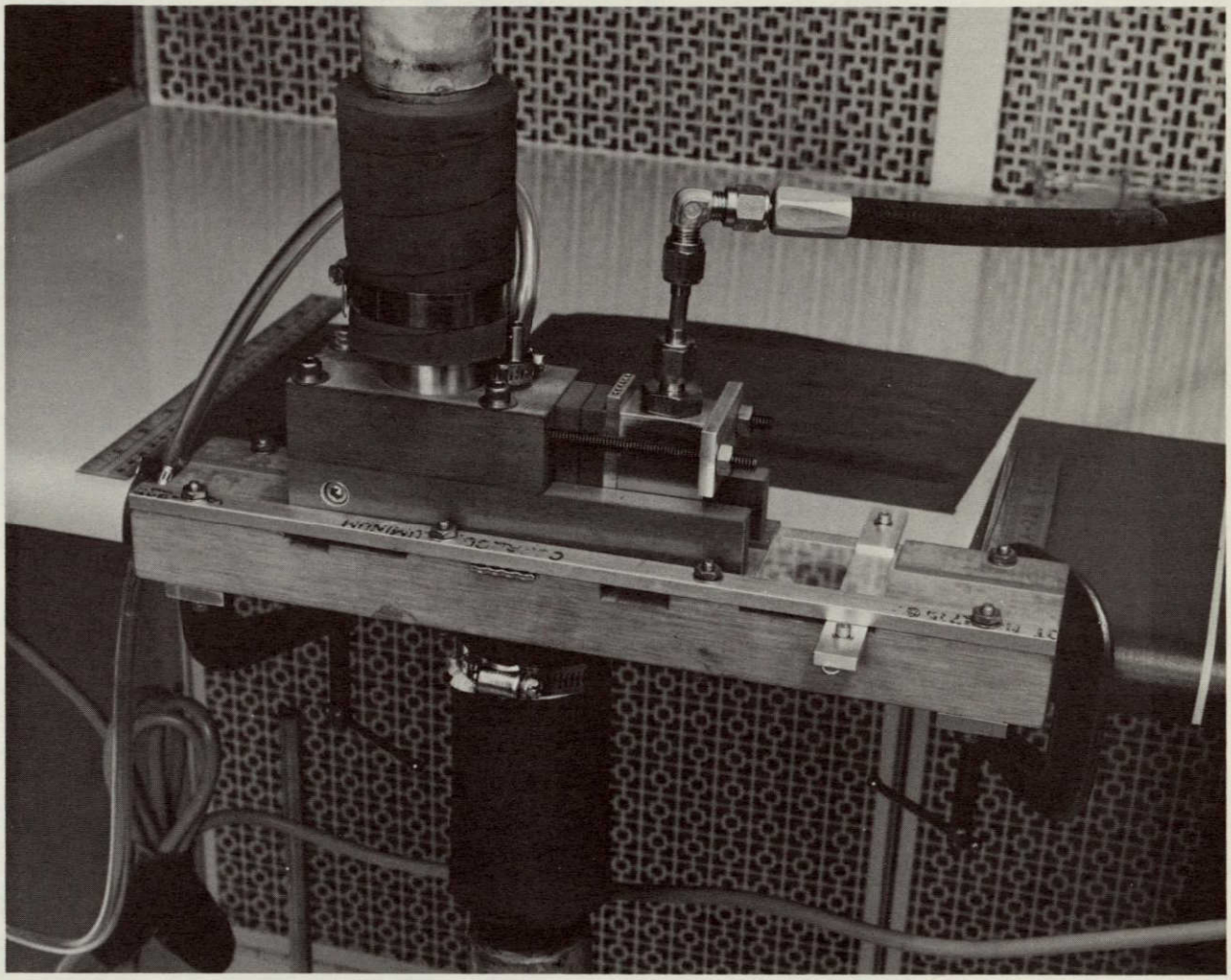

Fig. 4-A.2. Linear brush test apparatus working position

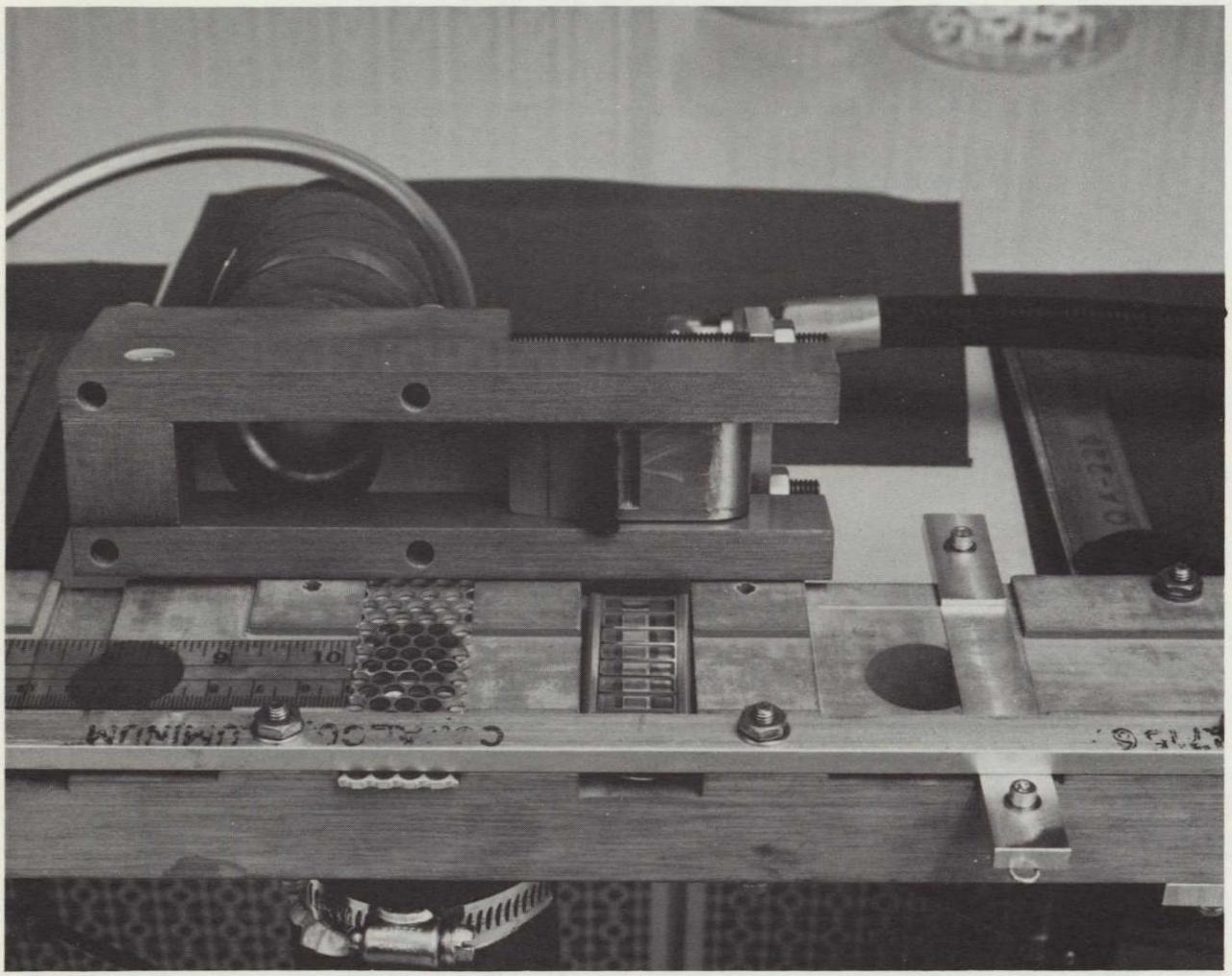

Fig. 4-A.3. Linear brush test apparatus view at test brush and accessories

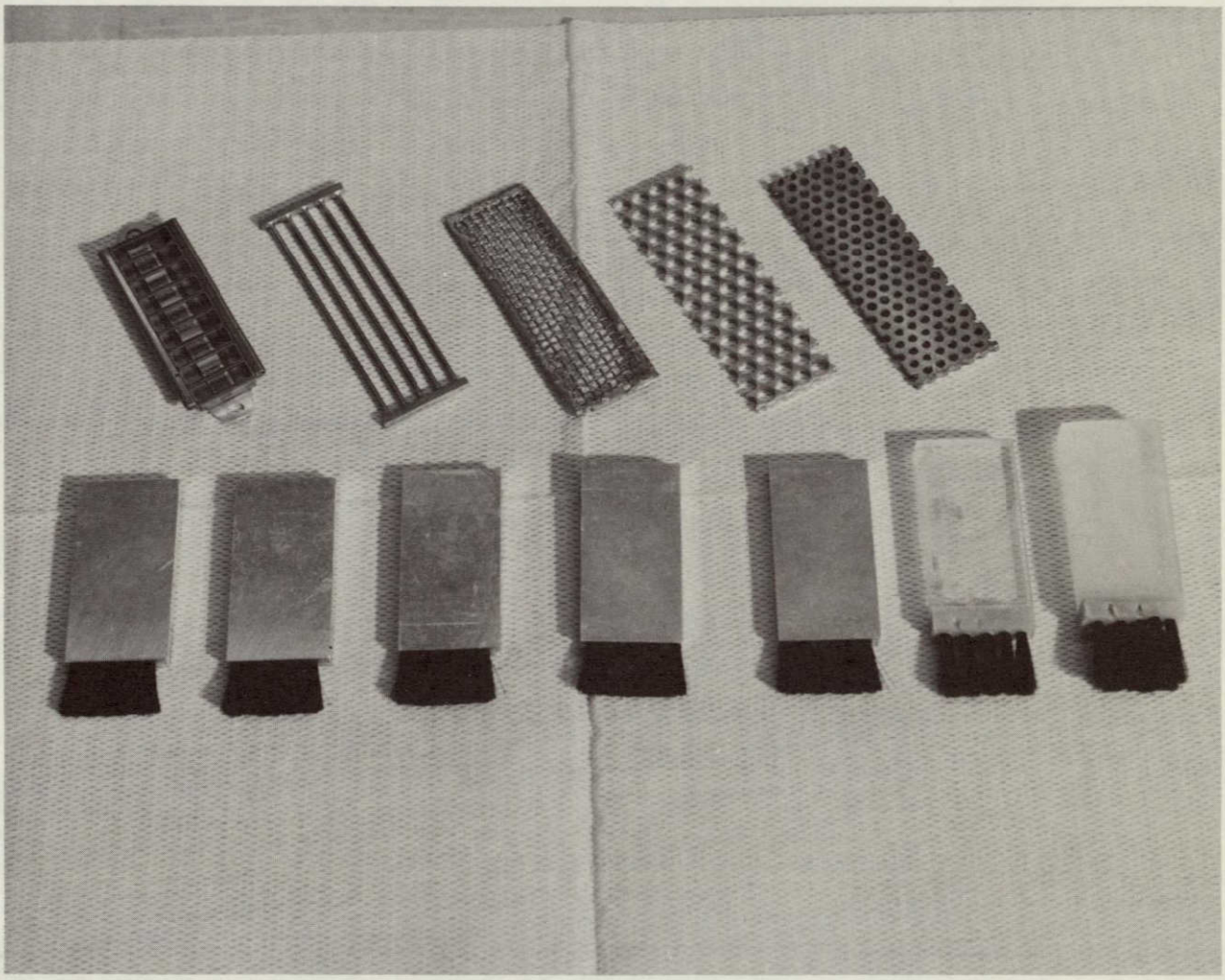

Fig. 4-A.4. Apparatus accessories; top - plutonium ship and vacuum grids; bottom - test brushes

During all tests (see Fig. 4-A.6) the brushes were adjusted in such a manner that the straightened hair would extend below the sample surface (8) just clear of the shedding slide (9). This would affect an acceptable hair-bending in the order of 60° relative to the surface and a uniform tip-contact with the swept surface.

4.1.3 Accomplishments

4.1.3.1 Flow Studies. The facility vacuum system produced an average vacuum of 150 mm Hg. If connected to the upper portion (2) of the test device, with the throttle (6)* open, this would produce excessive bending of the fibers with the grid (11) vacuum connection open or plugged. To maintain hair contact with the sample surface the flow had to be choked by lowering the throttle (6) to a distance of 1 mm from the surface. Since a distance of 3 mm was a self-imposed ground rule for the minimum standoff from the surface, the application of top vacuum to the apparatus was abandoned. If the vacuum was applied to the base connection through the grid (11) only, the slide had to be lowered to an acceptable distance of 5 mm from the surface to avoid fiber deflection and lift-off from the surface. The upper vacuum connection had to remain unplugged.

In this configuration, upon fully opening the slide, the fiber would flex over the striker bar (13) for cleaning, where desirable. A bypass area on the order of twice the inlet area was necessary to assure hair contact with the sample surface during vacuum flow through the grid (11).

4.1.3.2 Single Fiber Tests. Initial tests with the described apparatus were conducted with single fibers (rather then with brushes) to obtain information pertaining to specific fiber properties, such as the effects of flagging (tapering) and charging on particule adherence to the fiber. To accomplish this, four fibers were glued abreast to a flat plate, spaced 5 mm from each other, and were installed into the apparatus as described in para. 4.1.2 for test brushes.

---

*Numbers enclosed in parenthesis throughout Subtask A refer to nomenclature displayed in Fig. 4-A.1.

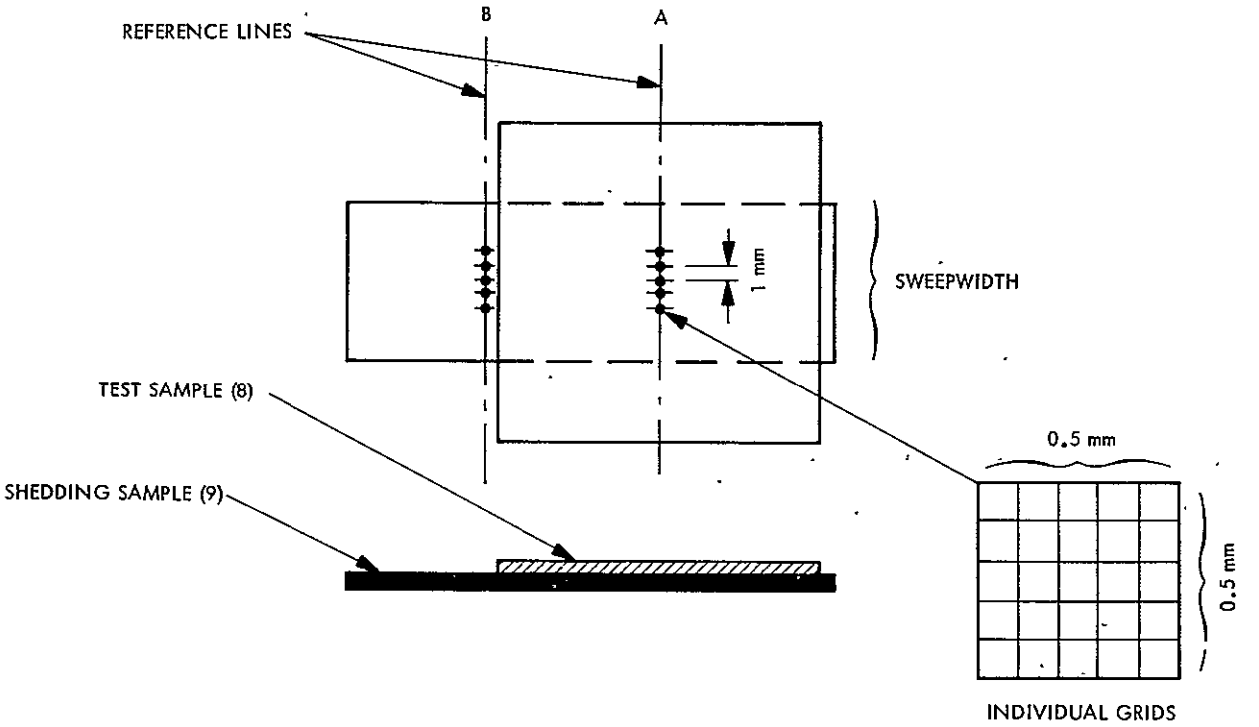

Fig. 4-A. 5. Arrangement of samples and counting areas

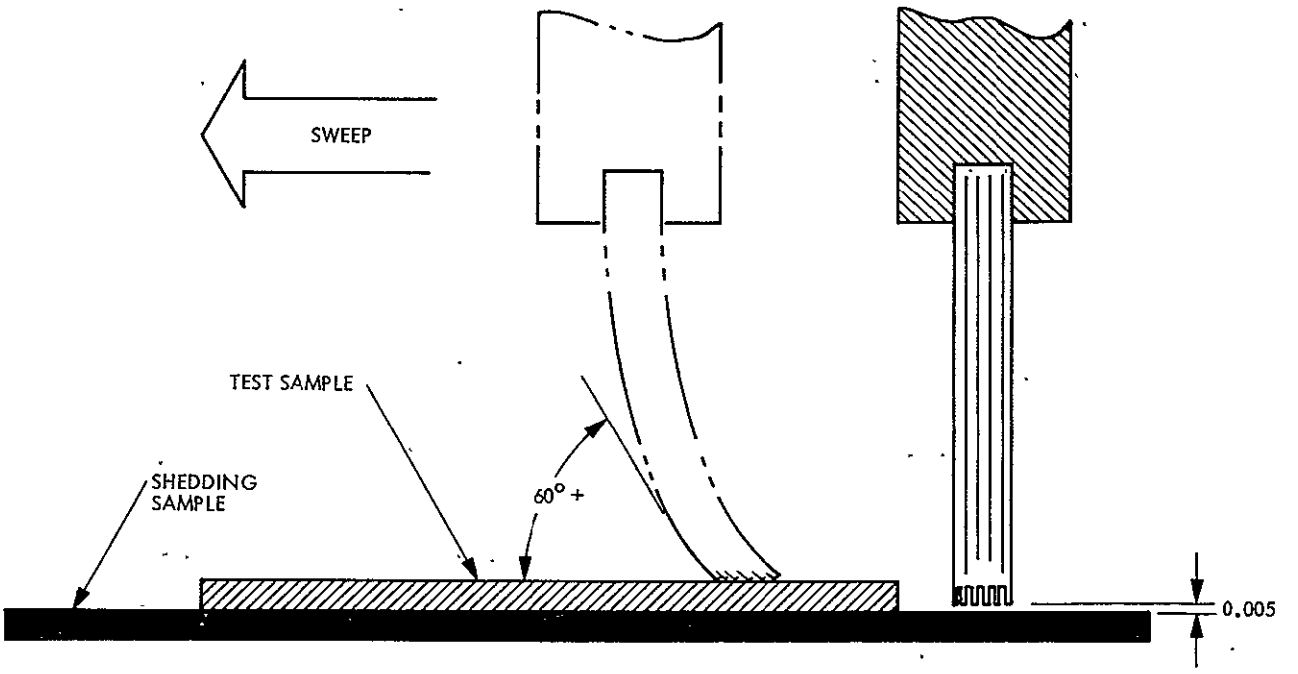

Fig. 4-A. 6. Brush adjustment

For test, the fibers were thoroughly vacuum cleaned using the filter probe (13), inspected under 100X, charged where prescribed, and were briskly swept over a sample slide seeded with GM 1543637 standard dust. Field of view counts then were taken from the fibers over a 1 mm length from the fiber tip.

The results are shown in Fig. 4-A.7. On a dry surface charging the fiber strongly enhanced the pick-up capability by a factor of two. On the fogged surface charging the fiber did not seem to have noticable effects probably because the charge flows off immediately upon contact with the surface. In all cases, the flagged fibers picked up considerably (up to twice) more particles than the trimmed fibers. The reason for this should be the roughness of the fiber surface generated by the abrasive process applied to produce the flagged end (see microphotos, Report No. 900-655, p. A-10).

An identical series of tests were conducted to establish the effect of flagging and charge on particle detachment from the fiber. To induce detachment the fibers were lowered onto a clean surface followed by a reversed 2 mm stroke which would cause a reversed buckling of the fiber such as may occur when touching a surface with a brush without sweeping.

Plotted in Fig. 4-A.8 are the numbers of all particles ≥ 5 μm counted from the tips of fibers swept over a dry or fogged sample, prior to and after buckling. The counts essentially substantiate the conclusions drawn from the previous tests that charging and flagging considerably enhances particle adhesion. The detachment due to buckling indicated in percent is on the order of 15-40 and does not seem to be conclusive where charge or flagging are concerned.

4.1.3.3 Restoration of Fiber Cleanliness. Restoration of fiber cleanliness was simulated by sweeping a clean brush over a seeded sample followed by (a) performing one single stroke over the vacuum grid (11), or by flexing the fibers over the striker bar (12) which, as described in para. 4.1.3.1, can be accomplished by pulling the throttle (6) all the way open. The degree of restoration achieved was established by vacuuming the fibers by means of the filter probe (13) and by comparing the filter counts.

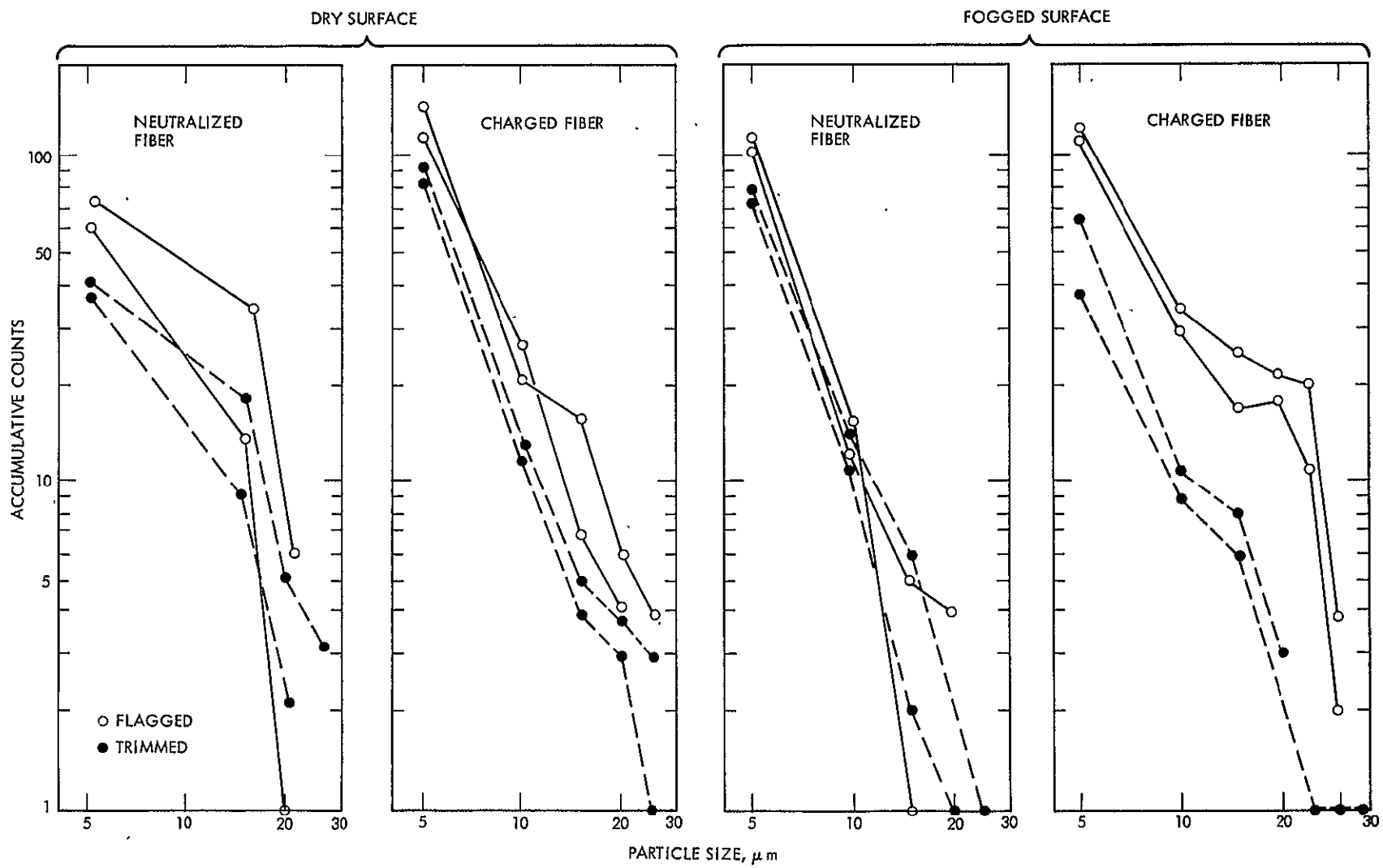

Fig. 4-A. 7. Effect of tip shape and static charge on particle adherence to

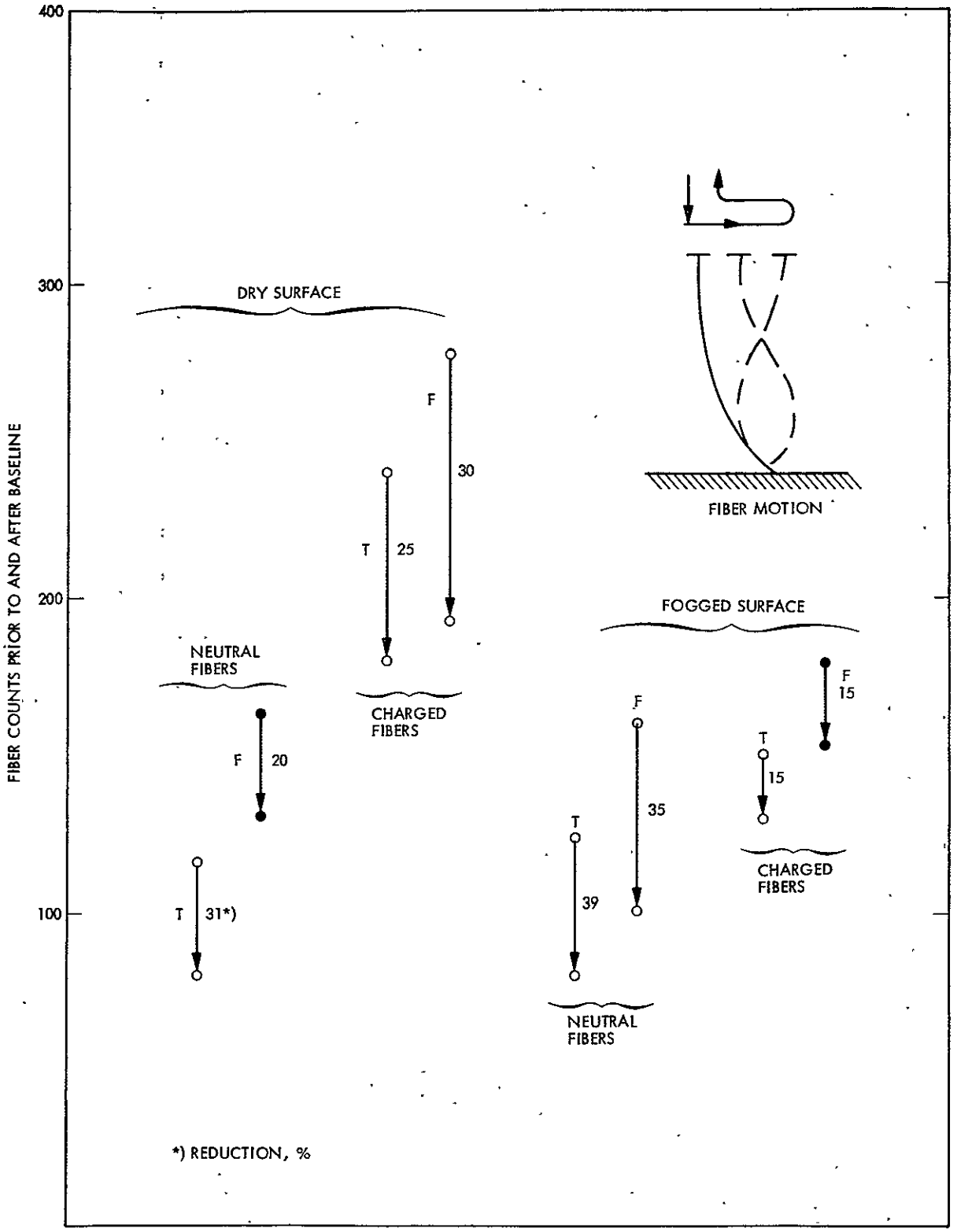

Fig. 4-A. 8 Single fiber shedding test; T - trimmed fibers; F - flagged fibers

Original fiber cleanliness could be fully restored by sweeping single fibers or brushes over the vacuum grid regardless of speed and type of grid installed. Repeated striking over the bar was necessary to restore fiber cleanliness. As shown in Fig. 4-A.9 charged fibers swept over the dry surface were hardest to remove (7 strikes). All the particles swept from a fogged surface came off after only 3 strokes because, as will be discussed later, of lumping.

4.1.3.4 Single Sweep Tests with Five Tufts Abreast. A number of single sweep tests were conducted first to study distributions, and to verify evaluation methods.

Fig. 4-A.10 shows a typical distribution of removal efficiency across the reference line of the test sample. From this test and other data obtained it appears that the brush is more efficient between the tufts where the fibers are spread due to bending on the surface. Plotted in Fig. 4-A.11 are line distributions across the shedding sample at different distance from the edge of the test sample, after sweeping dry samples seeded with 5-10 μm glass beads. A certain variation across the lines with tuft spacing is evident, but relation to the tuft axes is little conclusive because of lateral spreading of the particles due to hair snapping when sweeping over the edge of the test sample.

Figure 4-A.12 shows the line average from identical tests with dry and with fogged samples plotted versus distance from the edge of the test sample. It can be seen that edge shedding drops off sharply with distance from the edge. The shedding sample was found clear of any particles beyond a 3 mm distance from the edge.

4.1.3.5 Multiple Sweep Tests with Five-Abreast Felor Tufts.

1. Effect of Moisture and Repeated Sweeping on Cleaning Efficiency. In these tests the brush was swept repeatedly over dry and fogged samples seeded with 5-10 μm glass beads. Line counts were taken between sweeps from the test and from the shedding sample. The brush was only cleaned once prior to the test. The results are shown in Fig. 4-A.13 and 4-A.14.

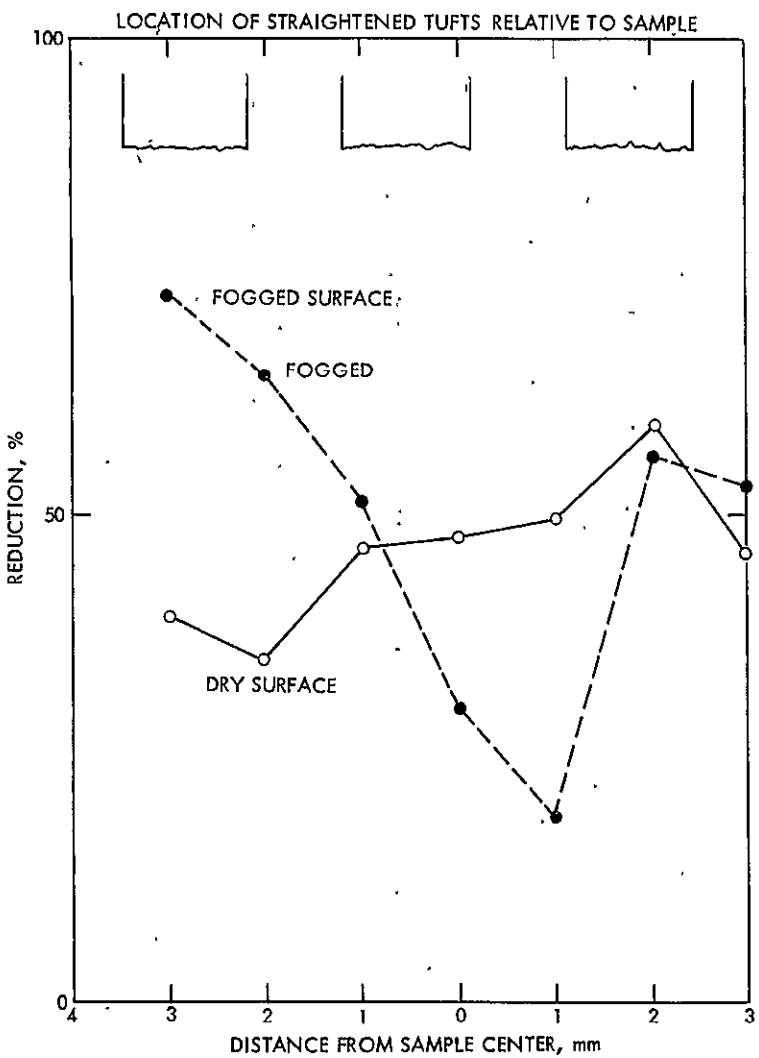

Fig. 4-A.9. Typical efficiency distribution across test sample with uncharged fiber

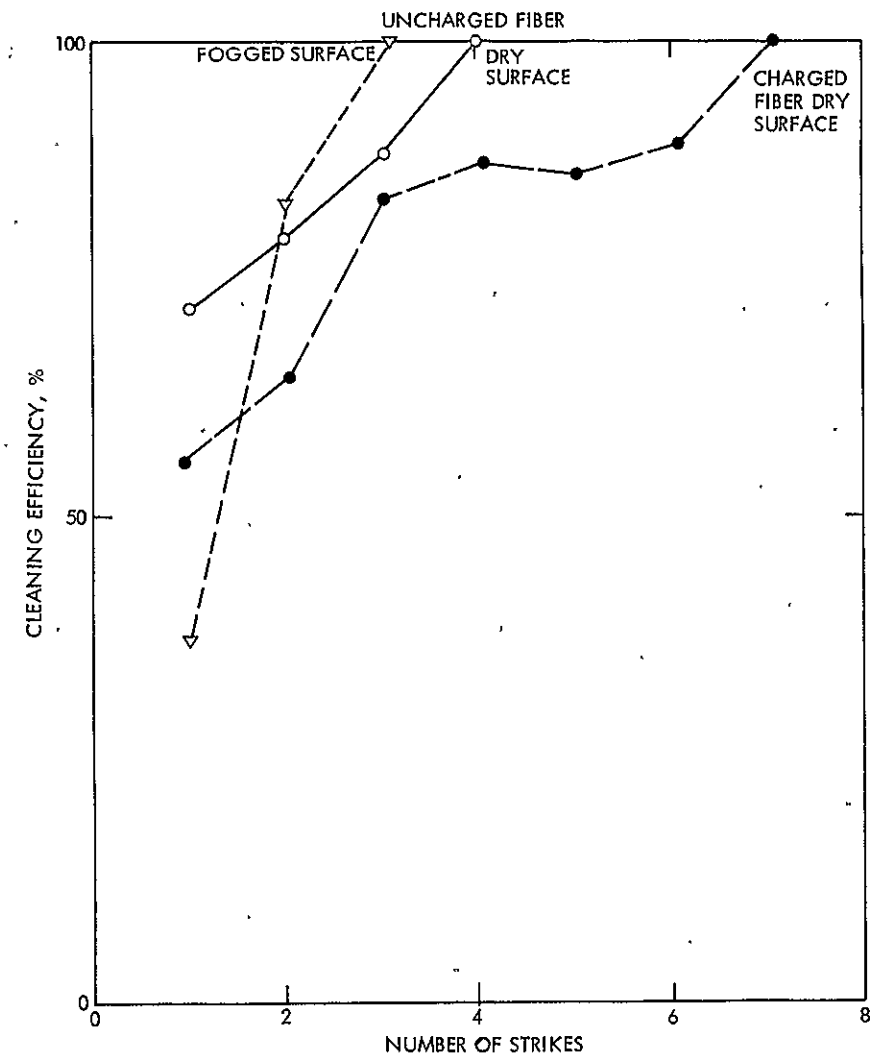

Fig. 4-A.10. Restoration of fiber - cleanliness of striker bar in vacuum flow

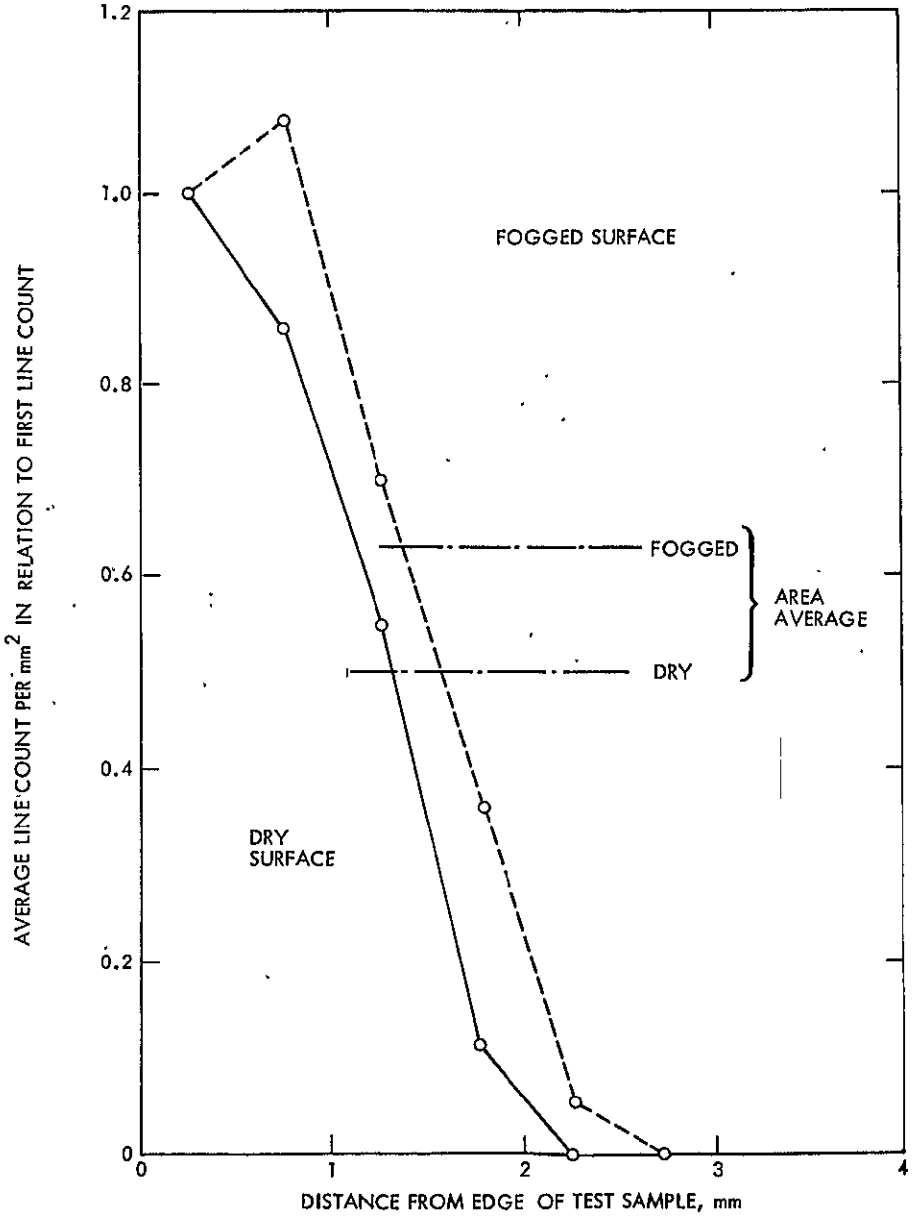

Fig. 4-A-11. Typical particle distribution over length of shedding sample

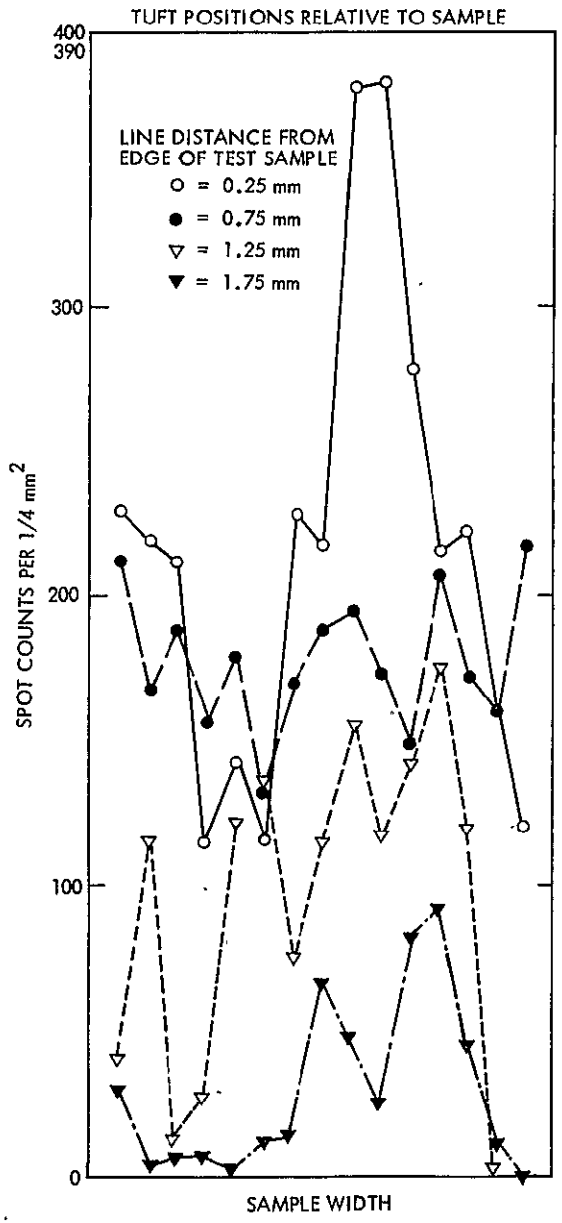

Fig. 4-A-12. Typical lateral particle distribution on a shedding slide

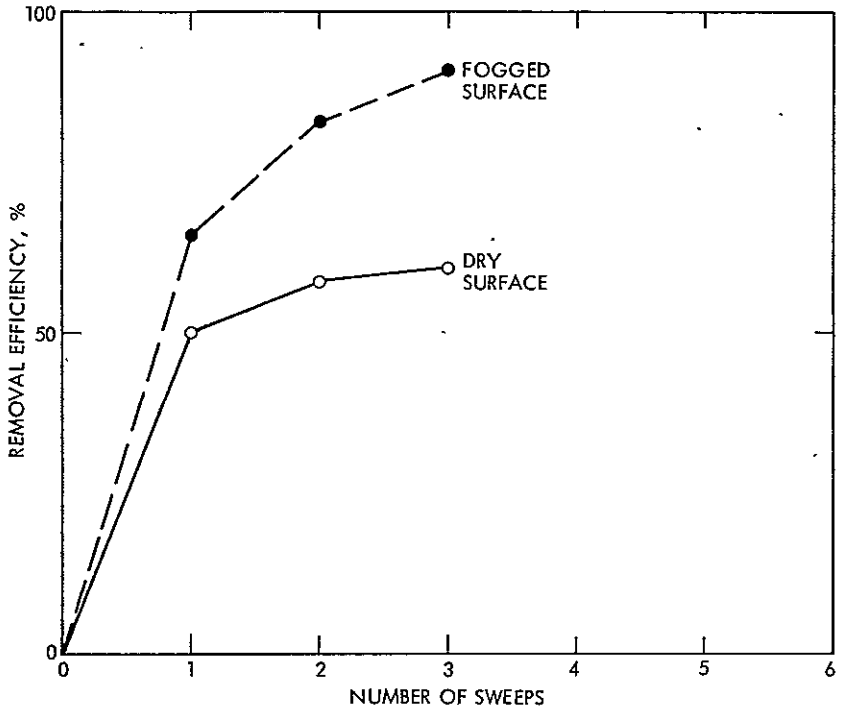

Fig. 4-A. 13. Effect of moisture and number of sweeps on removal efficiency

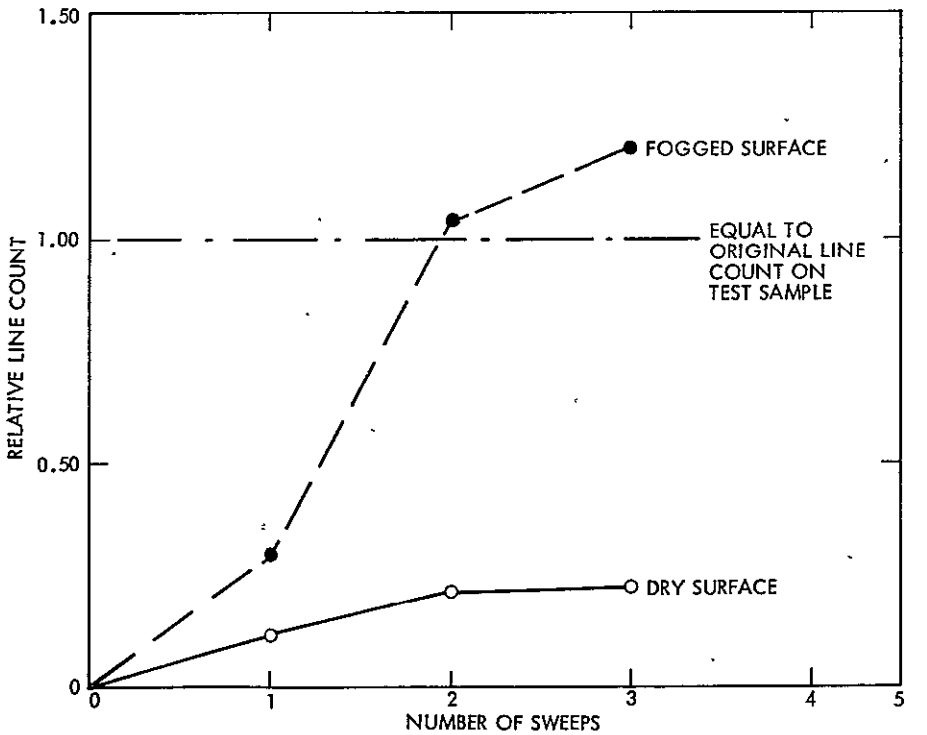

Fig. 4-A. 14. Effect of moisture and number of sweeps on edge-shedding

The tests substantiate earlier observations that repeated sweeping improves cleaning efficiency, but only the first few strokes represent a gain. The presence of moisture did improve the removal efficiency of glass beads, but shedding from the fibers also drastically increased if compared to the dry sample. The reason for this, as discussed in earlier reports, is lumping of the glass beads due to the formation of droplets after fogging. This does not generally imply that fogging the surface improves cleaning efficiency. This is only the case where size increase due to lumping strongly dominates the increase of adhesion caused by moisture. In previous tests with materials other than glass beads (random fallout, GM-standard dust) the presence of moisture did impair cleaning efficiency in most cases, depending upon size, shape and hygroscopic behavior of the contaminants. Because of the complexity of this problem, and the difficulties encountered with counting lumped particles, further tests with fogged samples were discontinued.

2. Effect of Static Charge. In this series of tests the test brush was cleaned and neutralized, or was cleaned and charged prior to tests as prescribed in para. 4.1.2. In addition to the line counts taken from the glass samples, the brush was vacuumed with the filter probe (13) between sweeps to establish the number of particles adhering to the brush. This represented a cleaning of the brush such as moving the brush over the vacuum grid (11) between sweeps. The results are shown in Fig. 4-A.15 through 4-A.18.

It is obvious that charging the fiber greatly enhances particle adherence to the fiber and cleaning efficiencies, but edge shedding is also more pronounced. Step efficiencies (Fig. 4-A.15) increases with repeated sweeping probably due to friction and charge build-up resulting from repeated sweeping.

Summarized in Table 4-A.1 are the cumulative total counts obtained from the described sampling methods compared to the initial total number of test particles within reach of the brush, in percent. The data also indicate increased efficiency and shedding with the charge. The effect of the charge on particle adherence to the fiber becomes particularly evident when comparing the amounts not accounted for, and the total amounts that have to be entrained into the main vacuum flow.

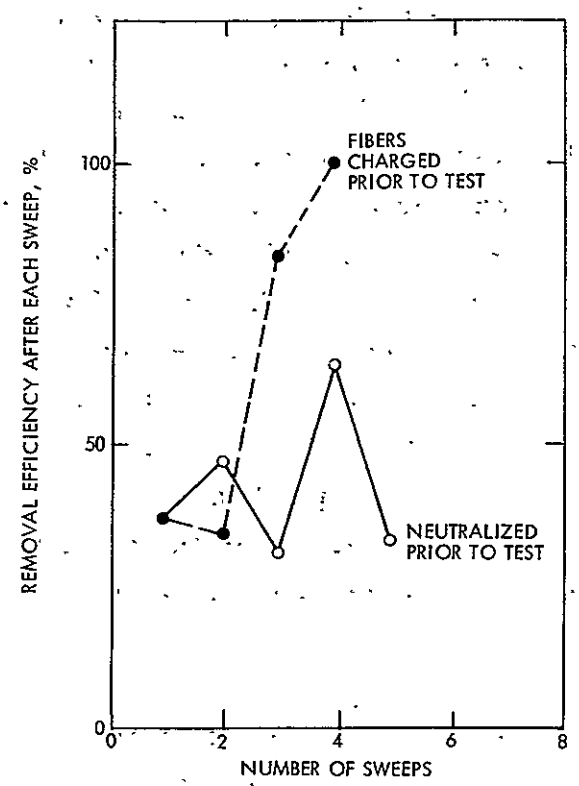

Fig. 4-A. 15. Effect of static charge on step-efficiency

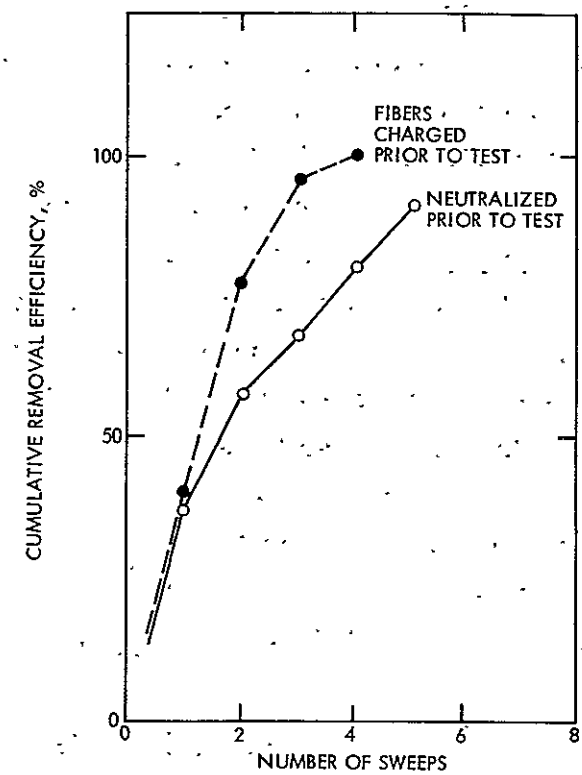

Fig. 4-A. 16. Effect of static charge on accumulative removal efficiency

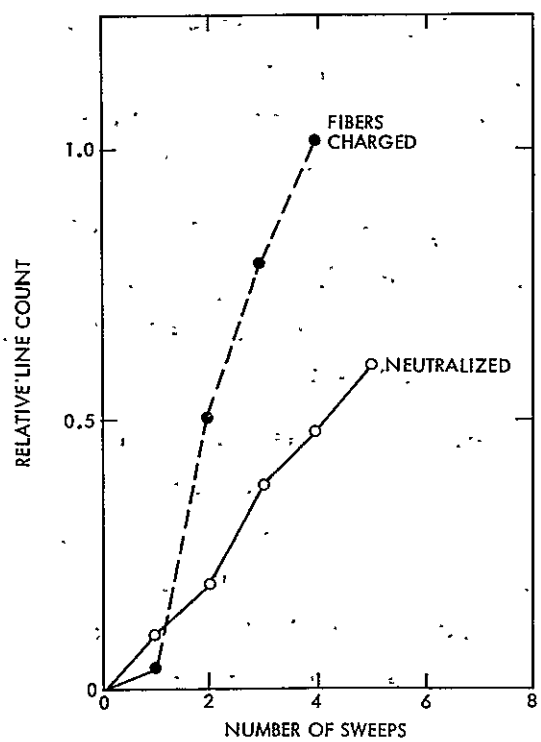

Fig. 4-A. 17. Effect of static charge on edge shedding

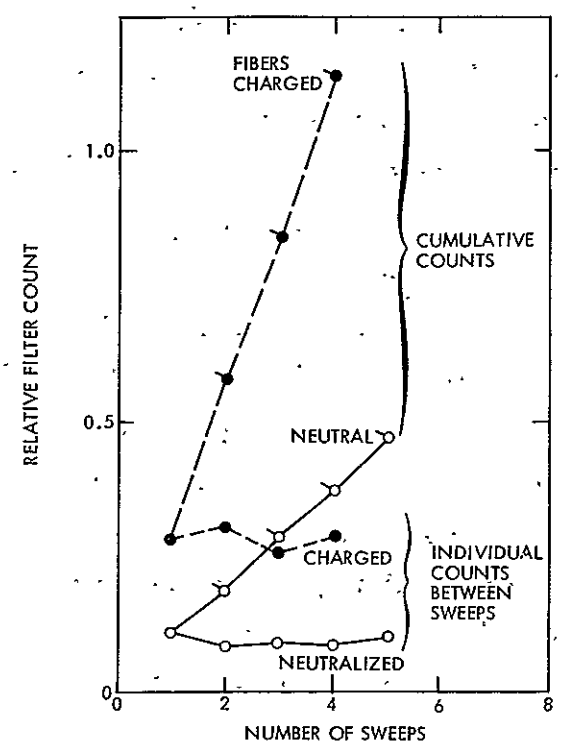

Fig. 4-A. 18. Effect of static charge particle adherence to brush

Table 4-A. 1. Effect of Static Charge on Edge Shedding and Adherence to Fiber

Item No.	Conditions of Fibers Prior to Test / Accounts	Neutralized	Charged
1	Amounts remaining on test sample	10	0
2	Amounts swept over the edge of test sample onto shedding sample	5	10
3	Amounts recovered from test brush by means of filter probe, functioning as vac grid	60	90
4	Amounts unaccounted for	25	0
5	Total to be reentrained into main vac flow (Items No. 2 and 4)	30	10

Data in percent initial test sample count within reach of brush.

During tests with the uncharged fiber, about 60% of the initial amount that potentially could have been removed from the test sample was found to adhere to the fibers after the test. A remainder on the order of 25% was unaccounted for. All of the particles removed from the test sample, less the amounts shed when clearing the sample edge, were found on the fibers when the fibers were charged. The amounts that have to be entrained by the main-flow (i. e., the particles shed and the ones unaccounted for in the test) are in the order of three times higher if the fibers are uncharged. The particles adhering to the fiber can efficiently be entrained into the system by means of a vacuum grid, which, as demonstrated, does not represent a problem. This leaves, in essence, no doubt that it would be of advantage from the removal efficiency and from the entrainment standpoint to charge the fibers, if compatible from the safety standpoint.

4.1.4 Summary

1) Particle adherence to the fiber upon contact with the surface was greatly enhanced if the fiber was mechanically flagged and/or charged. Either method increased the pick-up capability of the fiber by a factor of 1.5 to 2.0. Charge did not show any effect if the surface was fogged.

2) The amounts of particles shed from the fibers upon contact with the surface (buckling test) varied between 15 and 40% and were not conclusive where charge and fogging are concerned.

3) Fiber cleanliness could be completely restored by one single sweep over the vacuum grid. Repeated (up to 5 times) flexing of the tufts over the striker bar was necessary to completely restore fiber cleanliness.

4) Removal efficiencies were higher between the tufts; whereas shedding appeared to be more pronounced right in line with the tuft axes, where fibers are most densely spaced.

5) The removal of glass beads swept from fogged surfaces was more efficient, but edge shedding had also greatly increased. Both effects were attributed to lumping of the beads. This depends strongly upon the nature of the contaminants, and does <u>not</u> suggest fogging as a measure to improve cleaning efficiency.

6) Single sweep efficiency was on the order of 40-50% with the uncharged brush and appeared to rise slightly during repeated sweeping. The single sweep efficiency of the charged brush did rise strongly up to 100% after a few (4 to 5) sweeps. Progressive charging of the fiber as well as decreasing surface particulate density are believed the causes for this.

7) A 100% removal was achieved with the charged brush after the fourth sweep. The efficiencies achieved with the uncharged brush at the same number of strokes was on the order of 80%. A total of six or more strokes were needed to achieve a near 100% removal with uncharged brushes.

8) The cumulative particle adherence to the fibers and edge shedding observed in multi-sweep tests were three times higher with charged brushes, if compared to test with uncharged brushes, neutralized prior to test.

4.1.5 Conclusions

In regard to the overall task objective the following conclusions are drawn from this reporting period:

1) Mechanically flagged fiber appears to be the best choice for use in cleaning brushes.

2) Charging the fiber is most effective for single stroke cleaning with hand operated brushes.

3) For multisweep cleaning the charge mainly effects the number of sweeps needed to accomplish efficient removal which should not be of significance in motorized brushes. The observed natural charge build-up during the repeated rapid sweeping of dielectric surfaces will possibly have to be eliminated by sweeping over a grounded surface to comply with spacecraft safety requirements.

4) Sweeping the fiber tips of a vacuum grid is the most efficient method to restore fiber cleanliness. The tested method is applicable for rapid sweeping as occurring in motorized brushes.

5) Flexing the fibers over a striker bar in vacuum flow also efficiently restores fiber cleanliness but the bar has to be struck a minimum of five times. A grid of 5 bars or more has to be provided to clean the fibers in one sweeping motion.

6) A staggered tuft arrangement with two (or more) rows of tufts abreast is recommendable to even out, and to further increase, the efficiency of the brush.

7) The flow concept has to assure that the particles swept over the edge of the surface and shed from the brush before the brush hits the vacuum grid, are reentrained into the main flow without the fibers losing tip contact with the surface during sweeping.

4.1.6 Future Activities

The problem of entraining shed particles without losing fiber contact with the surface during cleaning still has to be resolved. Because this problem is strongly dependent on the sweep velocity and on the fiber dynamics, it was decided to discontinue hand-operated linear motion tests at this point, and proceed with a motorized version of the discussed felor brush, which is shown in Fig. 4-A.19. The device represents an operational cleaning tool where rotor diameter, tuft size and spacing are concerned. The mechanical design is experimental and allows for a variation of parameters still to be determined, such as the flow controlling areas and the stand-off from the surface. The design and fabrication of the device is in progress.

In the meantime, activities under this task will shift to the earlier described centrifugation experiment with the objective to generate quantitative data on particle adhesion to surfaces. These data will be used to support the final evaluation of all the mechanical cleaning tests conducted under this task, and to support post launch recontamination analysis work.

4.1.7 Presentation

None

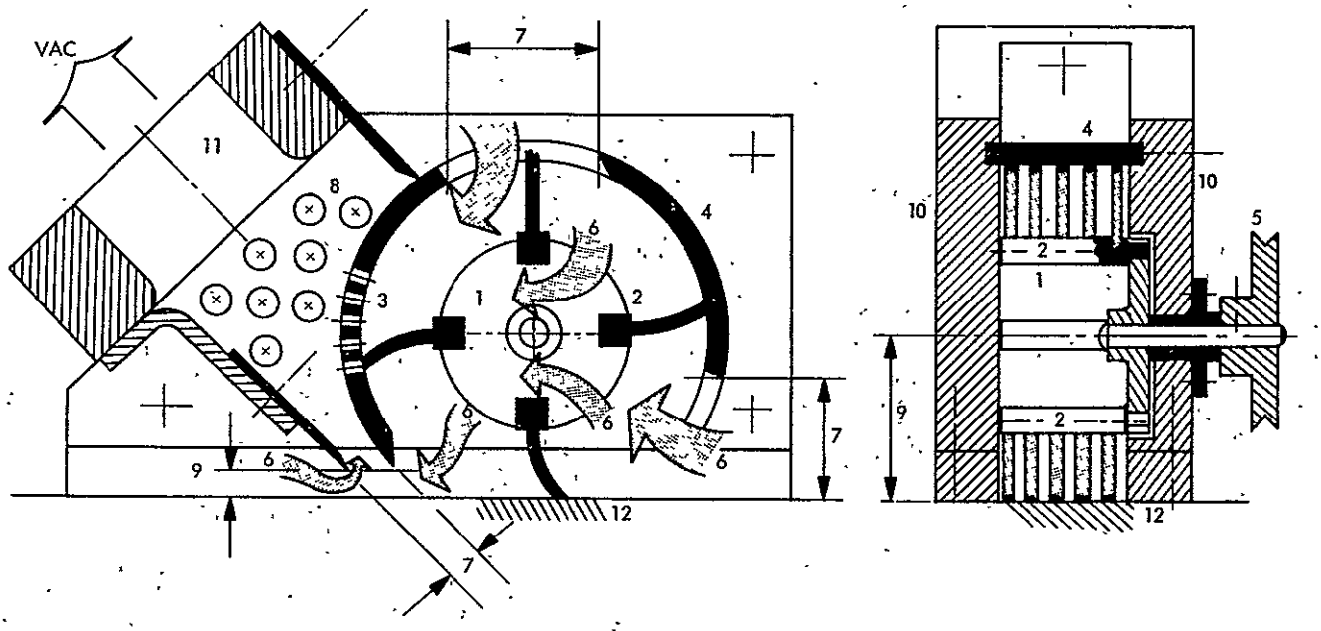

MAJOR DESIGN FEATURES:

1 - FREEBREEZING CAGE TYPE ROTOR
2 - EXCHANGEABLE STANDARD COMPUTER TAPE BRUSHES
3 - ADJUSTABLE VACUUM GRID SEGMENT
4 - CHARGE OR GROUNDING SHOE
5 - EXCHANGEABLE PULLEYS
6 - ROTOR CROSS FLOW
7 - VARIABLE FLOW CONTROLLING AREAS
8 - BYPASS ORIFICES, PLUGGED OR OPEN
9 - VARIABLE STAND OFF FROM SURFACE
10 - PLEXIGLAS SIDEWALLS (FOR STROBE OBSERVATION)
11 - VAC HOSE TO FACILITY VAC SYSTEM
12 - USE WITH BASE OF BRUSH TEST APPARATUS

Fig. 4-A.19. Experimental rotary brush 25.4 mm (1 inch) sweep width

4.2 EVALUATION OF PLASMA CLEANING AND DECONTAMINATION TECHNIQUES

4.2.1 Subtask B Introduction

The objective of this phase of work was to determine the effectiveness of plasma gas in contacting and sterilizing surfaces of different geometric configurations.

Capillary tubing of varied lengths and internal diameters, and stacked discs of mated surfaces were tested. Samples of metal and glass were selected because of differences in conductive electrical properties.

4.2.2 Approach

Test samples were contaiminated with controlled numbers of Bacillus subtilis var. niger spores and exposed to helium plasma. Plasma production values of 150 watts (rf), 0.2 mm Hg pressure, and 20 cc per minute helium flow were maintained during all exposures. Plasma exposures were for 15 and 60 minutes. Bioassay for recovery of surviving spores was conducted with techniques previously outlined. The test matrix is shown in Table 4-B.1.

Capillary tubing of three different internal diameters were tested. Originally, the test plan was to use tubing of 1.0, 0.5 and 0.1 cm inside diameter (I.D.). However, test results of the 0.1 cm tubing revealed that more meaningful data would be obtained if we selected even smaller tubing for the remainder of the investigation. Tube size availability and spore recovery problems limited the investigation to tubing of 0.1, 0.07 and 0.05 cm I.D.

Tubing lengths of 4, 8 and 12 cm long were assembled from 4 cm segments. They were attached end to end and formed a continuous length of tubing of uniform diameter. The test tubing was clipped to a circular glass ring placed at chamber position 1. Figure 4-B.1 depicts the test sample orientation in the chamber. Following plasma exposure, each 4 cm segment was assayed separately to determine the extent of penetration or sterilization.

Table 4-B.1. Test Matrix to Determine the Effectiveness of Helium Plasma in Penetrating and Sterilizing Various Sample Configurations

Sample Configuration	Dimensions, cm		Glass			Stainless Steel		
			[a] Helium Plasma, min.			Helium Plasma, min.		
	I.D.	Length	0	15	60	4	15	60
Capillary Tubes	0.1	4.0	[b] A 1	A 4	A 7	B 10	B 13	B 16
	0.1	[c] 8.0	A 2	A 5	A 8	B 11	B 14	B 17
	0.1	12.0	A 3	A 6	A 9	B 12	B 15	B 18
	0.07	4.0	(TUBING NOT AVAILABLE)			D 28	D 31	D 34
	0.07	8.0				D 29	D 32	D 35
	0.07	12.0				D 30	D 33	D 36
	0.05	4.0	E 37	E 40	E 43	F 46	F 49	F 52
	0.05	8.0	E 38	E 41	E 44	F 47	F 50	F 53
	0.05	12.0	E 39	E 42	E 45	F 48	F 51	F 54
Stacked Discs	Diameter							
	4.0		G 55	G 56	G 57	H 58	H 59	H 60

(a) Helium plasma, 150 watts rf, 0.2 mm Hg pressure, 20 cc He flow, chamber position 1.
(b) Five replicates
(c) Lengths longer than 4 cm consisted of 4 cm sections attached end to end.

Mated surfaces were investigated by using stacked discs of mated pairs. A stack consisted of two sterile discs sandwiched between two inoculated discs. Figure 4-B.2 shows the arrangement of a mated surface test stack. After exposure, the discs were analyzed separately. However, the data obtained were evaluated for each pair of discs. Some of the disc pair were overlayed with a nutrient medium for subsequent visual inspection for indication of plasma gas penetration.

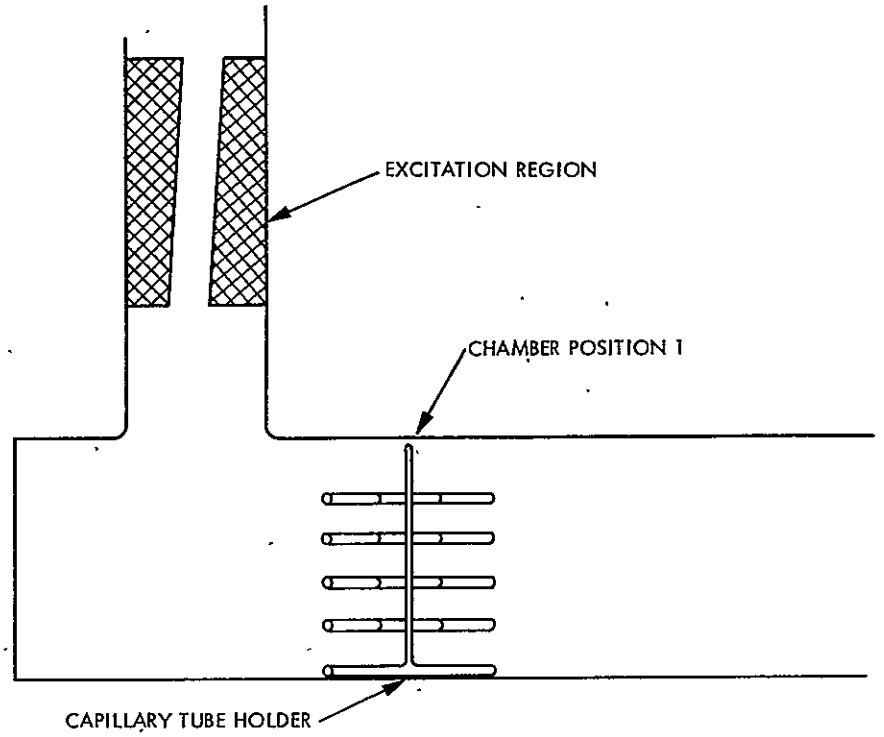

Fig. 4-B.1. Schematic of test sample orientation

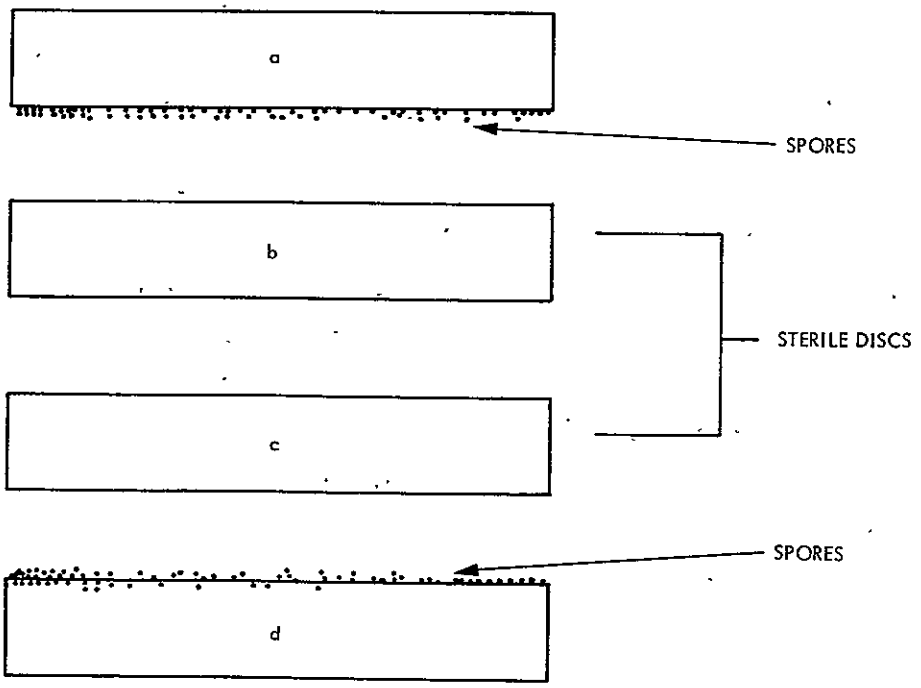

Fig. 4-B.2. Schematic of mated surface test stack

4.2.3 Significant Accomplishments

The analyses for spore survivors in plasma treated capillary tubes showing the percent spore survival are presented in Tables 4-B.2 and 4-B.3. Helium plasma was effective in reducing the total number of microorganisms present in all lengths and diameters of capillary tubing tested. The longer plasma exposure time of 60 minutes was more effective in reducing spore numbers. Also, spores inoculated in the glass capillaries died at a faster rate than did the spores inside the stainless steel tubes. This may be partially explained in that intense irradiation levels, sufficient to kill, passed through the glass walls of the tubes.

The distance that plasma penetrated is not easily concluded from the data obtained. However, in most cases, (Tables 4-B.2 and 4-B.3) tube lengths of 12 cm show a higher percentage of spore survival for the middle 4 cm segment. It appears that plasma was more effective at both 4 cm ends of the 12 cm tubes.

Table 4-B.2. Mean Percent Survival of Bacillus subtilis var. niger Spores in Glass Tubing After Exposure to Helium Plasma

Sample Diameter, Centimeters	Helium Plasma Exposure, Minutes	Tube Length Centimeters	Mean Percent Survival/ Tube	Mean Percent Survival/Tube Segments		
				4 cm	4 cm	4 cm
0.102	15	4	0.22	0.22		
		8	1.25	0.74	1.75	
		12	1.59	2.68	0.90	1.19
	60	4	0.00	0.00		
		8	0.13	0.01	0.01	
		12	0.00	0.00	0.00	0.00
0.051	15	4	1.00	1.00		
		8	2.24	2.22	2.26	
		12	0.57	0.42	1.09	0.19
	60	4	0.02	0.02		
		8	0.12	0.09	0.14	
		12	0.05	0.03	0.14	0.00

Table 4-B.3. Mean Percent Survival of Bacillus subtilis var. niger Spores in Stainless Steel Tubing After Exposure to Helium Plasma

Sample Diameter, Centimeters	Helium Plasma Exposure, Minutes	Tube Length Centimeters	Mean Percent Survival/ Tube	Mean Percent Survival/Tube Segments		
				4 cm	4 cm	4 cm
0.127	15	4	87.53	87.53		
		8	71.43	72.65	70.20	
		12	78.91	75.92	100.00	60.82
	60	4	2.37	2.37		
		8	5.55	7.06	4.04	
		12	13.80	8.46	28.29	4.66
0.071	15	4	4.60	4.60		
		8	5.96	6.59	5.32	
		12	14.14	1.80	28.80	11.82
	60	4	0.52	0.52		
		8	0.04	0.03	0.06	
		12	0.80	0.00	2.35	0.02
0.053	15	4	21.89	21.89		
		8	25.40	27.17	23.64	
		12	22.30	20.50	28.89	17.50
	60	4	4.35	4.35		
		8	3.77	4.58	2.95	
		12	5.85	3.18	9.46	4.93

Although spore reduction had occurred with the helium plasma and the results obtained provided a comparison between the tube diameters and lengths, no sterilization was observed. Therefore, the plasma density was increased with plasma production at 300 watts rf power. All other test conditions remained constant. Inoculated tubing, exposed to helium plasma at the higher rf power value, was analyzed for survivors and the results are presented in Table 4-B.4. Sterility of the tubes was observed after a 60 minute plasma exposure.

Table 4-B.4. Mean Percent Survival of *Bacillus subtilis* var. *niger* Spores in Stainless Steel Tubing after Exposure to Helium Plasma[a]

Sample Diameter, Centimeters	Helium Plasma Exposure, Minutes	Tube Length Centimeters	Mean Percent Survival/ Tube	Mean Percent Survival/ Tube Segments		
				4 cm	4 cm	4 cm
0.071	15	4	0.00	0.00		
		8	0.00	0.00	0.00	
		12	1.04	0.11	2.39	0.63
	60	4	0.00	0.00		
		8	0.00	0.00	0.00	
		12	0.00	0.00	0.00	0.00

[a]300 watts rf

The ability of plasma to penetrate and sterilize contaminated, mated surfaces was investigated. Data obtained (Table 4-B.5) for the number of microorganisms surviving a plasma treatment of such surfaces show a slight reduction from those numbers originally present. These data are from mated aluminum discs. Studies performed with mated glass surfaces showed that few, or no organisms survived. However, as noted previously, it is felt that penetration along the surface did not occur, but that most of the kill was caused by ultraviolet irradiation of intense amounts penetrating through the thin glass. Additional investigation of glass mated surfaces is being conducted.

4.2.4 Summary and Conclusion

The results of this investigation have been evaluated and the following conclusions drawn:

1) Helium plasma (300 watts rf) sterilized metal capillary tubes 0.07 by 12.0 cm and contaminated with 10^4 spores, within 60 minutes, and

2) Helium plasma was not able to penetrate mated metal surfaces to any great extent.

Table 4-B.5. Bacillus subtilis var. niger Spores Recovered from Mated Metal Surfaces That Were Exposed to Helium Plasma for Sixty Minutes[a]

Helium Plasma Test	Number Surviving Spores Per Mated Surface		Control Number Of Spores Per Mated Surface (No Plasma)	% Surviving Spores Per Mated Surface		
	a + b	c + d		a + b	c + d	Mean
1	4280	5040	6640	64.46	75.90	70.18
2	2700	3840	6600	40.91	58.18	49.55
3	6334	6286	8586	73.77	73.21	73.49
4	4306	6106	7046	61.11	86.66	73.89
5	2486	5114	7306	34.03	69.99	52.01
Mean	4021	5277	7236	55.57	72.93	64.25

[a]300 watts rf

From the data obtained to date it would appear that plasma is a surface sterilant. If objects are exposed to plasma gas for sufficient time, sterilization of all surfaces will occur.

4.2.5 Future Activities

The final phase of this contracted effort will be to study the compatibility of plasma on selected spacecraft material. The materials that will be tested are those used primarily for thermo control since these materials are considered the most sensitive to any environmental stress. The specific materials will include: 1) metallized Teflon, Mylar and Kapton; 2) optical coating; 3) black coating; 4) vacuum deposited gold or aluminum; and 5) graphite/epoxy sheets.

4.2.6 Presentation

Fraser, S., "Evaluation of Plasma Cleaning and Decontamination Techniques" presented at the NASA Spacecraft Sterilization Seminar, Cocoa Beach, Florida, December, 1974.

4.3 PLANETARY QUARANTINE (PQ) CONSIDERATION FOR SHUTTLE LAUNCHED SPACECRAFT

4.3.1 Subtask C Introduction

The objectives of this task are to assess the impact of planetary quarantine on Shuttle launched spacecraft and to determine the application of present and proposed monitoring and decontamination techniques to Shuttle operations.

4.3.2 Significant Accomplishments

The Space Transportation System (STS) will be used to launch a variety of planetary missions during the 1980s and 90s. The thrust of the task during this reporting period was oriented toward developing and implementing a detailed plan that will insure identification of the potential PQ impact on these missions for both the Shuttle operators and potential users, and to suggest solutions and alternatives.

The plan identified four major task areas:

1) Mission model assessment
2) STS operations assessment
3) Recontamination assessment, and
4) Research application assessment.

Within each task area pertinent subtasks were identified. A brief synopsis of these follows:

4.3.2.1 Task 1 – Mission Model Assessment. The January '73 NASA Mission Model is to be examined and updated per the latest Space Science Board (SSB) and HQ input, with the most probable mission set being selected for task usage. This mission set is to be categorized in a manner consistent with potential operators and users.

Probable PQ requirements will be identified by mission category. These requirements will be based on latest SSB and HQ input, and the types of PQ research needed to meet the requirements of the mission model categories will be listed.

4.3.2.2 Task 2 – STS Operations Assessment. This task will review the present STS contamination requirements in terms of their adequacy to achieve estimated missions PQ requirements. The contamination requirements will be updated and reevaluated through participation in the Shuttle Contamination Requirements Definition Group meetings.

Typical STS operational scenarios will be evaluated for potential contaminating events including prelaunch, launch, on-orbit, injection, and/or abort/return. Major differences will be identified for probes, orbiters, landers, and surface sample return missions.

Problem areas will be identified in terms of the system/Shuttle interface. An estimate of the impact on operations will be made as well as applicable solutions and alternatives.

4.3.2.3 Task 3 – Recontamination Assessment. This task will identify the potential recontamination problems a PQ sensitive payload may encounter from launch through injection. Drawing on Viking experience, a recontamination acceptance matrix will be constructed (by mission type). The dynamic events will be identified and sized, and contamination levels will be estimated. Analyses will be performed to size the overall problem and identify potential problem areas.

4.3.2.4 Task 4 – Research Applications Assessment. This task will assess the applicability of present PQ techniques to meet identified PQ/Shuttle requirements. Potential problems and impact will be discussed.

New research requirements will be identified within a mission matrix along with suggested lead times and recommendations.

Manned access option missions will be identified along with potential access/interface problems for PQ sensitive payloads. Operational scenarios for such missions including sample processing, retrieval, repair, storage and return will be investigated. Potential problems will be identified and recommendations will be suggested.

Since the plan has been completed and reviewed, the assessment of the current models has been completed. Operationally, several scenarios relative to payload integration (Cape) have been evaluated for potential contamination problems. A preliminary assessment of STS shroud options (no shroud, reusable, and disposable) has been completed, and an initial version of the recontamination acceptance matrix (by mission type) has been constructed.

4.3.3 Future Activities

The future effort on this task will be to update the mission model as appropriate to identify new missions or a change in research lead time. Operations from prelaunch through injection will continue to be examined for several payload categories. The recontamination effort will evaluate the operations for dynamic events (launch through injection) and will size the events for modeling.

4.3.4 Presentation

None

SECTION V

PLANETARY QUARANTINE LABORATORY ASSAY ACTIVITIES (AFETR) NASA No. 193-58-63-05

Contents	Title and Related Personnel
Subtask A para. 5.1	PLANETARY QUARANTINE LABORATORY ASSAY ACTIVITIES (AFETR)

Cognizance: J. R. Puleo

Associate Personnel:
- G. Oxborrow
- N. Fields
- S. Bergstrom
- L. Maull
- K. Gantner (Bionetics)
- G. Hayes (Bionetics)

PRECEDING PAGE BLANK NOT FILMED

5.1 PLANETARY QUARANTINE LABORATORY ASSAY ACTIVITIES (AFETR)

5.1.1 Subtask A Introduction

The objective of this subtask is to determine and document the quantitative and qualitative microbiological profiles of pertinent automated outbound spacecraft which may carry terrestrial organisms to the planets.

This type of work is required by NASA policy and lays a foundation upon which future policy can be formulated.

5.1.2 Significant Accomplishments

The Planetary Quarantine Laboratory (PQL) located in Building 49635, at Cape Canaveral Air Force Station (CCAFS), Florida, was modified to support the Viking 75 Program. The additional 600 square feet of laboratory space increased the PQL facilities to approximately 2400 square feet.

Three separate laboratory areas were established and equipped to support the Viking microbiological assay activities. These laboratories will house the bioassay teams from Martin-Marietta Aerospace (MMA), JPL Viking Orbiter (JPL-VO) and PQL.

Supplies and equipment needed to perform the required microbiological assays were purchased. Specified laboratory equipment was calibrated and/or certified as required by the Viking 75 Program Microbiological Assay and Monitoring Plan, M75-148-0. The entire PQL was fully operational and certified for Viking usage by December 31, 1974.

In addition, office facilities located in the Hanger N Annex were provided for the Planetary Quarantine Officer and personnel from the responsible organizations associated with the various functions of the bioassay activities. These organizations include, JPL-VO, MMA, Exotech Systems, Inc., and Bionetics Corporation.

5.1.3 Future Activities

Bioassay of the Viking Lander Capsule and Orbiter will be completed. Bacterial colonies resulting from the Viking bioassays will be picked randomly from culture plates, gram stained and identified. These isolates will be maintained on the appropriate media, subsequently lyophilized and stored for future reference. Microbiological profiles will be conducted on other pertinent spacecraft as requested by Planetary Quarantine Officer. The quantitative and qualitative microbial assessment of the intramural environment where spacecraft are assembled and tested will be completed.

5.1.4 Presentations

Puleo, J. R., Planetary Quarantine Laboratory Bioassay Activities (AFETR), Thirteenth Semi-Annual NASA Spacecraft Sterilization Technology Seminar, December 1974, Cocoa Beach, Florida.

SECTION VI

PLANETARY QUARANTINE LABORATORY - RESEARCH ACTIVITIES
(NASA No. 193-58-63-06)

Contents	Title and Related Personnel
Subtask A para. 6.1	TEFLON RIBBON EXPERIMENTS Cognizance: J. R. Puleo Associate Personnel: G. Oxborrow N. Fields S. Bergstrom
Subtask B para. 6.2	PYROLYSIS GAS - LIQUID CHROMATOGRAPHY STUDY Cognizance: G. Oxborrow Associate Personnel: N. Fields J. R. Puleo

PRECEDING PAGE BLANK NOT FILMED

6.1 TEFLON RIBBON EXPERIMENTS

6.1.1 Subtask A Introduction

The objective of this study is to characterize the thermal resistance profiles of naturally occurring bacterial spores associated with assembly facilities at Kennedy Space Center.

The validity of the currently accepted sterilization cycle should be confirmed. The cycle, to be valid, should be effective on bacterial spores associated with spacecraft in residence at Kennedy Space Center, Florida.

6.1.2 Significant Accomplishments

6.1.2.1 Results. The teflon ribbon study was continued. The details of the thermal apparatus and experimental test procedures were described in para. 5.1.2.1 of Jet Propulsion Laboratory (JPL) Doc. No. 900-655, April 1974. Naturally occurring airborne bacterial spores were collected on teflon ribbons exposed to the intramural environment of the Vehicle Assembly Building (VAB), Kennedy Space Center (KSC), Florida.

Due to modification of the high bay area in the VAB, the teflon ribbons were removed from the ground floor site, and were relocated on the 20th floor of the same high bay area.

The studies were broken into experimental groups to: 1) determine the ability of the "hardy" microorganisms to reproduce in a martian environment, 2) determine the geographical distribution of "hardy" microorganisms, and 3) evaluate the effects of moisture and temperature on survival of the "hardy" microorganisms when time is held constant.

The ability of "hardy" microorganisms to reproduce in a martian environment was evaluated in a cooperative study with Hardin-Simmons University (HSU) under the direction of Dr. Terry L. Foster. Ten experimental groups of teflon ribbons were subjected to the high thermal inertia cycle (JPL Doc. No. 900-655, April 1974) at 111.7C and 1.2 mg per liter moisture content in N_2. One-half of the ribbons from each experimental

C-2

run was retained at the Planetary Quarantine Laboratory (PQL), processed by the usual procedures, and served as controls. The remaining ribbons, upon their removal from the dry heat oven, were placed into sterile jars with filter-vented lids which allowed the aseptic exchange of gas inside of the jar. These were then placed into sterile, metal pressure-vacuum containers, where an N_2 atmosphere of five inches of water pressure was maintained. The teflon ribbons were transported by car to HSU and subjected to various experimental conditions; i.e., 1) ribbons used in five experiments were stored under a nitrogen atmosphere for three weeks, and then subjected to a vacuum of 10^{-6} Torr, 2) ribbons used in four experiments were exposed to a simulated martian environment at 15C, and 3) one set of ribbons received no treatment, in order to determine the effect of shipping on recovery of heat survivors (HSU Report No. 5, January 1975).

Table 6-A.1 compares the number of survivors, the MPN per ribbon and the survivor fraction to the PQL controls for each experiment. The data showed that exposure to nitrogen-vacuum did not appear to affect the number of heat survivors recovered. When ribbons were subjected to the experimental martian environment at 15C, a definite decrease in the number of survivors was noted. This effect could be the result of the low incubation temperature. Shipping had no apparent effects on the recovery of the heat survivors. Identification of the thermal survivors is now in progress.

Teflon ribbons were sent to JPL, Pasadena, California, and to Martin-Marietta Aerospace (MMA), Denver, Colorado, to assess the geographical distribution of "hardy" microorganisms. The ribbons sent to JPL were exposed for a period of seven days in the structural test laboratory where no environmental control was exercised. After the exposure period, the ribbons were collected, placed into sterile plastic containers, returned to PQL, and subsequently subjected to the thermal cycle described previously. Table 6-A.2 shows the numerical results after 28 days of incubation. Survivors were recovered in five of the six experiments. The survivor fraction is approximately the same as the fraction observed at the VAB-KSC area. All survivors were identified to see if the ratio of species types was similar. Table 6-A.3 shows the types of microorganisms and the frequency of biochemical tests observed. As was previously seen in results obtained

Table 6-A.1. Thermal Resistance of Bacterial Spores Collected on Teflon Ribbons - VAB - KSC

Temp. 111.7C

Moisture Content 1.2 mg/l

Experiment Number	N_o Spores	Positive/Total		MPN for Ribbon		Survivor Fraction N_H/N_o	
		PQL	HSU[a]	PQL	HSU	PQL	HSU
T1	2.3×10^2	2/12	0/12	0.182	0	7.9×10^{-4}	0
T2	6.7×10^2	4/12	6/12	0.406	0.693	6.1×10^{-4}	1.0×10^{-3}
T3	8.0×10^2	9/12	4/12	1.387	0.406	1.7×10^{-3}	5.1×10^{-4}
T4	1.7×10^3	9/12	4/12	1.387	0.406	8.2×10^{-4}	2.4×10^{-4}
T5	1.1×10^3	8/12	6/12	1.099	0.693	9.7×10^{-4}	6.3×10^{-4}
T6	3.6×10^2	2/12	0/12	0.182	0	5.1×10^{-4}	0
T7	6.5×10^2	5/12	0/12	0.539	0	8.3×10^{-4}	0
T8	6.1×10^2	10/12	2/12	1.792	0.182	3.0×10^{-3}	3.0×10^{-4}
T9	1.0×10^3	4/12	0/12	0.406	0	4.0×10^{-4}	0
T10	8.8×10^2	4/12	3/12	0.406	0.287	4.6×10^{-4}	3.3×10^{-4}

[a]Hardin-Simmons University
T1 - T5: Ribbons stored under nitrogen-vacuum environment.
T6 - T9: Ribbons stored under simulated martian environment (15C).
T10: Ribbons received no treatment.

Table 6-A. 2. Thermal Resistance of Bacterial Spores Collected on Teflon Ribbons - JPL/PASADENA

Temp. 111. 7C

Moisture Content 1. 2 mg/l

Experiment Number	N_o Spores	Positive/Total	MPN for Ribbon	Survivor Fraction N_H/N_o
JPL-1	3.8×10^2	4/24	0.182	4.8×10^{-4}
JPL-2	4.8×10^2	3/24	0.134	2.8×10^{-4}
JPL-3	2.9×10^2	2/24	0.087	3.0×10^{-4}
JPL-4	2.4×10^2	2/24	0.087	3.7×10^{-4}
JPL-5	3.4×10^2	3/24	0.134	3.9×10^{-4}
JPL-6	2.6×10^2	0/24	0.000	0.0

Table 6-A. 3. Biochemical Test Reactions of Heat-Stressed Environmental Isolates

JPL-Pasadena

Temp. 111. 7C

Moisture Content 1. 2 mg/l

Organism	No. of Isolates	Mannitol	Tyrosine	Phenyl-alanine	Casein	Starch	Voges-Proskauer	Citrate	Nitrate	Anaerobic Growth
B. brevis	1	-	+	-	+	+	-	-	-	-
B. firmus	1	-	-	+	-	+	-	-	+	-
B. lentus	4	-	-	-	-	+	-	-	-	-
B. macerans	1	-	-	-	-	+	-	-	+	+
B. pumilus	1	+	-	-	+	-	-	+	-	-
Atypical Bacillus	5	-	-	-	-	-	-	-	-	-
Atypical Bacillus	1	-	-	-	-	+	-	-	+	-

from the VAB (JPL Doc. No. 900-675, September 1974), the atypical bacillus (42.9%) and the lentus (21.4%) groups comprise the majority of the isolates.

The ribbons sent to MMA were exposed in the return air plenum located under the floor of the class 100,000 area where the Viking spacecraft was being assembled. The returned ribbons were treated as described in the study with JPL. Table 6-A.4 shows the results of the experiments. All experiments showed at least one positive ribbon. The survival fraction is also approximately the same as the above mentioned. The identification results (Table 6-A.5) show that the atypical bacillus and the lentus groups were the most predominant survivors. The remaining six survivors were identified as actinomycetes.

Results from the above experiments show the "hardy" microorganisms to be widely distributed geographically. The thermal survivors found in all three areas were similar although the ratio of one type to another was dissimilar.

A summary of the above experiments showed 84 survivors were recovered from a total of 408 teflon ribbons which had been exposed to airborne microbial fallout and subsequently subjected to the thermal sterilization cycle. Only three organisms were capable of anaerobic growth.

The incubation period of 28 days was examined to assure that an adequate time for microbial growth was being allowed. Table 6-A.6 shows the data collected from the VAB, JPL and MMA thermal experiments and the incubation period required prior to observing a positive culture. Greater than 85% of the positive cultures were observed at the end of 14 days incubation, with the exception of the MMA experiments. The delayed number of positive cultures obtained in the MMA experiments can be explained by the high percent of slow growing actinomycete cultures surviving the thermal treatment. The average percent of positive cultures obtained at 28 days (5.2%) is considered small and incubation extended beyond that period would not be expected to significantly increase the number of positive test ribbons.

Evaluation of a thermal process for effectively inactivating naturally occurring spores is difficult to obtain by direct experimentation due to variations in initial spore concentration (N_o) from experiment to experiment.

Table 6-A. 4. Thermal Resistance of Bacterial Spores Collected on Teflon Ribbons - Martin-Marietta/Denver

Temp: 111. 7C

Moisture Content 1. 2 mg/l

Experiment Number	N_o Spores	Positive/Total	MPN for Ribbon	Survivor Fraction N_H/N_o
MMA-1	1.3×10^2	3/24	0.134	1.0×10^{-3}
MMA-2	1.6×10^2	2/24	0.087	5.6×10^{-4}
MMA-3	2.4×10^2	4/24	0.182	7.7×10^{-4}
MMA-4	1.4×10^2	2/24	0.087	6.1×10^{-4}
MMA-5	1.2×10^2	1/24	0.043	3.7×10^{-4}
MMA-6	9.8×10^1	1/24	0.043	4.4×10^{-4}

Table 6-A. 5. Biological Test Reactions of Heat-Stressed Environmental Isolates

Martin-Marietta Aerospace

Temp. 111. 7C

Moisture Content 1. 2 mg/1

Organism	No. of Isolates	Mannitol	Tyrosine	Phenyl-alanine	Casein	Starch	Voges-Proskauer	Citrate	Nitrate	Anaerobic Growth
B. lentus	4	-	-	-	-	+	-	-	-	-
B. macerans	1	-	-	-	-	+	-	-	+	+
Atypical Bacillus	1	-	-	-	-	-	-	-	-	-
Atypical Bacillus	1	-	-	-	-	+	-	-	+	-

Table 6-A. 6. Positive Cultures Detected at Various Incubation Periods

Location	Temp. °C	Moisture Content mg/l	No. Positive Teflon Ribbons	Percent Positive Days of Incubation 7	14	21	28
VAB[a]	113	<0.01	124	66.9	12.9	11.3	8.9
VAB	113	1.2	72	72.2	13.9	11.1	2.8
VAB	111.7	1.2	183	84.7	8.2	4.4	2.7
JPL[b]	111.7	1.2	14	64.3	21.5	7.1	7.1
MMA[c]	111.7	1.2	13	23.1	46.1	15.4	15.4
		Total	406				
		Percent		74.4	12.3	8.1	5.2

[a]Vehicle Assembly Building, KSC, Florida

[b]Jet Propulsion Laboratory, Pasadena, California

[c]Martin-Marietta Aerospace, Denver, Colorado

Activity, personnel density, and climatic conditions in a given area are factors which could greatly influence the spore concentration and species distribution. However, the comparative effectiveness of thermal processes, with differing spore N_o, can be estimated by determining the survivor fraction after the thermal treatment.

Figure 6-A.1 shows the expected effects of three different thermal processes on naturally occurring spores. The thermal process of 113C, < 0.01 mg moisture content per liter N_2, is shown to be more effective than the presently accepted thermal process of 111. 7C, 1.2 mg moisture content per liter N_2. Both temperature and moisture content are shown to dramatically affect the number of survivors.

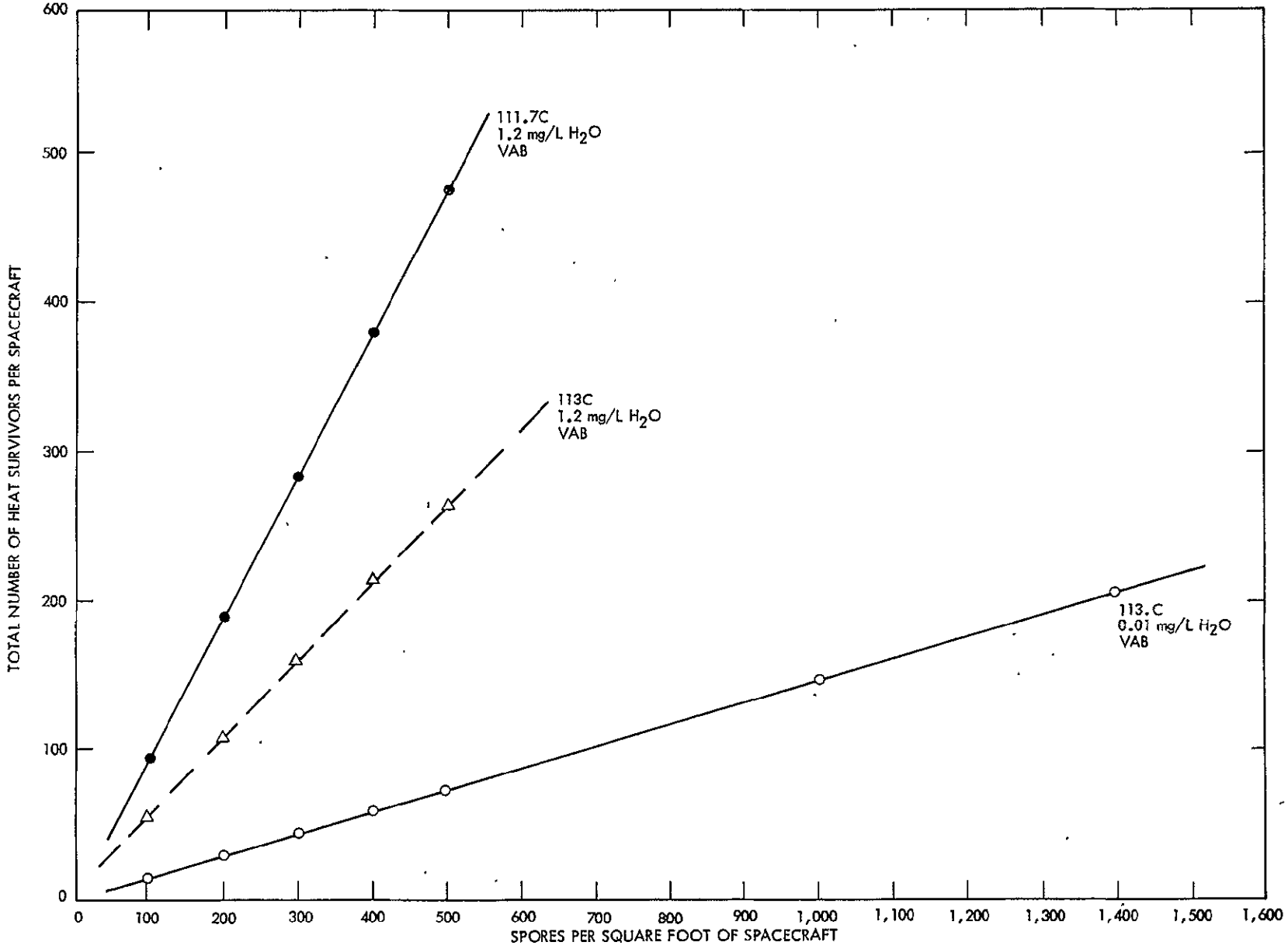

Figure 6-A. 1. Expected effects of thermal processes on naturally occurring spores

6.1.3 Future Activities

Future work will be directed to: (1) Characterize the thermal resistance profiles of naturally occurring bacterial spores from assembly facilities at KSC, JPL, MMA. (2) Develop thermal death curves using various tempreatures, water concentrations and duration of thermal exposure. (3) Cooperative studies with Hardin-Simmons University to determine the occurrence of thermal resistance of anaerobic microorganisms. (4) Thermal inactivation kinetics of bacterial spore populations isolated from the Viking Lander and Orbiter spacecraft.

6.1.4 Presentations

Puleo, J. R., "Review of Hardy Organisms Results; Factors of Temperature and Humidity", AIBS Planetary Quarantine Panel, Denver, Colorado, July 1974.

Puleo, J. R., "The Occurrence and Characteristics of Hardy Organisms at KSC, JPL, and Denver". Conference on the Significance of Hardy Organisms to the Viking Biopackage, Ames Research Center, Moffett Field, California, November 18-19, 1974.

Puleo, J. R., "Teflon Ribbon Experiments at KSC: Current Status of Thermal Resistance Studies", presented at Thirteenth Semi-Annual NASA Spacecraft Sterilization Technology Seminar, Cocoa Beach, Florida, December 1974.

6.1.5 References

1. Planetary Quarantine Semi-Annual Review, "Space Research and Technology", 1 July - 31 December 1973, JPL Document 900-655. April 1974.

2. "Response of Selected Microorganisms to Experimental Planetary Environments," Semi-Annual Report No. 5 of Planetary Quarantine Activities, 1 July - 31 December 1974, Hardin-Simmons University, January 1975.

3. Planetary Quarantine Semi-Annual Review, "Space Research and Technology", 1 January - 30 June 1974, JPL Document 900-675, September 1974.

6.2 PYROLYSIS GAS-LIQUID CHROMATOGRAPHY STUDY

6.2.1 Subtask B Introduction

Microbial survivors from the Viking Terminal Heat Cycle are difficult to identify by conventional morphological and biochemical methods. Isolates are generally slow growing, have few positive biochemical characteristics and are difficult to sporulate. Isolates with identical biochemical characteristics often have different colonial, cellular and spore morphology. From 132 isolates subjected to the pertinent battery of tests, approximately 40% did not fit the biochemical scheme and were classified as atypical Bacillus spp. Two possibilities are apparent for recovering such a large atypical group; a) they are unique species with an inherent genetic ability to withstand the heat cycle or, b) they are known species having individual spores physiologically superior to allow survival even though they may be permanently injured. These difficulties and questions have led to a search for a more reliable method of identification or characterization.

6.2.2 Approach

Pyrolysis gas-liquid chromatography (PGLC) has been shown by Dr. Simmonds (1) of the California Institute of Technology to be a rapid, sensitive method of bioorganic anaysis. This method, in conjunction with mass spectroscopy is part of the life detection package of the Viking spacecraft. Current literature has revealed several researchers have successfully differentiated various microbial groups or species using PGLC. Dr. Reiner, of the Center for Disease Control (CDC) in Atlanta, has been able to consistently identify species of the genus Mycobacterium, Salmonella and Leptospira (2, 3, 4, 5). Other researchers such as Dr. Kulik (6) of the University of Manchester in England have been using PGLC to identify and characterize species of Aspergillus and other fungi. Dr. Hall (7) from Purdue is speciating cockroaches with this method.

Another approach to chromatography identification is being developed by Dr. Moss (8), CDC, and others. Their method is to derivitize whole cell lysates, extract the derivitized fatty acids and obtain chromatograms from the extraction. This method of identification has also been somewhat successful.

6. 2. 3 Experimental Conditions

Pyrolysis was the method of choice because it is a more direct method, not requiring chemical combinations and extractions. The equipment used was a Pyroprobe 150 and a Varian Aerograph 2800 Chromatograph with a recorder and digital integrator as shown in Figure 6-B. 1. The pyrolysis unit was programmed to increase in temperature at the rate of 0. 1° C per millisecond until a temperature of 800° C was reached. It then held that temperature for 10 seconds before cooling to the 200° C constant temperature of the interface oven (Table 6-B. 1). The pyrolysis products were swept from the interface oven into the chromatograph column by a He flow of 25 ml per minute.

The injector temperature of the chromatograph was maintained at 230° C and the flame ionization detectors at 260° C. The column and column oven was regulated by a multilinear temperature programmer using the temperature program shown (Table 6-B. 2). Several column lengths and packings were evaluated before accepting a 10 foot by 1/8 inch coiled column packed with 7% carbowax 20M TPA terminated on Anakrom ABS support (100-120 mesh).

Cultures were prepared for pyrolysis (Figure 6-B. 2) while in the log growth phase to assure more uniform and pronounced cellular physiology. Cultures were grown on Trypticase Soy Agar (TSA) supplemented with 0. 1% yeast extract and 0. 2% soluble starch. Slants from original cultures were incubated at 32° C. Cells were harvested by washing from the plates with 10ml of sterile buffered distilled water and placed in centrifuge tubes. Prior to centrifugation three washings of each culture were made by shaking on a rotary shaker for 1-5 minutes. Between each centrifugation the supernatant was decanted and replaced by fresh sterile buffered distilled water.

6. 2. 3. 1 Results. Chromatograms from *Bacillus globgii* and 15 ATCC and NRS stock *Bacillus* species were visually compared. Differences were seen between all species examined. Chromatographs 6-B. 3 thru 6-B. 5 show some of the chromatograms obtained of different species. It is easily seen that the peak area indicated by A in chromatograph 6-B. 3 is not present in 6-B. 4 or 6-B. 5. Chromatogram 6-B. 4 is easily separated from the others when area B is compared.

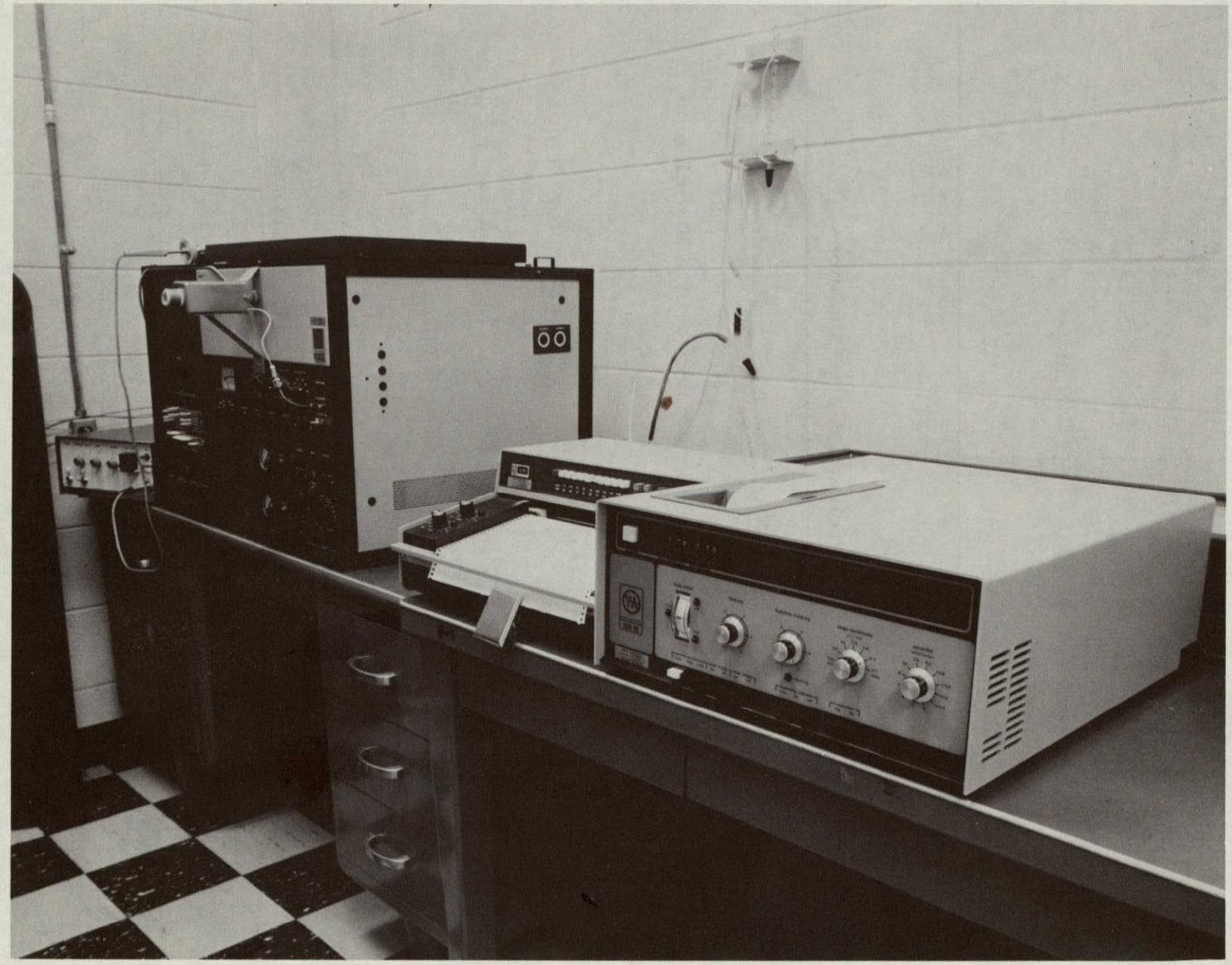

Fig. 6-B.1. Chromatographic Equipment

Table 6-B. 1 Pyrolysis Conditions

INTERFACE TEMP.	200°C
RAMP.	0. 1°C/MS
INTERVAL	10 sec.
FINAL TEMP.	800°C

Table 6-B. 2. Chromatography Conditions

Column	Solid: ANAKROM ABS	Liquid 7% CW-20M
Flows	HE 25 H 30 ml/min	Air 300 ml/min
Electrometer	Range 10^{-11}	
Injector Temp. 230 °C		Detector Temp. 260°C
Temp. Program	Initial 80°C	Step Interval 3 min
Steps	Rate - °C	Final Temp.
1	0	80. 0
2-5	6. 5	158. 0
6-14	1. 25	191. 75
15	6. 5	211. 25
16-18	0	211. 25

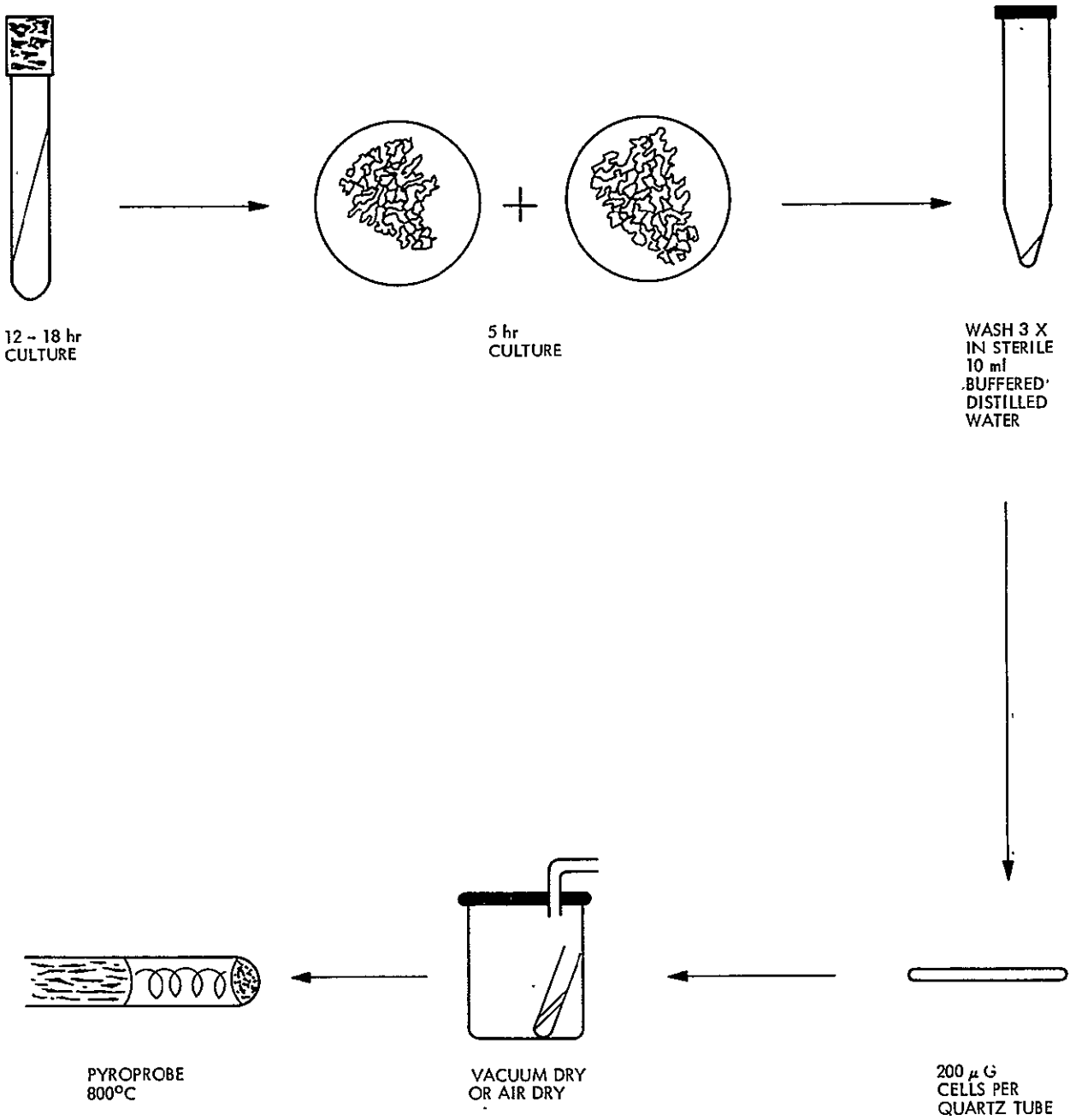

Fig. 6-B.2. Assay Techniques

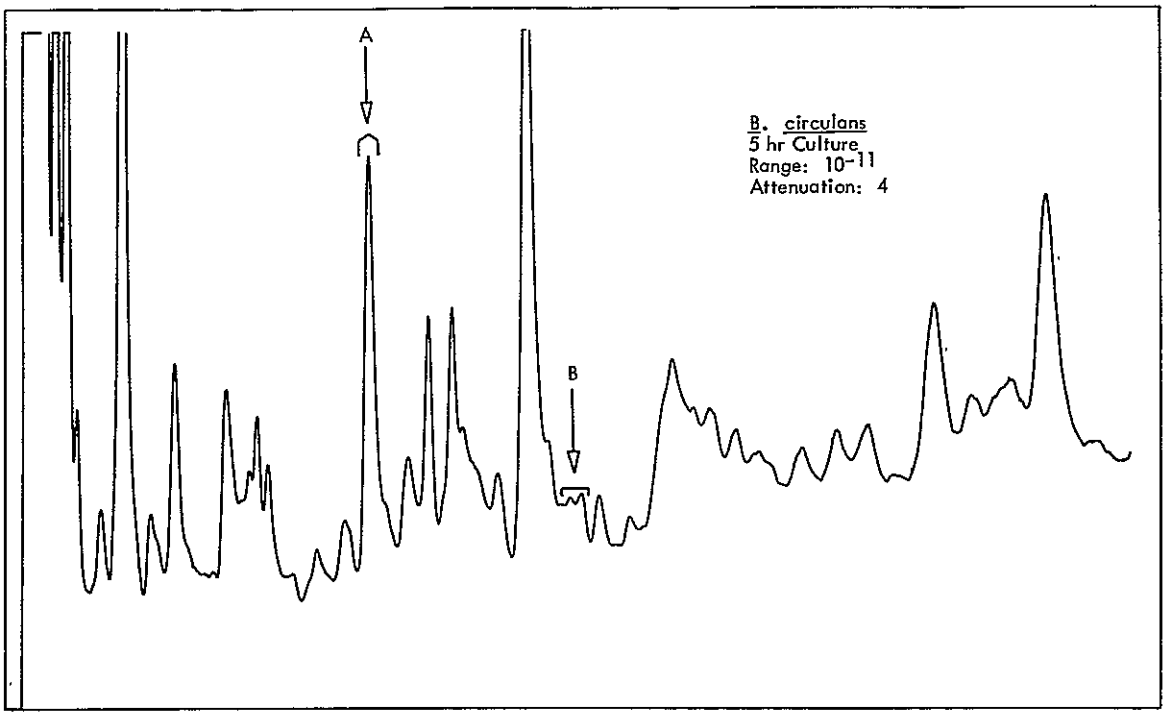

Fig. 6-B.3. Chromatogram of B. circulans

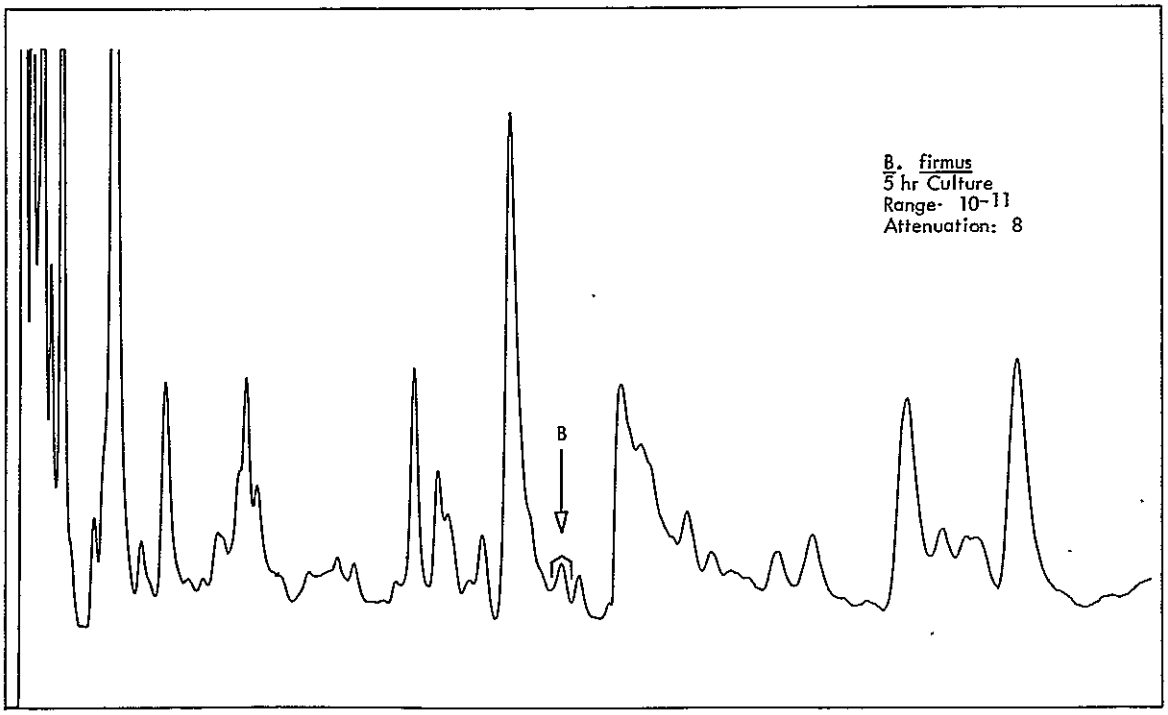

Fig. 6-B.4. Chromatogram of B. firmus

Physiological changes in cells can easily be demonstrated by the presence of spores in a culture. Chromatogram 6-B. 6 show the effects of sporulation on the peak area C when compared to chromatogram 6-b. 5.

A survivor from the terminal heat cycle (Figure 6-B. 7) is compared to the chromatograms from the stock cultures. Area D is obviously much different suggesting a different culture metabolism.

Computer pattern recognition analysis of six replicate samples of the above culture integrator data is being evaluated by the ADAPT family of computer programs. Preliminary results show the Bacillus spp. being separated into their individual groups.

6. 2. 4 Future Activities

Future activities in this study will concentrate on comparing Bacillus spp. in various physiological conditions and their resultant chromatograms; complete a chromatographic catalog of Bacillus spp. ; evaluate glass capillary columns and use a digitizer to prepare a data base for computer analysis; identify or characterize dry heat resistant microorganisms; evaluate a pattern recognition computer identification system; and chemically identify resultant chromatographic peaks using mass spectroscopy.

6. 2. 5 Presentation

Oxborrow, G. S. , "Identification of Microorganisms using Pyrolysis Gas Chromatographic Equipment and Computer Manipulation of Data", presented at Thirteenth Semi-Annual NASA Spececraft Sterilization Technology Seminar, Cocoa Beach, Florida, December 1974.

6. 2. 6 References

1. Simmonds, P. G. , G. P. Shulman and Stembridge, "Organic Analysis by Pyrolysis Gas-Liquid Chromatography - Mass Spectrometry A Candidate Experiment for the Biological Exploration of Mars", J. Chromatog. Sci. 7, 36 (1969).

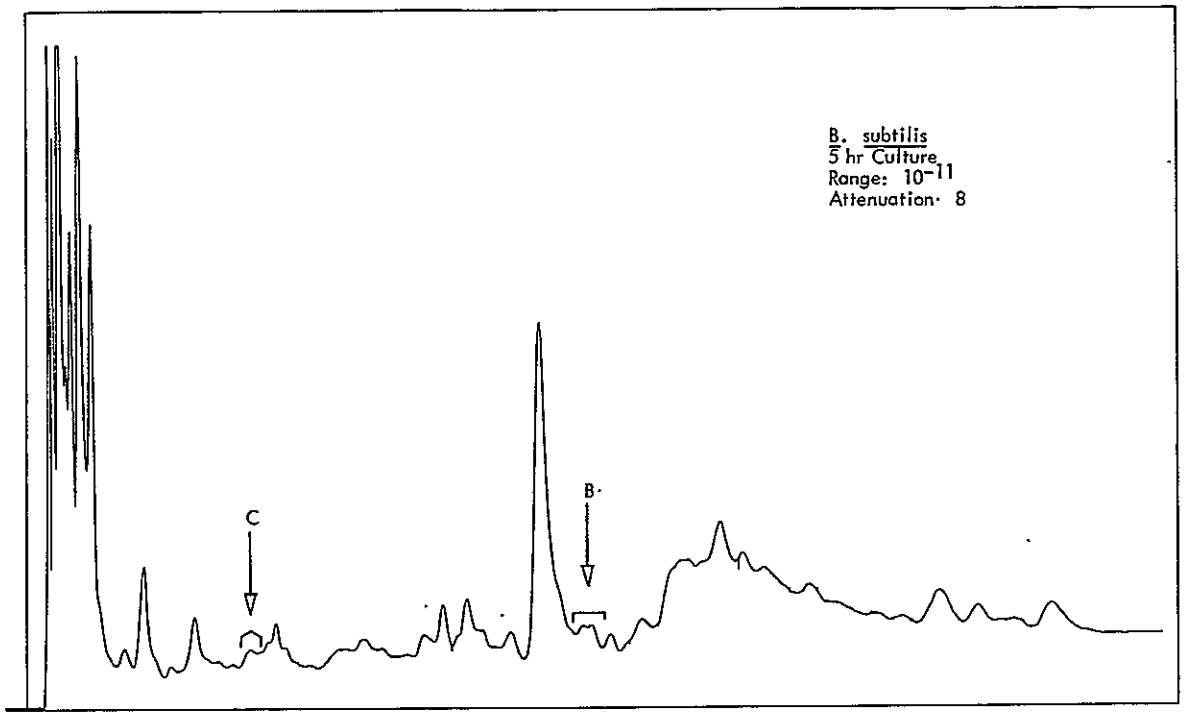

Fig. 6-B.5. Chromatogram of B. subtilis

2. Reiner, E. and Kubica, "Predictive Value of Pyrolysis Gas-Liquid Chromatography in the Differentiation of Mycobacteria", American Review of Respiratory Diseases, Vol. 99 (1969).

3. Reiner, E., "Studies on Differentiation of Microorganisms by Pyrolysis Gas-Liquid Chromatography", J. of G. C., Feb. (1967)

4. Reiner, E., and W. H. Ewing, "Chemotaxonomic Studies of Some Gram Negative Bacteria by Means of Pyrolysis Gas-Liquid Chromatography", Nature, Vol. 217, Jan. (1968).

5. Reiner, E., J. J. Hicks and C. R. Sulzer, "Leptospiral Taxonomy by Pyrolysis Gas-Liquid Chromatography", Canadian J. of Microbiol., Vol. 19, 10 (1973).

6. Vincent, P. G. and M. M. Kulik, "Pyrolysis Gas-Liquid Chromatography of Fungi: Differentiation of Species and Strains of Several Members of the Aspergillus flavus Group", Applied Microbiol., Vol. 20, 6, Dec. (1970).

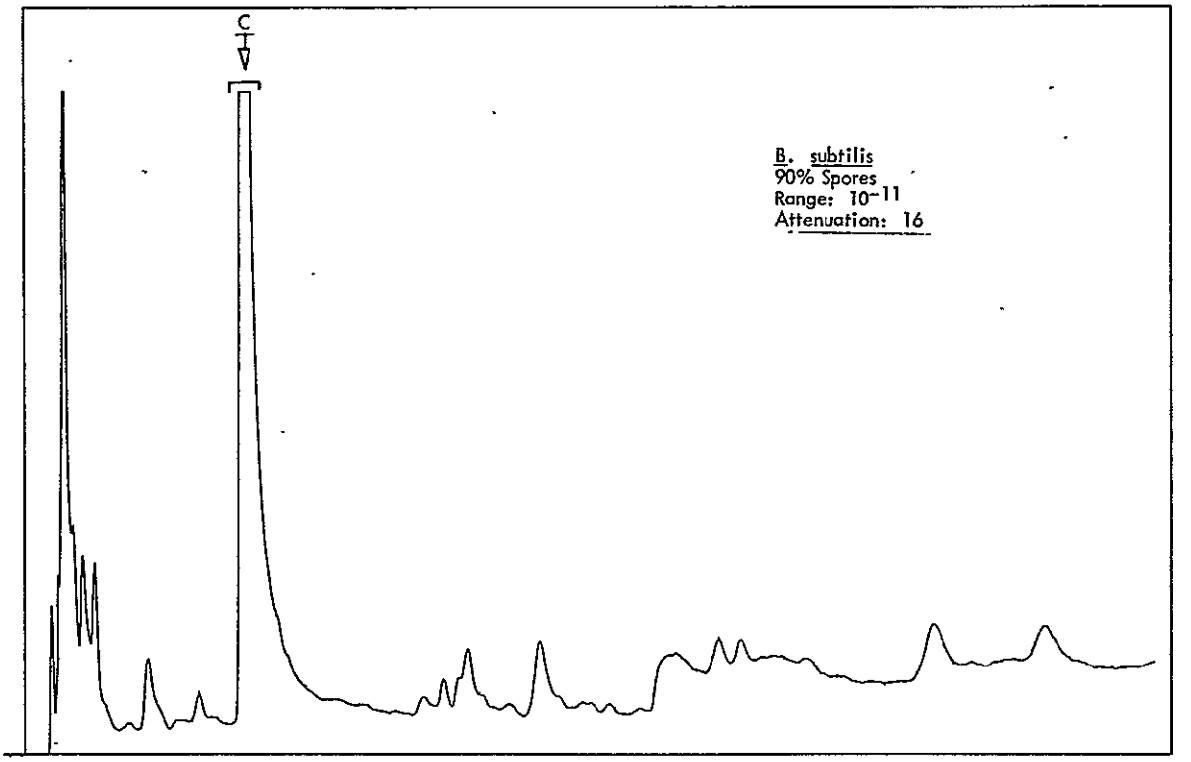

Fig. 6-B.6. Chromatogram of B. subtilis (90% spores)

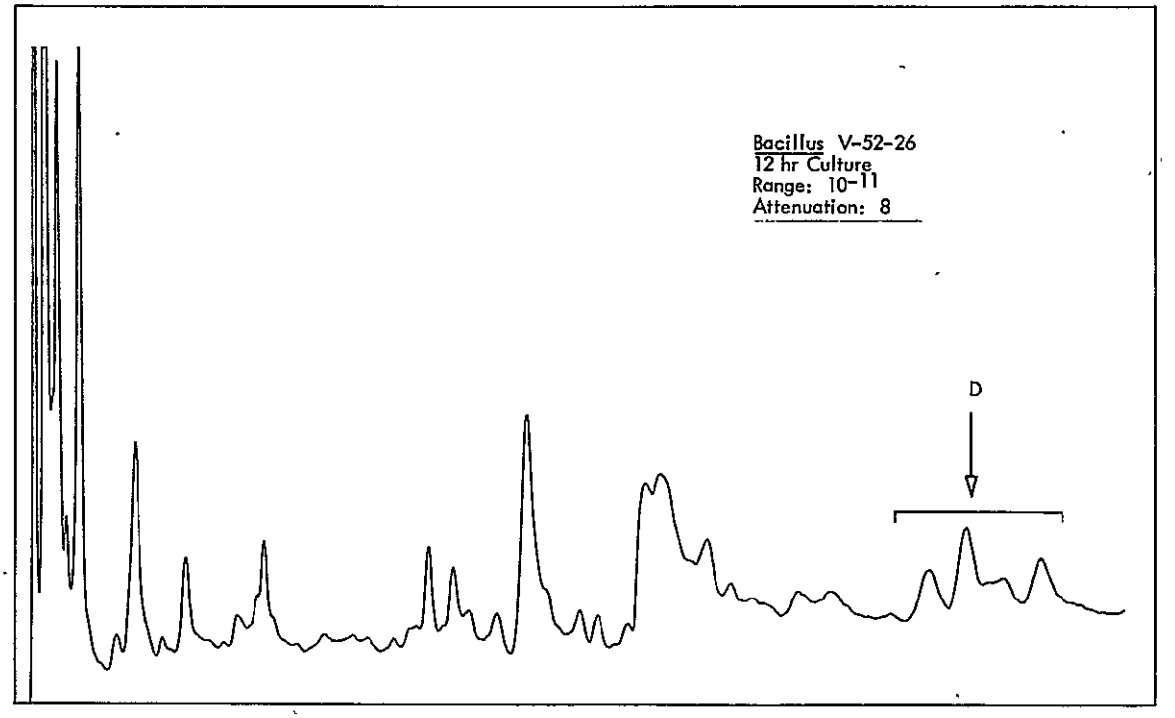

Fig. 6-B.7. Chromatogram of heat survivor Bacillus V-52-26

7. Hall, R. C. and G. W. Bennett, "Pyrolysis Gas-Liquid Chromatography of Several Cockroach species", J. Chromatog. Sci. Vol. 11, Aug. (1973).

8. Farshtchi, D. and C. W. Moss, "Characterization of Bacteria by Gas Chromatography: Comparison of Trimethylsilyl Derivatives of Whole-Cell Hydrolysates", Appl. Microbiol., Vol. 17, 2, Feb. (1969).

NASA — JPL — Coml., L.A. Calif.

DISTRIBUTION

Alcorn, D.	179-203
Caird, H.	111-118
Craven, C.	180-805
Hess, D. S.	233-208
Hoffman, A.R. (2)	233-206
Puleo, J. R. (14)	179-203
Small, J. G. (3)	180-703
Taylor, D. M. (75)	233-206